

**Moderation of rRNA gene activity  
triggers metabolic adaptation promoting  
geroprotection in *Caenorhabditis elegans***

**Dissertation**

To Fulfill the  
Requirements for the Degree of  
„doctor rerum naturalium” (Dr. rer. nat.)

**Submitted to the Council of the Faculty  
of Biological Sciences  
of the Friedrich Schiller University Jena**

**by Mohamed Samin Sharifi, M.Sc., B. Sc.  
born on 26.08.1991 in Kabul**

First referee: Dr. rer. nat. Holger Bierhoff, Friedrich Schiller University Jena

Second referee: PD Dr. rer. nat. Christian Kosan, Friedrich Schiller University Jena

External referee: PD Dr. rer. nat. Matthias Schaefer, Medical University of Vienna

Date of defense: June 3<sup>rd</sup>, 2022

## TABLE OF CONTENTS

Table of contents .....	I
List of figures .....	V
List of tables.....	VI
List of Abbreviations .....	VII
Summary.....	X
Zusammenfassung.....	XII
1 Introduction .....	1
1.1 Aging.....	1
1.1.1 Aging definition.....	1
1.1.2 Dietary restriction signaling pathways .....	2
1.2 <i>Caenorhabditis elegans</i> as a model in aging research .....	3
1.2.1 <i>Caenorhabditis elegans</i> anatomy and development.....	3
1.2.2 <i>Caenorhabditis elegans</i> in aging research .....	5
1.3 Ribosomal RNA synthesis .....	7
1.3.1 Ribosome biogenesis .....	7
1.3.2 Ribosomal RNA synthesis in <i>Caenorhabditis elegans</i> .....	8
1.3.3 Link between ribosomal RNA genes and aging .....	9
2 Aim of this study .....	11
3 Materials .....	13
3.1 Primers .....	13
3.2 Chemicals.....	13
3.3 Software .....	16

3.4	Consumables .....	17
4	METHODS.....	18
4.1	Buffers and media .....	18
4.2	<i>Caenorhabditis elegans</i> experiments .....	20
4.2.1	Strains and maintenance .....	20
4.2.2	RNAi bacterial plate preparation .....	20
4.2.3	Age-synchronization .....	20
4.2.4	RNA interference experiments .....	21
4.2.5	Lifespan analysis .....	21
4.2.6	Burrowing assay .....	22
4.2.7	Smurf assay .....	22
4.2.8	Nucleolar size measurement .....	22
4.2.9	Worm size determination .....	23
4.3	Molecular biology techniques .....	23
4.3.1	Genotyping .....	23
4.3.2	RNA extraction .....	24
4.3.3	cDNA synthesis .....	24
4.3.4	Reverse transcription and quantitative polymerase chain reaction .....	24
4.3.5	ATP measurement .....	25
4.3.6	Western blot analysis .....	25
4.4	Lipidomics and proteomics .....	26
4.4.1	Lipidomics .....	26
4.4.2	Proteomics .....	27
4.5	Statistical analysis .....	27

5	Results.....	28
5.1	rRNA gene activity hinders longevity .....	28
5.1.1	Increased RNA polymerase I transcriptional activity is detrimental for lifespan...28	
5.1.2	Moderation of rRNA gene activity through TIF-IA knockdown extends lifespan...32	
5.1.3	rRNA gene activity is inversely correlated to healthspan .....	33
5.2	Proteomic adaptations to curbed rDNA activity .....	39
5.2.1	Moderation of rRNA gene activity adjusts metabolism at old age .....	39
5.2.2	Abundance of vitellogenins is reduced in TIF-IA knockdown worms.....	41
5.2.3	TIF-IA knockdown promotes longevity only partly via translation inhibition .....	42
5.3	Reduction of rRNA gene activity remodels energy and lipid metabolism .....	46
5.3.1	Curtailment of rRNA gene activity increases cellular ATP levels.....	46
5.3.2	Moderation of rRNA gene activity alters lipid metabolism.....	48
5.4	Inhibition of rDNA activity late in life promotes healthy longevity .....	51
5.4.1	Knockdown of RNA polymerase I subunit RPOA-2 extends lifespan .....	51
5.4.2	RPOA-2 knockdown late in life extends lifespan .....	53
5.4.3	RPOA-2 knockdown late in life improves healthspan .....	55
6	Discussion.....	58
6.1	RNA polymerase I transcriptional activity is a modulator of longevity .....	58
6.2	Lowering rRNA gene activity is a promising late-life intervention .....	59
6.3	Moderate rDNA activity provides geroprotection through preserving energy levels	60
6.4	Curbed pre-rRNA synthesis modulates lipid metabolism and reduces lipotoxicity ...	62
6.5	Decreased rRNA gene activity alleviates proteostatic stress.....	63
6.6	Perturbation of pre-rRNA synthesis as an anti-aging strategy .....	65
7	References .....	68

Acknowledgments .....	XIV
Declaration of independent assignment Ehrenwörtliche Erklärung .....	XVI

## LIST OF FIGURES

Figure 1: Schematic illustration of the <i>C. elegans</i> life cycle .....	4
Figure 2: Formation of the pre-initiation complex and pre-rRNA synthesis.....	7
Figure 3: NCL-1 knockdown increases pre-rRNA synthesis and shortens lifespan .....	29
Figure 4: TIF-IA overexpression shortens lifespan through overlocking of rRNA genes .....	31
Figure 5: TIF-IA knockdown decreases rRNA gene activity .....	33
Figure 6: TIF-IA knockdown decreases nucleolar size and extends lifespan.....	34
Figure 7: Knockdown of TIF-IA and NCL-1 affect body size in opposite directions.....	35
Figure 8: Aging-associated loss of neuromuscular health is worsened by knocking down NCL-1 but improved upon TIF-IA knockdown .....	36
Figure 9: Loss of intestinal integrity at old age due to knockdown of NCL-1.....	38
Figure 10: TIF-IA knockdown rescues proteins involved in aging-related metabolic decline...	40
Figure 11: Restriction of rRNA synthesis lowers the expression of vitellogenins .....	41
Figure 12: Production of ribosomal proteins and total protein content is reduced upon TIF-IA knockdown .....	43
Figure 13: Lifespan extension by TIF-IA knockdown is not improved by concomitant translation inhibition .....	45
Figure 14: Reduction of rRNA gene activity increases ATP levels and counteracts the loss of cellular energy upon aging .....	47
Figure 15: Moderation of pre-rRNA synthesis partially rescues worms from age-related metformin toxicity.....	48
Figure 16: Knockdown of TIF-IA changes the composition of membrane and storage lipids...	50
Figure 17: Knockdown of the RNA polymerase I subunit RPOA-2 extends lifespan .....	52
Figure 18: Knockdown of RPOA-2 late in life extends lifespan .....	54
Figure 19: Moderation of rRNA gene activity late in life improves neuromuscular health .....	55
Figure 20: Knockdown of RPOA-2 late in life improves intestinal integrity in old worms .....	57
Figure 21: Model depicting the geroprotective changes induced by moderation of rDNA activity.....	65

## LIST OF TABLES

Table 1: List of primers for reverse transcription-quantitative polymerase chain reaction.....	13
Table 2: List of chemicals, antibodies, enzymes, and commercial kits .....	13
Table 3: List of used software.....	16
Table 4: Recipe buffers and media .....	18



## LIST OF ABBREVIATIONS

AD	adulthood day
ADP	adenosine diphosphate
age-1	ageing alteration 1
AMP	adenosine monophosphate
AMPK	5' AMP-activated protein kinase
APS	ammonium peroxydisulfate
ATP	adenosine triphosphate
ATPase	adenosine triphosphatase
Brat	Brain tumor protein
cDNA	complementary DNA
<i>C. elegans</i>	<i>Caenorhabditis elegans</i>
CGC	Caenorhabditis Genetics Centre
CHX	cycloheximide
CT	threshold cycle
DAF-2	abnormal dauer formation 2
DAF-16	abnormal dauer formation 16
DAPI	4',6-diamidino-2-phenylindole
<i>D. melanogaster</i>	<i>Drosophila melanogaster</i>
DMSO	dimethyl sulfoxide
DNA	deoxyribonucleic acid
DR	dietary restriction
dsRNA	double-stranded RNA
eat-2	eating abnormal 2
<i>E. coli</i>	<i>Escherichia coli</i>
EDTA	ethylenediaminetetraacetic acid
ERC	extrachromosomal rDNA circle
et al.	et alia
EtOH	ethanol
FA	fatty acid
FFA	free fatty acid
FIB-1	fibrillarin family 1
FOXO	forkhead box O
GFP	green fluorescent protein
GTP	guanosine triphosphate
GTPase	guanosine triphosphatase
HRP	horseradish peroxidase
IFE-2	initiation factor 4E family
IGF-1	insulin-like growth factor 1
IGS	intergenic spacer
IIS	insulin & IGF-1 signaling
IPTG	isopropyl $\beta$ -D-1-thiogalactopyranoside
ITS	internal transcribed spacer

KD	knockdown
KPB	Potassium phosphate buffer
LB	lysogeny broth
LCFA	long-chain fatty acid
LET-363	lethal 363
MCFA	medium-chain fatty acid
Met	metformin
MoSCI	Mos1-mediated single-copy insertion
mRNA	messenger RNA
mTOR	mechanistic target of rapamycin
MUFA	monounsaturated fatty acid
NAD <sup>+</sup>	nicotinamide adenine dinucleotide
NCL-1	abnormal nucleoli
NGM	nematode growth medium
NOR	nucleolar organizing region
NP-40	Nonidet P40
ns	not significant
OE	overexpressing
PAGE	polyacrylamide gel electrophoresis
PC	phosphatidylcholine
PCA	principal component analysis
PCR	polymerase chain reaction
PE	phosphatidylethanolamine
PG	phosphatidylglycerol
PGC-1 $\alpha$	peroxisome proliferator-activated receptor gamma coactivator 1-alpha
PI	phosphatidylinositol
PIC	pre-initiation complex
PI3K	phosphatidylinositol 3 kinase
PS	phosphatidylserine
Pol I/II/III	RNA polymerase I/II/III
POLR1B	RNA polymerase I subunit RPA2
pre-rRNA	pre-ribosomal RNA
proteostasis	protein homeostasis
PUFA	polyunsaturated fatty acid
RCF	relative centrifugal field
rDNA	rRNA genes
RNA	ribonucleic acid
RNAi	RNA interference
RNase	ribonuclease
RP	ribosomal protein
RPOA-2	RNA polymerase I (A) subunit
rRNA	ribosomal RNA
RT	room temperature

RT-qPCR	reverse transcription-quantitative PCR
SCFA	short-chain fatty acids
SD	standard deviation
SDS	sodium dodecyl sulfate
SIRT1	sirtuin 1
SL1	selectivity factor 1
TAE	Tris/acetic acid/EDTA
TAG	triacylglycerol
TBST	Tris-buffered saline with Tween 20
TEMED	N,N,N',N'-tetramethylethylenediamine
TIF-IA	transcription initiation factor IA
TRIM2/3	tripartite motif-containing 2 and 3
TRIS	tris(hydroxymethyl)aminomethane
U	Units
UBF	upstream binding factor
UPLC-MS/MS	ultra performance liquid chromatography tandem mass spectrometry
V	Volt
VIT	Vitellogenin
v/v	volume per volume
w/v	weight per volume
WT	wild type

## SUMMARY

Despite aging being inevitable, the rate of aging is malleable. An energy-saving, catabolic state promotes longevity, whereas major anabolic activities like ribosome biogenesis and protein synthesis are linked to accelerated aging. Both processes are hinged on the transcription of rRNA genes (rDNA) into a pre-ribosomal RNA (pre-rRNA) by RNA polymerase I (Pol I). Pol I accounts for most of the cell's transcriptional output and presides over major pathways of macromolecule biosynthesis; however, its role in aging is not well understood. To investigate how the Pol I transcription machinery impacts lifespan and healthspan, its activity was manipulated in the roundworm *Caenorhabditis elegans* (*C. elegans*). First, NCL-1, a general repressor of ribosome biogenesis, was knocked down, leading to elevated pre-rRNA levels but reduced lifespan. The negative correlation between pre-rRNA synthesis and lifespan was corroborated by overexpression of the essential and evolutionarily conserved transcription initiation factor IA (TIF-IA). In contrast, TIF-IA depletion impaired rDNA activity and prolonged the survival of worms. Comparing NCL-1 and TIF-IA knockdown (KD) worms revealed striking differences in their fitness at young and old age. Early in life, NCL-1 KD worms were markedly bulkier and excelled in locomotive performance. However, later in life, the neuromuscular and intestinal health of NCL-1 KD worms deteriorated dramatically. Albeit the fitness of TIF-IA KD animals was initially lower, it was preserved far into adulthood, indicating an extended healthspan. Notably, a similar improvement of healthspan was achieved by KD of a Pol I subunit even in older worms, supporting the geroprotective effect of curbing pre-rRNA synthesis.

To understand how TIF-IA KD promotes longevity, metabolic adaptation to moderate pre-rRNA synthesis was investigated. Proteomic analyses showed that ribosomal proteins were depleted already from early adulthood on, corroborating reduced ribosome biogenesis. Moreover, TIF-IA KD repressed the age-dependent accumulation of yolk proteins, revealing another way of alleviating the metabolic burden. Accordingly, old and young TIF-IA depleted worms exhibited a marked increase in ATP levels compared to age-matched control worms. Given the close relationship between energy and lipid metabolism, lipidomics demonstrated

that the profile of membrane and storage lipids was altered towards a longevity signature upon TIF-1A KD.

Taken together, this study has uncovered how moderation of pre-rRNA synthesis concerts metabolic responses that promote healthy aging in *C. elegans*. Based on the structural and functional conservation of the Pol I machinery, these insights are likely translatable to mammalian aging, rendering Pol I a prime candidate for novel aging interventions.

## ZUSAMMENFASSUNG

Alterung gilt als unausweichlich, dennoch ist die Geschwindigkeit des Alterns beeinflussbar. Langlebigkeit wird durch einen energiesparenden, katabolischen Stoffwechsel gefördert, während anabolische Vorgänge wie Ribosomenbiogenese und Proteinsynthese mit beschleunigter Alterung in Verbindung stehen. Beide Prozesse sind von der Transkription der rRNA-Gene (rDNA) durch die RNA Polymerase I (Pol I) abhängig. Die dabei erfolgende Synthese der prä-ribosomalen RNA (prä-rRNA) macht einen Großteil der zellulären Transkriptionsaktivität aus. Obwohl Pol I die Biosynthese wichtiger Makromoleküle steuert, wird ihre Rolle bei der Alterung bisher wenig verstanden.

Um den Einfluss des Pol I-Transkriptionsapparats auf die Lebens- und Gesundheitsspanne zu untersuchen, wurde seine Aktivität in dem Fadenwurm *Caenorhabditis elegans* manipuliert. Zuerst wurde NCL-1, ein zentraler Repressor der Ribosomenbiogenese, durch RNA-Interferenz (RNAi) depletiert, was zu einer Erhöhung der prä-rRNA-Synthese bei gleichzeitiger Verringerung der Lebensspanne führte. Diese negative Korrelation wurde durch Überexpression des essentiellen und evolutionär konservierten Transkriptionsinitiationsfaktors IA (TIF-IA) bestätigt. Es wurde wieder eine verstärkte prä-rRNA-Synthese und eine verkürzte Lebensdauer festgestellt, während RNAi gegen TIF-IA den gegenteiligen Effekt erzielte. Ein Vergleich von Fadenwürmern, die mit RNAi entweder gegen TIF-IA oder NCL-1 behandelt wurden, ergab klare Fitnessunterschiede im frühen und fortgeschrittenen Alter. In jungen Würmern führte die Depletion von NCL-1 zu einem deutlich massiveren Körperbau sowie zu einer effizienteren Fortbewegung. Hingegen nahmen in alten NCL-1-defizienten Tieren die neuromuskuläre Kapazität sowie die Darmintegrität dramatisch ab. Obwohl diese Fitnessparameter durch die TIF-IA RNAi im frühen Alter leicht reduziert waren, nahmen sie mit der Zeit kaum ab, sodass diese Würmer im Alter die beste Gesundheit aufwiesen. Diese Verlängerung der Gesundheitsspanne konnte auch nach Depletion einer Pol I-Untereinheit beobachtet werden, sogar wenn die RNAi-Behandlung erst in älteren Würmern begonnen wurde. Diese Ergebnisse legen eine Verzögerung des Alterns durch verminderte prä-rRNA-Synthese nahe.

Um genauer aufzuklären, wie TIF-IA RNAi die Langlebigkeit fördert, wurde die Anpassung des Metabolismus untersucht. Proteom-Analysen zeigten, dass mit der reduzierten prä-rRNA-Synthese eine Verminderung der ribosomalen Proteine einherging. Somit war bereits in jungen Würmern eine allgemeine Hemmung der Ribosomenbiogenese zu beobachten. Daneben war in TIF-IA-defizienten Tieren die metabolische Belastung, die durch die aberrante Anreicherung von Dotter-Proteinen im Alter auftritt, verringert. Entsprechend führte die TIF-IA RNAi in jungen und alten Würmern zu deutlich höheren ATP-Spiegeln im Vergleich zu gleichaltrigen Würmern der Kontrollgruppe. Aufgrund der starken Vernetzung von Energie- und Fettstoffwechsel wurden weiterhin Lipidomik-Studien durchgeführt. Hierbei stellte sich heraus, dass sich durch TIF-IA-Depletion bei den Membran- und Speicherlipiden eine für Langlebigkeit charakteristische Zusammensetzung einstellte.

Zusammenfassend zeigt diese Studie, dass die Verminderung der prä-rRNA-Synthese eine Umstrukturierung des Metabolismus bewirkt, wodurch die gesunde Alterung von *Caenorhabditis elegans* gefördert wird. Ausgehend von der strukturellen und funktionellen Konservierung des Pol I Transkriptionsapparats ist es wahrscheinlich, dass diese Erkenntnisse auch auf das Altern in Säugern übertragbar sind. Damit ist Pol I ein ideales Ziel für neue Ansätze, um dem Alterungsprozess entgegenzuwirken.

# 1 INTRODUCTION

## 1.1 Aging

### 1.1.1 Aging definition

Aging can be simply defined as a time-dependent accumulation of damage and deterioration of cellular processes resulting in reduced viability and increased vulnerability—consequently, physiological functions of organs decline [1]. The evolution of aging can be explained with the antagonistic pleiotropy theory first described by G.C. Williams in 1957 [2]. Briefly, organisms in natural conditions will most likely die of extrinsic hazards such as predation, disease, or starvation rather than aging. Therefore, dealing with these hazards has higher selective pressure than the reduction of life force over time. This selection can lead to genes that provide an advantage early on but a disadvantage later on (antagonistic pleiotropy). This includes anabolic processes that stimulate growth and reproduction, but in return, promote aging, such as protein synthesis [3]. Thus, aging is a side effect of other evolutionary changes required for the species' survival.

The functional decline with age affects most organs, e.g., a decrease in muscle mass results in lower strength and speed output [4, 5]. Additionally, aging is accompanied by chronic low-grade systemic inflammation in the absence of infections, so-called immunoaging [6]. Moreover, the gut and its microbiota are involved in immunoaging, as intestinal homeostasis plays a crucial part in regulating the immune system [7-9]. Interestingly, lifespan in *Drosophila melanogaster* (*D. melanogaster*) is directly linked to intestinal barrier function [10].

In addition, aging-associated functional decline can develop into chronic diseases. Currently, several age-related diseases are among the deadliest globally [11]. Therefore, prevention of aging could decrease global mortality rates, pinpointing the importance of understanding aging.



### 1.1.2 Dietary restriction signaling pathways

In order to slow down aging, interventions for aging-modulated pathways have to be developed. Lifespan and healthspan can be extended either with a pharmacological or nutritional approach. One of the most well-studied anti-aging interventions is dietary restriction (DR), which is achieved by reducing calorie intake or restricting certain amino acids, such as methionine, without malnutrition [12]. DR effectively extends lifespan in a broad range of model organisms, from yeast to rhesus monkeys [13, 14]. DR-mediated longevity is achieved mainly through the conserved nutrient-sensing pathways, including the mechanistic target of rapamycin (mTOR) and insulin & insulin-like growth factor 1 (IGF-1) signaling (IIS), 5' AMP-activated protein kinase (AMPK), and sirtuin 1 (SIRT1) pathways.

The IIS pathway is a hormonally regulated signaling pathway, with phosphatidylinositol 3-kinase (PI3K) being its key signal transducer. The inhibition of IIS extends lifespan in worms, flies, and mice [15-17]. Furthermore, PI3K positively regulates the mTOR pathway [18]. mTOR is a central nutrient-sensing protein and regulates a wide range of cellular processes, including promoting mRNA translation initiation, inhibiting autophagy core machinery, positively regulating genes involved in anabolic processes, and inhibiting autophagy genes [19-22]. It responds mainly to amino acid availability but also indirectly senses cellular levels of oxygen and ATP [23]. Both genetic and pharmacological inhibition of mTOR leads to lifespan extension [24, 25].

AMPK is a cellular energy sensor activated by adenosine diphosphate (ADP) or adenosine monophosphate (AMP), which can be inhibited competitively by adenosine triphosphate (ATP) [26]. Thus, AMPK activation requires low total cellular energy [27]. DR changes the cell's energy level, increasing AMP/ATP ratio, and the ratio between oxidized and reduced nicotinamide adenine dinucleotide ( $\text{NAD}^+/\text{NADH}$ ). Hence, DR activates AMPK, and AMPK itself has been shown to mediate longevity [28]. In addition, AMPK also alters the  $\text{NAD}^+/\text{NADH}$  ratio, promoting  $\text{NAD}^+$ -dependent enzymes such as SIRT1 [29].

SIRT1 is an  $\text{NAD}^+$ -dependent deacetylase that has been associated with increased genome stability [30]. The yeast homolog Sir2 plays an important role in the stability of ribosomal RNA genes, which has been linked to the longevity of yeast (explained in section

1.3.3) [31, 32]. Interestingly, SIRT1 inhibits mTOR and activates AMPK [33-35]. Furthermore, SIRT1 activates the mitochondrial biogenesis master regulator 'peroxisome proliferator-activated receptor gamma coactivator 1-alpha' (PGC-1 $\alpha$ ), which promotes longevity in *D. melanogaster* [36, 37]. SIRT1 is positively correlated with longevity and has been targeted for aging interventions [38-40].

Additionally, inhibition of mTOR and the IIS pathway curb mRNA translation initiation, which is partially responsible for the pro-longevity effect [41]. Attenuation of translation has been shown to decrease proteolytic stress [42, 43]. Protein homeostasis (proteostasis) is compromised upon aging, and loss of proteostasis has been characterized as one of the hallmarks of aging [1]. Impairment of proteostasis eventually leads to the accumulation of cytotoxic protein aggregates, which cannot be resolved by the protein surveillance machinery [44-47]. Translation attenuation can alleviate the overwhelming burden of the aged proteostatic system, consequently reducing proteotoxicity.

## 1.2 *Caenorhabditis elegans* as a model in aging research

### 1.2.1 *Caenorhabditis elegans* anatomy and development

The nematode *Caenorhabditis elegans* (*C. elegans*) has its natural habitats in soil, rotten fruits, and vegetables and uses bacteria as its primary food source [48]. *C. elegans* has two natural sexes; the majority is hermaphrodite, with only a small fraction being male ( $\leq 0.02\%$ ) [49]. The roundworms have a relatively simple anatomy with a small number of tissues and a fixed somatic cell number of 959 and 1033 for hermaphrodites and males, respectively. After development, the somatic cells are in a post-mitotic state. The head consists of an excretory system, the feeding organ (the pharynx), and a collection of neurons forming the 'brain'. The body comprises the intestine and gonads. Body wall muscles are arranged in four rows, two on the ventral and two on the dorsal side. The whole body is enveloped into a sturdy collagenous cuticle [50].

The nematodes undergo four larval stages, L1-L4, before reaching adulthood. The development from L1 to L4 stage takes around two days, depending on the temperature, and can be arrested at two distinct time points. After hatching, the L1 worms will start their post-

embryonic development only in the presence of food; however, in the absence of food, they will remain arrested and can survive approximately a week. The second decision point is at the L1-L2 molt. Under adverse conditions, the larvae will enter the more resilient dauer stage. This arrested state does not affect the lifespan of a post-dauer adult. After exiting dauer, the worm develops into L4 larvae, carrying fully developed gonads. Finally, the L4 worm develops into an adult and is considered fully matured when (self-)fertility is reached (**Figure 1**). Adult worms lay eggs for approximately three to six days, depending on the temperature, and live around three weeks [51, 52].

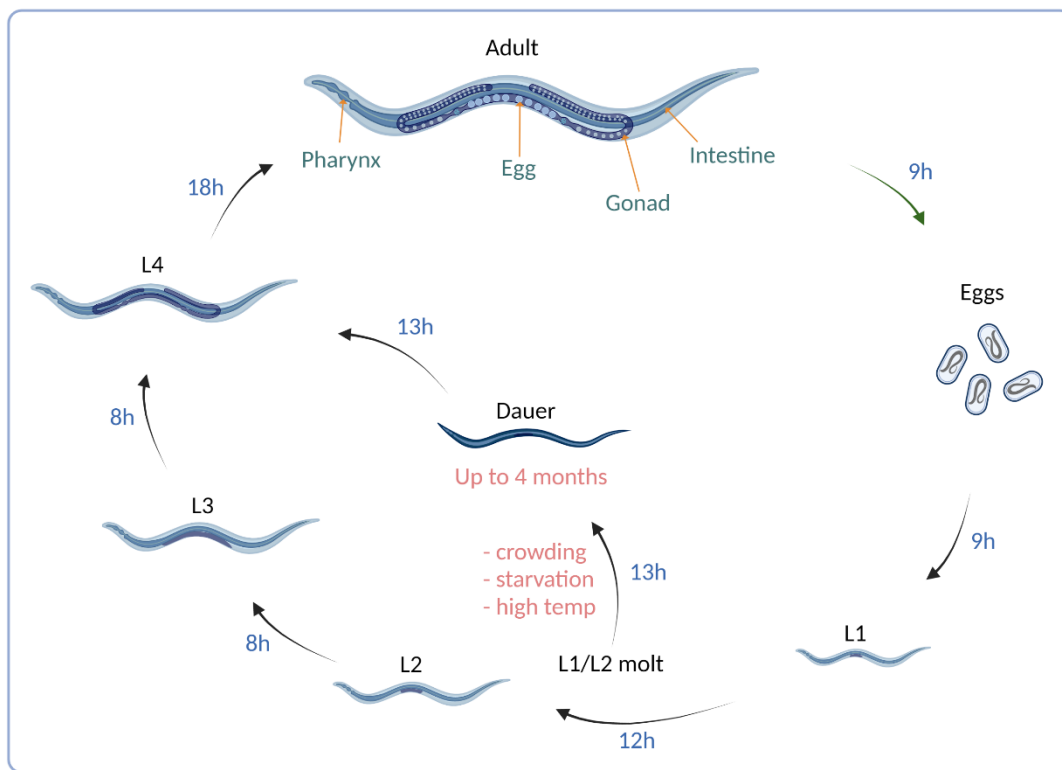


**Figure 1: Schematic illustration of the *C. elegans* life cycle.**

After hatching, nematodes go through four larval stages (L1-L4) to develop into adults. In the presence of environmental stressors during the L1/L2 transition, the worms switch to a diapause stage termed dauer. After reaching adulthood, a hermaphrodite is capable of laying eggs within 9 hours. Development times are based on 22 °C.

### 1.2.2 *Caenorhabditis elegans* in aging research

*C. elegans* requires relatively low maintenance and has a short lifespan [52]. Reproduction occurs mainly via self-fertilization (99.9%), creating genetically identical offspring [53]. The worms are also amenable to genetic manipulation, especially by RNA interference (RNAi), which is optimal for studying gene function. Besides, for 83% of *C. elegans* proteins, human homologs have been predicted [54]. All these features make *C. elegans* a versatile model organism that has been extensively used in aging research.

In fact, the first long-lived mutant was found in *C. elegans*, harboring a disruption of the *age-1* gene (ageing alteration 1) [55]. *age-1* was later found to encode the catalytic subunit of PI3K, which belongs to the IIS pathway [56]. Interestingly, a mutation in the *C. elegans* ortholog of the IGF-1 receptor, *daf-2* (abnormal dauer formation 2), prolonged lifespan by two-fold, representing the biggest gain in lifespan owing to a single gene mutation in *C. elegans* [15]. The longevity of *daf-2* and *age-1* mutants depend on DAF-16 (abnormal dauer formation 16), a protein belonging to the family of FOXO (forkhead box O) transcription factors that are conserved in metazoans [15, 57].

*daf-2* mutation extends lifespan partially through reducing expression of the vitellogenins VIT-2 and VIT-5 [58]. Vitellogenins are yolk proteins and function as nutrient and fat transporters from the intestine to the germline. Worms load yolk into oocytes throughout their reproductive phase, ending around adulthood day 6 (AD6). Due to inappropriate programming of the yolk protein-encoding genes, after the reproductive phase, the yolk accumulates. This accumulation continues during aging and rises to pathological levels. The accumulated vitellogenins can form proteotoxic aggregates in the cell [47]. Moreover, high yolk results in ectopic fat disposition and eventually in lipotoxicity [59, 60]. Thus, yolk accumulation can cause lipotoxic and proteotoxic stress, which *daf-2* mutation may prevent.

Besides yolk, other lipids have also been shown to play a role in aging. Lipids play an essential role in signal transduction, the structure of cellular membranes, and energy metabolism [61]. Lipid composition is linked to longevity, including high ratios of short- versus long-chain fatty acid (SCFA:LCFA) and high monounsaturated fatty acid versus polyunsaturated fatty acids ratio (MUFA:PUFA) [62]. MUFAs are more resistant to lipid peroxidation than

PUFAs, and therefore, higher MUFA rates protect the membrane from peroxidative damage [63]. However, higher MUFA rates decrease membrane fluidity, which can be compensated by decreasing the fatty acid chain length. Changes in fatty acid chain lengths in *C. elegans* longevity strains are expected to play a role in membrane fluidity [62]. Furthermore, triacylglycerides (TAGs) are the main storage lipids that serve as the primary energy reserve in *C. elegans*, and their level is increased in *daf-2* mutant worms. Additionally, supplementation of various lipids to *C. elegans* extended lifespan [64-73], underscoring the importance of lipids and lipid metabolism in aging and longevity.

In worms, lifespan extension by DR was shown for the first time in 1977 [74], and since then, 20 different methods have been developed to induce or mimic the DR state (reviewed in [75]). One widely used DR method is by using worms harboring a mutation in *eat-2* (eating abnormal 2). This mutation causes deficiency in pharyngeal pumping and thereby limits the intake of bacteria, and *eat-2* mutants live approximately 1.4-fold longer than wild-type worms [76, 77]. *eat-2* mutant worms exhibit reduced activity of LET-363 (lethal 363, ortholog of mTOR) and thereby activate lipophagy, which contributes to longevity [59, 78]. Additionally, the *eat-2* mutation restricts protein synthesis, and inhibition of mRNA translation *per se* has been shown to extend lifespan in *C. elegans* [41, 79, 80]. Interestingly, *eat-2* mutant worms as well as several other long-lived mutants, including *daf-2*, have a common cellular feature, namely small nucleoli [81]. These non-membrane-bound organelles in the nucleus are the sites of ribosome biogenesis and their size and activity are tightly linked [82]. The fact that nucleolar size anti-correlates with longevity implies that ribosome biogenesis restricts lifespan.

## 1.3 Ribosomal RNA synthesis

### 1.3.1 Ribosome biogenesis

Nucleoli are formed around nucleolar organizing regions (NORs), originally identified by Barbara McClintock in maize [83]. NORs comprise the ribosomal RNA (rRNA) genes organized in multiple clusters in a head-to-tail orientation. Each gene body is around 13-15 kb in mammals and is separated by an intergenic spacer (IGS) of approximately 30 kb [84]. The rRNA genes (rDNA) are transcribed by RNA polymerase I (Pol I) into pre-rRNA (**Figure 2**), which is processed into the three largest rRNAs, 18S, 5.8S, and 25S-28S rRNA.

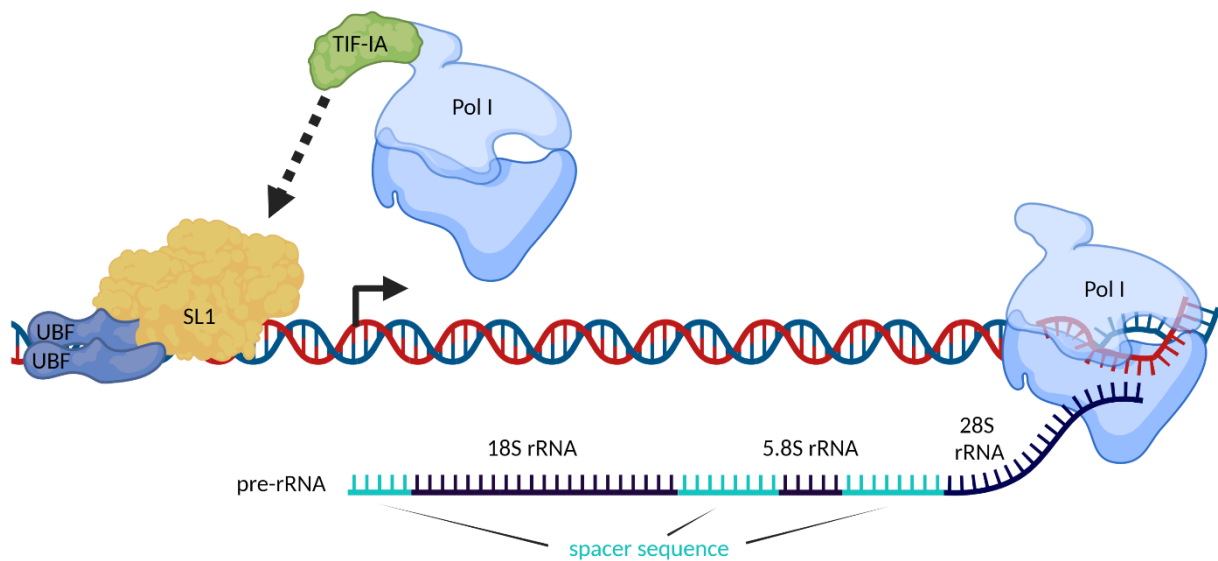


**Figure 2: Formation of the pre-initiation complex and pre-rRNA synthesis.**

After SL1 and a UBF dimer have bound to the promoter, TIF-IA recruits RNA polymerase I (Pol I) to the pre-initiation complex by interacting with SL1. Pol I transcribes the rRNA gene into a precursor transcript (pre-rRNA), which includes the 18S, 5.8S, and (in mammals) 28S ribosomal RNAs (rRNAs), separated by spacer sequences. The figure is not drawn to scale. [UBF = upstream binding factor, SL1 = selectivity factor 1, TIF-IA = transcription initiation factor IA]

Positioning of Pol I at the rDNA promoter depends on pre-initiation complex (PIC) formation. First, the upstream binding factor (UBF) and selectivity factor 1 (SL1) bind cooperatively to the promoter [85]. Pol I is guided by the transcription initiation factor IA (TIF-IA) to the UBF/SL1 complex, where TIF-IA interacts with SL1 [86, 87]. TIF-IA is conserved from yeast to mammals [88, 89]. The interaction between TIF-IA and SL1 is essential for Pol I recruitment to the rDNA promoter [86, 87], making TIF-IA an excellent target for many signaling pathways to regulate the initiation of rRNA synthesis.

Ribosome biogenesis can be divided into several steps: synthesis, processing, modification, and folding of the pre-rRNA, synthesis of the 5S rRNA and ribosomal proteins (RPs), and assembly of the (pre-)ribosomal particles [90]. Both 40S and 60S pre-ribosomal particles are generated in the nucleolus and nucleoplasm. Eventually, they are exported to the cytoplasm, where the final maturation into translation-competent 80S ribosomes occurs [90, 91].

Ribosome biogenesis requires all three eukaryotic RNA polymerases, Pol I synthesizing pre-rRNA, Pol III transcribing the 5S rRNA genes, and Pol II generating the mRNAs of RPs. rRNA accounts for approximately 80% of the total cellular RNA, representing the major transcriptional output of cells. Ribosome biogenesis involves over 200 accessory factors, many of them being energy-consuming enzymes, including kinases, ATPases, GTPases, RNA helicases, and RNases [92-95]. Since the production of ribosomes is a highly energy-demanding process, it has to be properly controlled to avoid unnecessary energy expenditure. Being the initial step of ribosome biogenesis, pre-rRNA synthesis is tightly regulated according to cell growth, nutrient and energy availability, and stress [96].

### 1.3.2 Ribosomal RNA synthesis in *Caenorhabditis elegans*

The rRNA genes have been mapped in *C. elegans*. There are around 55 rRNA gene tandem repeats on chromosome I [97]. One repeat is 7.2 kb long and encodes a pre-rRNA harboring 18S (*rrn-1.1*), 5.8S (*rrn-2.1*), and 26S (*rrn-3.1*) rRNAs, that are each separated by spacer sequences [98]. In contrast to yeast and mammals, the regulation of rRNA gene transcription in *C. elegans* is not well studied. In worms, the Pol I (*rpoa* gene class) and

the Pol I/III shared subunits (*rpac* gene class) have been identified. Regarding the Pol I initiation factors, the TIF-IA ortholog (C36E8.1) and orthologs (TBP-1, Tag-51, and F23H11.2) of three human SL1 subunits (TBP, TAF1A, and TAF1B, respectively) are currently known in *C. elegans* [99-103]. Concerning UBF, it has been anticipated that orthologs exist in many animal phyla, and a closely related *C. elegans* protein, HMG-5, has been identified [104].

In *C. elegans*, the synthesis of rRNA is also controlled by a master regulator of ribosome biogenesis, which is a protein termed 'abnormal nucleoli 1' (NCL-1). NCL-1 is structurally and functionally closely related to the protein 'brain tumor' (Brat) in *D. melanogaster* [105], whereas the closest relatives in mammals, 'tripartite motif-containing 2 and 3' (TRIM2/3), have lost their nucleolar function [106]. NCL-1 negatively regulates pre-rRNA processing through inhibition of the rRNA processing factor fibrillarin (FIB-1). Moreover, NCL-1 also regulates Pol III transcription, as the accumulation of rRNA, including 5S rRNA, has been observed in oocytes of *ncl-1* mutant worms [107]. Furthermore, *ncl-1* mutants have been shown to have increased nucleolar size and elevated ribosome and protein biosynthesis [81, 107, 108], indicating that pre-rRNA synthesis is also increased. However, whether NCL-1 has a direct impact on Pol I transcriptional activity is not known.

### 1.3.3 Link between ribosomal RNA genes and aging

Since rDNA has a repetitive nature, it is prone to structural rearrangements by homologous recombination [109]. In yeast, it was shown that homologous recombination could result in looping out of the rRNA genes, giving rise to extrachromosomal rDNA circles (ERCs) [110]. Moreover, rDNA stability in yeast has been linked directly to lifespan. Both rDNA instability and ERCs accelerate with age, however, via two distinct mechanisms. rDNA instability lengthens the cell cycle via unknown signals, which will eventually result in senescence, i.e., a non-reversible post-mitotic state [111, 112]. ERCs, on the other hand, will sequester transcription factors from the chromosomal rDNA and will be aberrantly transcribed [113]. Intriguingly, ERCs that had been introduced into young yeast cells shortened lifespan [110]. In line with these findings, in *D. melanogaster*, heterochromatin formation led to more stable rDNA and less ERC formation, which was linked to longevity [114]. Extrachromosomal



circular elements, including to a small extent also ERCs, were recently discovered in humans and *C. elegans* [115, 116]; however, whether they play a role in the aging of animals remains unknown.

Partial ablation of Pol III has been shown to extend lifespan in fruit flies, indicating that reduced synthesis of 5S rRNA and tRNA feeds into a longevity-promoting metabolism [117]. Accordingly, inhibition of protein synthesis was observed, which phenocopied impaired mTOR activity. These findings are reminiscent of the mutation or knockdown of NCL-1 in *C. elegans*, which increases ribosome biogenesis as well as mRNA translation, and shortens lifespan [81, 107].

In line with these observations, it was recently found that partial inhibition of Pol I in *D. melanogaster* extends lifespan [118]. The study concluded that Pol I and Pol III act in the same longevity pathway, i.e., perturbation of either RNA polymerases mimics mTOR inhibition by reducing protein synthesis. In fact, curbing mRNA translation is a well-known intervention to prolong lifespan [41, 79, 80]. Nonetheless, interfering with ribosome biogenesis at the level of Pol I transcription, i.e., at the top of the synthesis hierarchy, is likely to trigger further pro-longevity mechanisms. For instance, curbing the high rDNA transcriptional activity will not only *per se* free cellular energy but will also significantly reduce the energetic costs caused by pre-rRNA processing and assembly of ribosomal particles [92-95].

Given that the nucleolus has been recognized as an important sensor of cellular insults, whose stress signaling is majorly induced by shut-down of rDNA activity [119], a moderate transcriptional inhibition might also lead to a hormetic response triggering metabolic adaptations that in turn increase longevity [120]. Thus, it is likely that depending at which level ribosome biogenesis and protein production are manipulated, different physiological responses are induced. Deciphering these differences is required to understand the role of this anabolic axis in aging thoroughly.

## 2 AIM OF THIS STUDY

The nucleolus is the site of Pol I-driven rRNA gene transcription and subsequent ribosome biogenesis, thus dictating the cell's capacity for protein synthesis. Owing to this pivotal role in cellular metabolism, nucleolar activity and structure are tightly regulated. Growth factor, nutrient, and energy-sensing pathways that primarily impinge on the Pol I machinery also strongly impact lifespan and healthspan. Accordingly, a recent study in the nematode *C. elegans* has shown that depletion of NCL-1, a general repressor of ribosome biogenesis, increases nucleolar size but shortens lifespan [81]. This observation raises the following questions:

- Does the pro-longevity function of NCL-1 also include repression of Pol I transcription?
- Can direct interference with Pol I transcription prolong lifespan? Moreover, if so, at which stage in life can it be applied to be beneficial?
- How does modulation of pre-rRNA synthesis affect organismal health?
- Which metabolic adaptations are triggered by pre-rRNA manipulations?

To answer these questions, Pol I gain- and loss-of-function studies in *C. elegans* will be performed. The presumed upregulation of pre-rRNA synthesis upon RNAi-mediated knockdown of NCL-1 will be tested, and the reported reduction of lifespan will be re-evaluated. To connect aberrant rDNA activity directly to accelerated aging, the essential Pol I transcription factor TIF-IA will be overexpressed, and lifespan will be assessed. On the other hand, interference with Pol I transcription will be achieved by knocking down TIF-IA, and, again, lifetime will be measured. Alternatively, a subunit of Pol I will be targeted by RNAi to corroborate the data from the TIF-IA knockdown. Tests will be performed to estimate at which stage of the *C. elegans* life cycle the perturbations can be most efficiently implemented to modulate longevity. Furthermore, knockdown of TIF-IA and NCL-1 will be contrasted in terms of growth, neuromuscular performance, and intestinal integrity of worms. Assaying these fitness parameters early and late in life will reveal the healthspan of *C. elegans* in response to either diminished or elevated rDNA activity.

Pol I transcription ultimately governs the cell's protein production capacity. Thus, it is conceivable that the TIF-IA knockdown affects longevity indirectly by inhibiting protein

synthesis, a bona fide anti-aging intervention [121]. To dissect this interplay, lifespan assays will be conducted after combining TIF-IA RNAi with genetic or pharmacological perturbation of mRNA translation. Furthermore, the impact of TIF-IA knockdown on the *C. elegans* proteome will be monitored by mass spectrometry, comparing protein profiles of young, middle-aged, and old animals treated with either control or TIF-IA RNAi. Likewise, lipidomics will be applied to understand how the lipid metabolism is adapted to attenuated Pol I transcription.

Given that pre-rRNA synthesis by itself is energetically costly and presides over major anabolic tasks, its mitigation is likely to counteract the decline of the cellular energy pool with age [122]. Therefore, changes in ATP levels during aging will be compared between control, TIF-IA-depleted, and translation-inhibited worms. These experiments will show how curbing synthesis of either pre-rRNA or proteins differs with regard to the conservation of cellular energy. Taken together, this study aims to elucidate the role of Pol I transcription in longevity and to unravel the different molecular mechanisms behind it.

### 3 MATERIALS

#### 3.1 Primers

Primers were designed using primer blast of NCBI. Primers were synthesized by Integrated DNA Technologies, Inc. or Metabion International AG.

**Table 1: List of primers for reverse transcription-quantitative polymerase chain reaction**

TARGET (GENE)	SEQUENCE	
	FORWARD PRIMER	REVERSE PRIMER
C36E8.1 (TIF-1A)	TGGAAATGCGAGCAAAACGA	CCGTGCACACTGAGTCCAAA
ncl-1	GCCGACGATTGAGCAACAAC	AGTGAAGTCTGGAACGGAG
pre-rRNA (1)	TGGCTTCACGGTCAGTTGAG	CATGGGTCTGGACAGTCACTAC
pre-rRNA (2)	AACCGCTATGTGTCTCCTGG	ATCACCGCATGTCCGTGAAG
rpoa-2	GCCGATTCCAGGAAGACGAT	CACAATATGCCGGTTCAGCG
<i>tbg-1</i> (Tubulin)	CAATGTGCCCATCAATTCGG	AACAAGAAGCGAGTGACGTC

#### 3.2 Chemicals

**Table 2: List of chemicals, antibodies, enzymes, and commercial kits**

CHEMICAL or SOLUTION	SOURCE	CATALOG NUMBER
2-Propanol	Carl Roth GmbH	7343.1
5X Colorless GoTaq® Flexi Buffer	Promega	M890A
5X Green GoTaq® Flexi Buffer	Promega	M891A
Acetic acid	Carl Roth GmbH	KK62.1
Agar	SERVA	11396.04
Ampicillin sodium salt	Carl Roth GmbH	K029.1
Ammonium peroxydisulfate (APS)	Carl Roth GmbH	9592.1
ATP Bioluminescence Assay Kit HS II	Hoffmann-La Roche	11699695001
Bacto peptone	BD Biosciences	211820
Bacto tryptone	Carl Roth GmbH	8952.2

Brilliant Blue FCF	Merck KGaA	3844-45-9
Bromophenol blue	Carl Roth GmbH	A512.1
Calcium chloride (CaCl <sub>2</sub> ) dehydrate	Merck KGaA	21097
Cholesterol	Merck KGaA	C8503
Cycloheximide (CHX)	Merck KGaA	01810
dATP Solution (100 mM)	Thermo Fisher Scientific Inc.	R0141
dCTP Solution (100 mM)	Thermo Fisher Scientific Inc.	R0151
dGTP Solution (100 mM)	Thermo Fisher Scientific Inc.	R0161
Dimethyl sulfoxide (DMSO)	Merck KGaA	D2438
Dipotassium phosphate (K <sub>2</sub> HPO <sub>4</sub> )	Carl Roth GmbH	T875.2
Disodium phosphate (Na <sub>2</sub> HPO <sub>4</sub> )	Carl Roth GmbH	4984.1
dTTP Solution (100 mM)	Thermo Fisher Scientific Inc.	R0171
Ethanol (EtOH), ≥99.8%, absolute	Carl Roth GmbH	9065.1
EtOH, 99.8%	Carl Roth GmbH	K928.4
Ethidium bromide 10 mg/ml	Thermo Fisher Scientific Inc.	15585011
Ethylenediaminetetraacetic acid (EDTA)	Carl Roth GmbH	8084.1
GeneRuler 1 kb Plus DNA Ladder	Thermo Fisher Scientific Inc.	SM1332
Gentamycin	Merck KGaA	48760
Glycerol	Carl Roth GmbH	3783.1
Glycine	Carl Roth GmbH	3790.2
GlycoBlue™ Coprecipitant	Thermo Fisher Scientific Inc.	AM9515
GoTaq® G2 Flexi DNA Polymerase	Promega	M780A
Isopropyl β-D-1-thiogalactopyranoside (IPTG)	Merck KGaA	I6758
Magnesium sulfate heptahydrate (MgSO <sub>4</sub> · 7H <sub>2</sub> O)	Carl Roth GmbH	P027.2

Maxima SYBR Green/ROX qPCR Master Mix (2X)	Thermo Fisher Scientific Inc.	K0222
Magnesium chloride (MgCl <sub>2</sub> ) solution	Promega	A351B
β-Mercaptoethanol	Carl Roth GmbH	4227.1
Metformin Hydrochloride	Tokyo Chemical Industry	M2009
Methanol	Carl Roth GmbH	4627.5
Monopotassium phosphate (KH <sub>2</sub> PO <sub>4</sub> )	Carl Roth GmbH	3904.1
Monosodium phosphate (NaH <sub>2</sub> PO <sub>4</sub> )	Carl Roth GmbH	K300.2
Mounting Medium with 4',6-diamidino-2-phenylindole (DAPI)	Abcam PLC	ab104139
Nonidet P40 (NP40) / IGEPAL® CA-630	Merck KGaA	I8896
Nystatin	Merck KGaA	N1638
Pluronic® F-127	Merck KGaA	P2443
Poly-L-lysine hydrobromide	Merck KGaA	25988-63-0
Potassium hydroxide (KOH)	Carl Roth GmbH	P747.2
Primer "random"	Merck KGaA	11034731001
Proteinase K	Roche Applied Science	3115879001
RiboLock RNase-Inhibitor (40 U/μl)	Thermo Fisher Scientific Inc.	EO0384
ROTIPHORESE® NF-Acrylamide/Bis solution 30%	Carl Roth GmbH	A124.1
Sodium chloride (NaCl)	Carl Roth GmbH	P029.2
Sodium dodecyl sulfate (SDS)	Carl Roth GmbH	CN30.1
Sodium hypochlorite (NaClO) 10%	Merck KGaA	105614
SuperScript™ IV First-Strand Synthesis System	Thermo Fisher Scientific Inc.	18091200

N,N,N',N'- Tetramethylethylenediamine (TEMED)	Merck KGaA	T9281
Tetracycline	Carl Roth GmbH	0237.1
Tris(hydroxymethyl)aminomethane (Tris)	Carl Roth GmbH	4855.1
anti- $\alpha$ -Tubulin antibody (Clone: DM1A; Species: Mouse)	Merck KGaA	T6199
Tween® 20	Carl Roth GmbH	9127.1
anti-Ty1 antibody (Species: Rabbit)	Purified by Dr. Lisa Lange from BB2 hybridoma cells	Ref: [123]
Whatman™ Gel Blotting Paper Grade GB003	Cytiva	10427804
Yeast extract	Carl Roth GmbH	2363.4

### 3.3 Software

**Table 3: List of used software**

SOFTWARE	SOURCE
BioRender	BioRender.com
FusionCapt Advanced 19.03	Vilber Lourmat GmbH
Prism 8.0.0 (224)	GraphPad Software, Inc.
QuantStudio™ Design & Analysis Software	Thermo Fisher Scientific Inc.
Venny 2.1.0	BioinfoGP
WormCat	Amy K Walker Labs
Zen, ZEN/ZEN-lite, Zen 2.6 blue edition	Carl Zeiss AG

### 3.4 Consumables

Basic laboratory consumables, such as Petri plates, pipette tips, conical centrifuge tubes, and multi-well plates, were purchased from Greiner Bio-One, and reaction tubes (1.5 ml, 2 ml) were used from Sarstedt AG & Co. KG. Plates and adhesive seals for RT-qPCR were purchased from Applied Biosystems. Ceramic beads (zirconium silicate beads, 1.0 mm; Cat. nr. ZSB10) were purchased from Witec AG, and nylon net filters (11  $\mu$ m,  $\varnothing$  47 mm; Cat. nr. NY1104700) were used from Merck KGaA.



## 4 METHODS

### 4.1 Buffers and media

**Table 4: Recipe buffers and media**

<b>BUFFER/SOLUTION</b>	<b>REAGENTS (dissolved in H<sub>2</sub>O)</b>
3x Laemmli buffer	<ul style="list-style-type: none"><li>- 150 mM Tris-HCl</li><li>- 6% SDS</li><li>- 30% Glycerol</li><li>- 0.3% Bromophenol blue</li><li>- 6% <math>\beta</math>-Mercaptoethanol</li></ul>
Lysogeny broth (LB) medium	<ul style="list-style-type: none"><li>- 1% Bacto tryptone</li><li>- 0.5% Yeast extract</li><li>- 0.5% NaCl</li></ul> <p>pH 7.5</p>
LB agar	<ul style="list-style-type: none"><li>- LB medium</li><li>- 1.5% Agar</li></ul>
M9 buffer	<ul style="list-style-type: none"><li>- 22 <math>\mu</math>M KH<sub>2</sub>PO<sub>4</sub></li><li>- 86 <math>\mu</math>M NaCl</li><li>- 42 <math>\mu</math>M Na<sub>2</sub>HPO<sub>4</sub>,</li><li>- 1 mM MgSO<sub>4</sub></li></ul>
Single Worm Lysis Buffer	<ul style="list-style-type: none"><li>- 30 mM Tris</li><li>- 8 mM EDTA</li><li>- 100 mM NaCl</li><li>- 0.7% NP40</li><li>- 0.7% Tween 20</li></ul>

Nematode growth medium (NGM) agar	<ul style="list-style-type: none"> <li>- 51 mM NaCl</li> <li>- 2.5% Bacto peptone</li> <li>- 1.7% Agar</li> <li>- 1 mM MgSO<sub>4</sub></li> <li>- 1 mM CaCl<sub>2</sub></li> <li>- 25 mM KPB</li> <li>- 5 µg/ml Cholesterol</li> <li>- 25 U/ml Nystatin</li> </ul>
NGM – IPTG agar	<ul style="list-style-type: none"> <li>- NGM agar</li> <li>- 200 µg/ml Ampicillin</li> <li>- 1.5 mM IPTG</li> </ul>
SDS-PAGE Running buffer	<ul style="list-style-type: none"> <li>- 25 mM Tris</li> <li>- 192 mM Glycine</li> <li>- 0.1% SDS</li> </ul> <p>pH 8.3</p>
TAE buffer	<ul style="list-style-type: none"> <li>- 40 mM Tris</li> <li>- 20 mM Acetic acid</li> <li>- 1 mM EDTA</li> </ul>
Protein transfer buffer	<ul style="list-style-type: none"> <li>- 25 mM Tris</li> <li>- 192 mM Glycine</li> <li>- 20% Methanol</li> </ul> <p>pH 8.3</p>
Tris-buffered saline with Tween 20 (TBST)	<ul style="list-style-type: none"> <li>- 50 mM Tris-HCl,</li> <li>- 150 mM NaCl</li> <li>- 0.1% Tween 20</li> </ul> <p>pH 7.5</p>

## 4.2 *Caenorhabditis elegans* experiments

### 4.2.1 Strains and maintenance

In this study, the following *C. elegans* strains were used: wild isolate (N2), *ife-2* mutant (KX15), FIB-1::GFP expressing strain (COP262), and TIF-1A overexpressing strain (COP2239). N2 and the *ife-2* mutant strains were purchased from Caenorhabditis Genetics Centre (CGC). The TIF-1A overexpressing strain was generated by InVivo Biosystems using the MosSCI method [124]: knuSi855 [ pNU2297 ( HBIE01 - eft-3p::3xTy1::C36E8.1::tbb-2u in ttTi5605, unc-119(+) ) II ; unc-119(ed3) III.

Worms were maintained and grown on standard nematode growth medium at 20 °C as described in ‘Wormbook’ unless indicated otherwise [125]. The worms were fed with OP50 *Escherichia coli* (*E. coli*), purchased from CGC, or, for RNA interference (RNAi) experiments, with HT115(DE3) *E. coli*. HT115(DE3) strains, harboring an L4440 plasmid derivative producing the double-stranded RNA (dsRNA) of interest, were taken from “Ahringer *C. elegans* RNAi collection” (Source BioScience Ltd.).

### 4.2.2 RNAi bacterial plate preparation

A colony of HT115(DE3) *E. coli* was inoculated in LB medium containing 200 µg/ml ampicillin, and the inoculate was incubated overnight at 37 °C. The next day, fresh LB medium was added (half the volume of the inoculates), and, thereafter, 2 mM IPTG was added to initiate dsRNA synthesis. Samples were incubated for 20 minutes at 37 °C and concentrated at least three times, before seeding on the NGM – IPTG agar plates.

### 4.2.3 Age-synchronization

To age-synchronize worms, bleaching was performed as previously described [126]. Briefly, the worms were washed off the plates with M9 buffer, and gravity settled. When the worms settled, the supernatant was removed, fresh M9 buffer and bleaching solution were added in a 1:1 ratio. The worms were vortexed for 2 minutes, and samples were washed three times with M9 buffer. Thereafter, per 1 ml of M9 buffer, the following antibiotics were added:

1  $\mu$ l of 100 mg/ml ampicillin, 1  $\mu$ l of 20 mg/ml gentamycin, and 0.5  $\mu$ l of 12.5 mg/ml tetracycline. The eggs were left overnight in M9 buffer to hatch. The next day, the synchronized L1 larvae were filtered using 11  $\mu$ m nylon filters to remove worm debris.

#### 4.2.4 RNA interference experiments

For knockdown of NCL-1 and TIF-1A, the worms were fed with bacteria producing the corresponding dsRNA for two generations. First, they were transferred at L4 stage on the dsRNA-producing bacteria and incubated overnight at 20 °C. The next day, bleaching was performed as described in 4.2.3. The L1 worms were seeded and kept for 48 hours at 20 °C. TIF-1A KD worms were seeded 4 hours earlier due to a slight delay in development. After 48 hours, the L4 worms were transferred to 15 °C and kept at this temperature for the rest of the experiment, unless stated otherwise.

To achieve RPOA-2 knockdown, the L4 larvae were transferred on the dsRNA-producing bacteria and kept throughout the experiment at 20 °C, unless indicated otherwise.

#### 4.2.5 Lifespan analysis

The lifespan of age-synchronized worms was measured on NGM (OP50 *E. coli* lawn) plates or NGM-IPTG (HT115(DE3) *E. coli* lawn) plates. The lifespan started when worms reached the L4 stage (adulthood day 0). 140 worms per condition were used, divided into two 6 cm Petri plates (70 worms per plate). Animals were transferred to fresh plates every 1-2 days in the reproductive phase and every 4-5 days in the post-reproductive phase. Worms were scored daily, and dead worms were removed from the pool.

For analysis of drugs on lifespan, the drug was added in the agar. Cycloheximide was added to a final concentration of 1  $\mu$ M, and treatment was started at L4 larval stage. Metformin was added to a final concentration of 50 mM. The worms were transferred at adulthood day 12 on the metformin-containing plates.

#### 4.2.6 Burrowing assay

The burrowing assay was performed as described previously [127]. Briefly, three 12-well plates per condition were used. A drop of 50  $\mu$ l of 26% pluronic F-127 gel (w/w, dissolved in water) was added to the well. After the drop was solidified, 40-45 worms per plate were transferred on top of the gel. Thereafter, 4 ml of the 26% pluronic F-127 gel was added on top and incubated at 20 °C for 5 minutes to solidify the gel. 20  $\mu$ l of concentrated OP50 *E. coli* suspension (100 mg/ml) was added as a chemoattractant on top of the solidified gel to initiate the experiment. The experiment was performed at 20 °C, animals on top were scored over time. The measurement time was 3 hours for young worms and 4 hours for old worms.

#### 4.2.7 Smurf assay

Smurf assay was performed as described elsewhere [128]. Worms were incubated in a 5% Brilliant Blue FCF, OP50 liquid culture for 3 hours at 18 °C. Afterward, worms with a dye-permeable intestine were scored (Smurf), and representative images were made using the ZEISS Axio Zoom.V16.

#### 4.2.8 Nucleolar size measurement

The FIB-1::GFP expressing strain was washed with M9 buffer and was transferred to Poly-L-lysine-coated microscopy slides. The M9 buffer was aspirated. 10  $\mu$ l of Ethanol (EtOH) were added on top, and samples were air-dried; this procedure was repeated twice. Slides were mounted with mounting media containing DAPI. Slides were incubated for 10 minutes in the dark and stored at 4 °C. Images were recorded with the Zeiss Axiovert 200 ApoTome (Carl Zeiss AG). Nuclear (DAPI) and nucleolar (GFP) areas were marked and measured using the ZEISS ZEN Imaging Software. The relative nucleolar size was calculated by normalizing the GFP signal to the DAPI signal.

#### 4.2.9 Worm size determination

Worms on NGM plates were imaged using the ZEISS Axio Zoom.V16. The area of individual animals was manually determined (encircled) and quantified using the ZEISS ZEN Imaging Software.

### 4.3 Molecular biology techniques

#### 4.3.1 Genotyping

##### Genomic DNA isolation

Worms were transferred to Single Worm Lysis Buffer containing proteinase K (100 µg/ml). One worm per 6 µl was used, incubated for 1 hour at 60 °C and 15 minutes at 95 °C.

##### Polymerase chain reaction

For genotyping of the mutants, a polymerase chain reaction (PCR) was performed. High-Performance GoTaq® G2 DNA Polymerase with Mg-Free Buffer System (Promega Corporation) was used for this purpose, however 1 µl of 25 mM MgCl<sub>2</sub> was added to each sample. According to the manufacturer's guidelines, PCR was performed where 3 µl of *C. elegans* genomic DNA was used in a total volume of 15 µl per reaction. Primers were designed to have optimal annealing at 60 °C. The PCR reaction was done for 38 cycles.

##### Gel electrophoresis

Samples were run on a 2% agarose gel in TAE buffer at 120 V for half an hour. A DNA ladder was included in every run. Gels were stained with the DNA-intercalating dye ethidium bromide (10 µg/ml) and imaged using ChemiDoc XRS+ System (Bio-Rad Laboratories, Inc.).

#### 4.3.2 RNA extraction

Worms were transferred to M9 buffer and washed twice with this buffer. The M9 buffer was removed, and TRI reagent was added. Samples were transferred to tubes containing zirconium silicate beads and were bead-beaten using “Precellys 24 tissue homogenizer” (Bertin Instruments) (settings: 6000, 20 seconds on, 30 seconds off, two rounds). 100 µl 1-Bromo-3-chloropropane was added to the samples per 1 ml TRI reagent. To increase the visibility of the pellet after precipitation, 1 µl of glycoblue (15 mg/ml) was added to the samples. Samples were shaken firmly for 1 minute and spun down for 15 minutes at 15,300 RCF at 4 °C. The upper aqueous phase was carefully transferred to a fresh tube, and ice-cold 2-propanol was added in a 1:1 ratio. The samples were kept overnight at -20 °C and spun down afterward at 15,300 RCF at 4 °C for 10 minutes. The supernatant was removed, the pellets were washed with 1 ml of 75% EtOH and then centrifuged for 3 minutes at 15,300 RCF at 4 °C. The supernatant was again removed, and the washing step was repeated. Thereafter, the supernatant was removed entirely, and the samples were left to air dry for 1-3 minutes (depending on the pellet size). The pellet was dissolved in water at 55 °C for 1 minute. The concentration of RNA was measured using the NanoDrop™ 2000c device (Thermo Fisher Scientific Inc.).

#### 4.3.3 cDNA synthesis

Following the manufacturer’s protocol, 1 µg of RNA was treated with DNase I (Merck KGaA), in the presence of 0.25 µl RNase inhibitor (Ribolock, Thermo Fisher Scientific Inc.) for 20 minutes. Half of the sample was used for the cDNA synthesis with SuperScript IV® Reverse Transcriptase (Thermo Fisher Scientific Inc.). Reactions (10 µl) were performed as recommended by the manufacturer, using random hexamers for cDNA priming.

#### 4.3.4 Reverse transcription and quantitative polymerase chain reaction

The reverse transcription-quantitative polymerase chain reactions (RT-qPCRs) were performed using Maxima™ SYBR™ Green/ROX 2X qPCR Master Mix (Thermo Fisher Scientific Inc.) and MircroAmp™ Fast Optical 96-well reaction plates (Applied Biosystems) on a

QuantStudio 3 PCR system (Thermo Fisher Scientific Inc.). A two-step cycling protocol was carried out with 60 °C for annealing and elongation and 40 cycles. The cDNA was diluted before pipetting it in the well. The dilution depended on the amplicon: 1:10 for mRNA amplicons, 1:100 for pre-rRNA amplicons. Technical triplets were used per sample, and per amplicon, a negative control, and a standard curve were included. Data were analyzed using the relative standard curve method. Tubulin mRNA levels were used for normalization.

#### 4.3.5 ATP measurement

Worms were transferred to M9 buffer and washed twice with M9 buffer. Samples were snap-frozen and boiled for 10 minutes, sonicated using Bioruptor® Plus sonication device (Diagenode) (10 cycles, 1 minute on, 30 seconds off) and spun down for 10 minutes at 15,300 RCF at 4 °C. Supernatants containing the worm lysate were transferred to new tubes. ATP measurement was carried out using “ATP Bioluminescence Assay Kit HS II” (Roche). Samples were prepared according to the user guide; samples were diluted 1:5 with the dilution buffer of the kit. Measurement was performed in technical triplicates using the Mithras LB 940 microplate reader (Berthold). For normalization, the protein concentration of the undiluted samples was used. Protein concentration was measured using NanoDrop™ 2000c (Thermo Fisher Scientific Inc.).

#### 4.3.6 Western blot analysis

##### Gel electrophoresis and blotting

Frozen pellets of worms were boiled for 5 minutes at 95 °C and sonicated using Bioruptor® Plus sonication device (Diagenode) for 10 cycles (1 minute on, 30 seconds off). The lysates were spun down for 10 minutes at 15,300 RCF at 4 °C. The supernatant containing the total protein was transferred to a new tube. Protein levels of lysates were measured with the NanoDrop™ 2000c (Thermo Fisher Scientific Inc.). Samples (30-50 µg) were mixed with 3x Laemmli buffer to a final 1X concentration and boiled for 5 minutes at 95 °C. Proteins were separated by polyacrylamide gel electrophoresis (PAGE). Samples were run for approximately 1.5 hours on a 10% polyacrylamide/bisacrylamide separating gel, with a 5% stacking gel at



100 V. Proteins were transferred to a nitrocellulose membrane; gel and membrane were placed between Whatman papers and soaked in transfer buffer. Blotting was done with the Trans-Blot® Turbo™ Transfer System (Bio-Rad Laboratories, Inc.), using the standard program for the mini-gel.

### Protein detection

To block non-specific binding of antibodies to the membranes, they were incubated with TBST containing 5% fat-free dry milk (Salites) for 1 hour at RT. Thereafter, another incubation step was performed with the primary antibody in 5% fat-free dry milk in TBST (1:5000), samples were kept overnight at 4 °C. The day after, the membranes were washed three times with TBST for 10 minutes and incubated with the corresponding horseradish peroxidase (HRP)-conjugated secondary antibody in 5% fat-free dry milk in TBST for 1 hour at RT. Afterward, membranes were rewashed three times with TBST for 10 minutes. ECL Western Blotting Substrates were used for protein visualization on the Fusion Solo 4S system (Vilber Lourmat), with the software FusionCapt Advanced 17.03 software (Vilber Lourmat). Detection of proteins was executed step-wise, using primary antibodies of different host species on the same membrane.

## 4.4 Lipidomics and proteomics

### 4.4.1 Lipidomics

Plates containing around 700 age-synchronized worms were transferred to M9 buffer, washed three times with M9 buffer, pelletized, and snap-frozen in liquid nitrogen. Thereafter, samples were boiled for 5 minutes at 95 °C and sonicated using Bioruptor® Plus sonication device (Diagenode) (10 cycles, 1 minute on, 30 seconds off). Samples were stored at -80 °C. Lipid extraction and analysis using tandem mass spectrometry were done by the groups of Prof. Dr. Werz and PD Dr. Koeberle at the department of Pharmacy, Friedrich Schiller University of Jena.

#### 4.4.2 Proteomics

Plates containing around 700 age-synchronized worms were transferred to M9 buffer, washed three times with M9 buffer, pelletized and snap-frozen in liquid nitrogen, and stored at -80 °C. Protein extraction and tandem mass spectrometry were performed by the proteomics core facility of the Fritz Lipmann Institute (FLI) Jena, who also performed the initial analysis. A more in-depth analysis of the data was done in collaboration with Prerna Chaudhari from the Ermolaeva group at the FLI.

#### 4.5 Statistical analysis

Statistical analysis was performed with Prism 8 (Graphpad Software Inc.) unless mentioned otherwise. For statistics, significance was determined at  $P < 0.05$ . The appropriate statistical test was chosen for each experiment as indicated in the figure legends.

## 5 RESULTS

### 5.1 rRNA gene activity hinders longevity

#### 5.1.1 Increased RNA polymerase I transcriptional activity is detrimental for lifespan

Small nucleoli have been shown to be a marker for longevity; in addition, impairment of NCL-1, a repressor of ribosome biogenesis, increases nucleolar size [81]. NCL-1 negatively regulates rRNA processing by repressing FIB-1, but whether NCL-1 alters the nucleolar size through Pol I regulation is unknown [107, 108]. To determine if NCL-1 directly impacts pre-rRNA synthesis, *C. elegans* was fed bacteria containing dsRNA against NCL-1. First, expression analysis was performed by RT-qPCR, comparing NCL-1 RNAi treated animals with worms that had ingested bacteria producing non-targeting dsRNA (control). Notably, an effective knockdown of NCL-1 mRNA levels to 40% required rearing worms at 15 °C for two generations on dsRNA-producing bacteria (**Figure 3A**).

To gauge Pol I transcriptional activity, the spacer sequence between the 18S and 5.8S rRNA sequences of pre-rRNA was monitored using RT-qPCR. Owing to the rapid processing of pre-rRNA, the spacer sequences are promptly removed and degraded [129]. Therefore, pre-rRNA levels serve as a proxy for rDNA activity. Treating worms with NCL-1 RNAi increased pre-rRNA levels by 2-fold (**Figure 3B**). This observation, together with the fact that pre-rRNA processing is rather enhanced by elevated FIB-1 levels upon NCL-1 knockdown (KD), supports the notion that NCL-1 directly represses Pol I activity [107].

To assess how this increase in pre-rRNA levels affects longevity, the survival of a synchronized worm population was scored daily throughout adulthood. This Lifespan analysis showed a significant increase in mortality in NCL-1 knockdown worms, with a median lifespan of 19 adulthood days (AD19), compared to control worms, with a median lifespan of AD25 (**Figure 3C**). Thus, it is conceivable that the shortened lifespan of NCL-1-depleted worms is partly caused by elevated pre-rRNA synthesis.

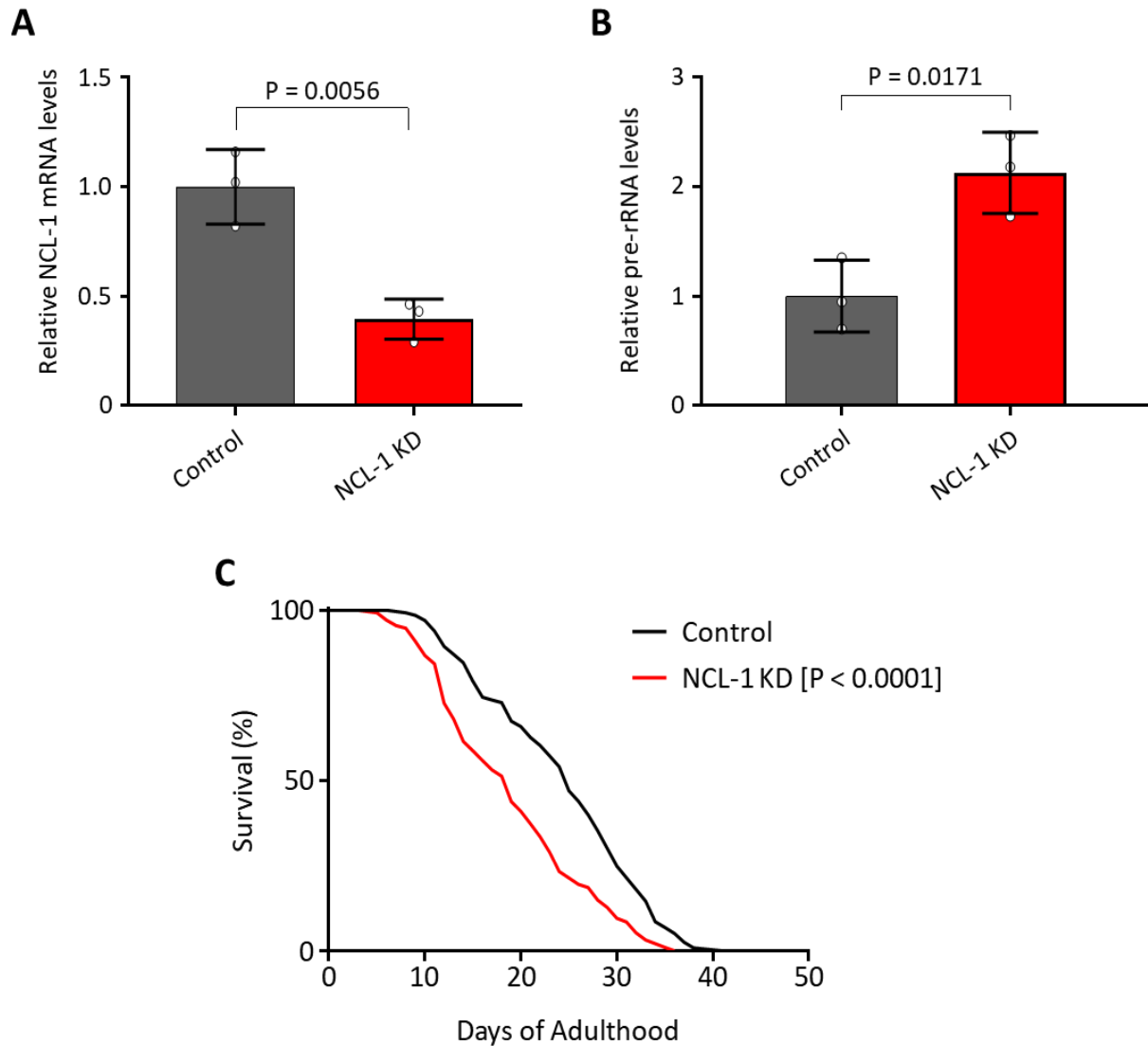


**Figure 3: NCL-1 knockdown increases pre-rRNA synthesis and shortens lifespan.** RT-qPCR analysis of **(A)** NCL-1 mRNA and **(B)** pre-rRNA levels comparing NCL-1 KD worms to control RNAi treated worms. Shown are the relative expression levels  $\pm$ SD normalized to tubulin mRNA, and each data point indicates an independent experiment ( $n = 3$ ). Sixty worms per condition were pooled for RNA extraction in each experiment. Statistical significance was calculated using unpaired Student's *t*-test **(C)** Representative plot of lifespan analysis from NCL-1 KD worms versus control worms at 15 °C. The population size was 140 worms per condition. At least three independent experiments were conducted. Statistical analysis was done using the Mantel-Cox test.

Since NCL-1 has pleiotropic effects, whether the increased mortality results from the dysregulation of other NCL-1 targets must be excluded; this can be elucidated by increasing rDNA activity via a distinct approach. TIF-IA is a transcription factor that plays an essential role in recruiting Pol I to the rDNA promoter [87]. TIF-IA overexpression is sufficient to increase rRNA synthesis in mammals and *D. melanogaster* [130, 131]. Accordingly, increasing TIF-IA levels should also increase rRNA gene activity in *C. elegans*. Hence, a TIF-IA overexpressing (TIF-IA OE) strain was generated by In Vivo Biosystems (Eugene, USA) using Mos1-mediated single-copy insertion (MoSCI) technique [124]. The ectopic gene encoded *C. elegans*' TIF-IA fused to a Ty1-epitope tag, and thus its expression could be detected on Western Blots using an anti-Ty1 antibody (**Figure 4A**). Harboring an additional gene copy, the TIF-IA OE strain should also have higher TIF-IA expression levels. Indeed, RT-qPCR analysis revealed a 2.5-fold increase of TIF-IA mRNA relative to wild-type animals (**Figure 4B**). Importantly, the surplus of TIF-IA correlated with 1.5-fold elevated pre-rRNA levels, demonstrating that the ectopic TIF-IA was functional and promoted rDNA transcription (**Figure 4C**). Having shown that TIF-IA OE animals increased pre-rRNA production, a direct link between rRNA gene activity and longevity could be investigated. Lifespan assays comparing wild-type and mutant worms revealed a drop in median survival from AD18 to AD13, i.e., a shorting of lifespan by 28% for the TIF-IA OE strain (**Figure 4D**). These data imply that supraphysiological rDNA transcription has an adverse effect on longevity.

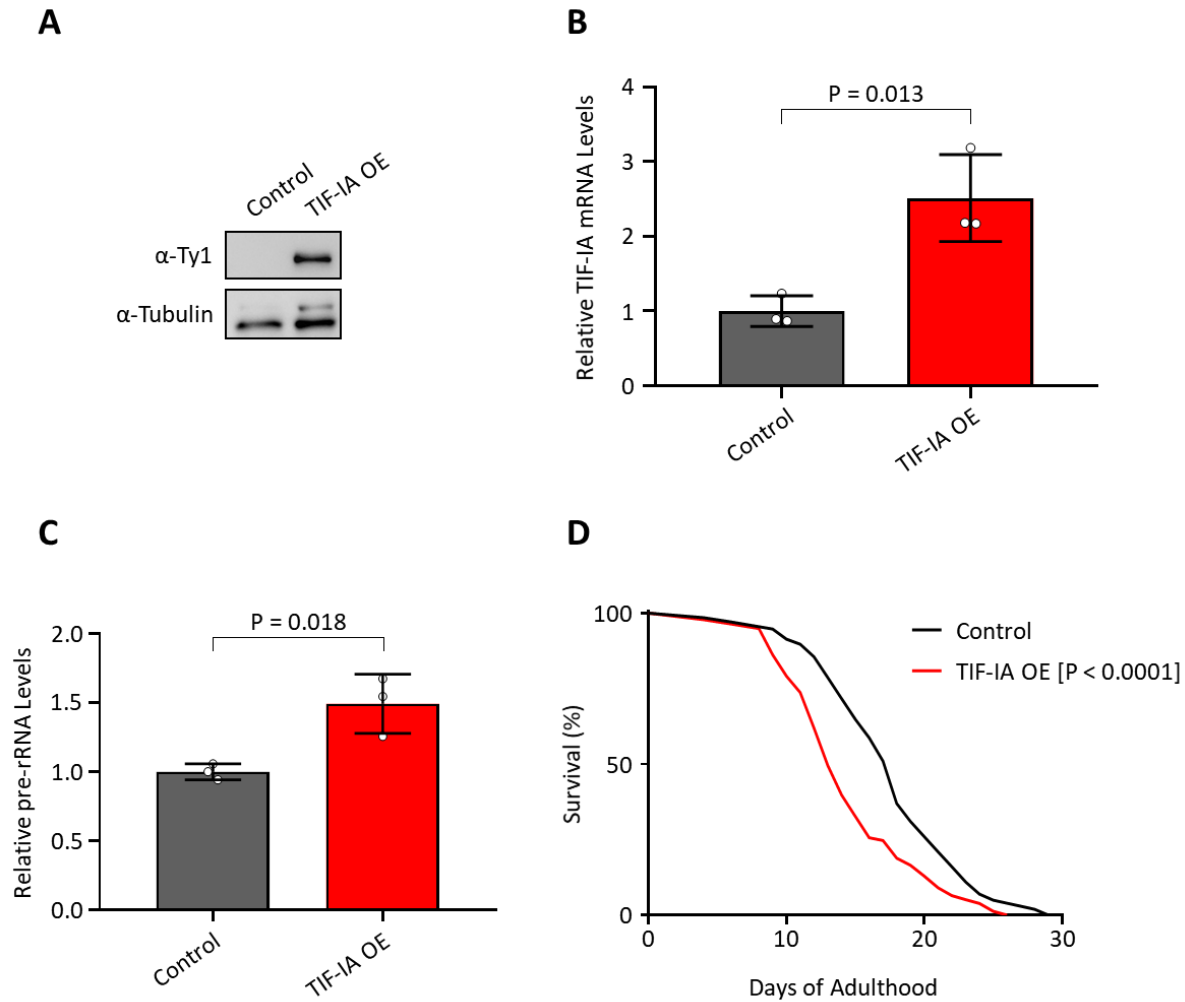


**Figure 4: TIF-IA overexpression shortens lifespan through overlocking of rRNA genes.** **A)** Western Blot analysis of Ty1-tagged TIF-IA in wild type (control) and TIF-IA overexpressing (OE) strain using an  $\alpha$ -Ty1 antibody. Tubulin was used as a loading control. **B & C)** RT-qPCR analysis of **(B)** TIF-IA mRNA and **(C)** pre-rRNA levels comparing TIF-IA OE with wild-type worms. Shown are the relative expression levels  $\pm$ SD normalized to tubulin mRNA levels, and each data point indicates an independent experiment ( $n = 3$ ). Sixty worms per condition were used in each experiment. Statistical significance was calculated using unpaired Student's *t*-test. **D)** Representative result of lifespan analysis of the TIF-IA OE strain and wild-type nematodes at 20 °C. The population size was 140 worms per condition. At least three independent experiments were conducted. Statistical analysis was done using the Mantel-Cox test.

### 5.1.2 Moderation of rRNA gene activity through TIF-IA knockdown extends lifespan

Given that enhanced rRNA gene activity restricts lifespan, decreasing rDNA activity might conversely extend it. To test this hypothesis, RNAi against TIF-IA was administered to diminish Pol I transcription. Similar to the NCL-1 knockdown, worms were cultivated for two generations at 15 °C on TIF-IA dsRNA-producing bacteria to achieve a high knockdown efficiency of 80% (**Figure 5A**). In accord with low TIF-IA expression, pre-rRNA levels were reduced by 65% upon TIF-IA depletion (**Figure 5B**). As the synthesis of pre-rRNA is an important determinant of nucleolar size, shrunken nucleoli in TIF-IA KD worms were expected. To test this hypothesis, a FIB-1::GFP strain harboring a fusion between the nucleolar processing factor FIB-1 and Green Fluorescent Protein (GFP)[132], was treated with control or TIF-IA RNAi. After immobilization and permeabilization of worms, nuclear DNA was stained with 4',6-diamidino-2-phenylindole (DAPI) to measure nucleolar relative to nuclear dimensions, i.e., GFP fluorescent signals relative to DAPI fluorescence. Taking only large polyploid cells into account that were readily visible [133], TIF-IA KD animals exhibited a reduction of 35% in nucleolar size (**Figures 6A,B**). This finding supports the strong impact of TIF-IA knockdown on pre-rRNA synthesis and points to a geroprotective effect, as small nucleoli are a hallmark of longevity [134].

To ultimately assess whether moderation of rRNA gene transcription extends the lifespan of nematodes, survival curves of control and TIF-IA KD animals were recorded. While about half of the control worms died at AD22, knockdown of TIF-IA caused a marked lifespan extension to AD28 (**Figure 6C**). Together, these data show that pre-rRNA synthesis negatively correlates with longevity, high synthetic activity shortens lifespan, whereas diminished rRNA gene transcription prolongs life.

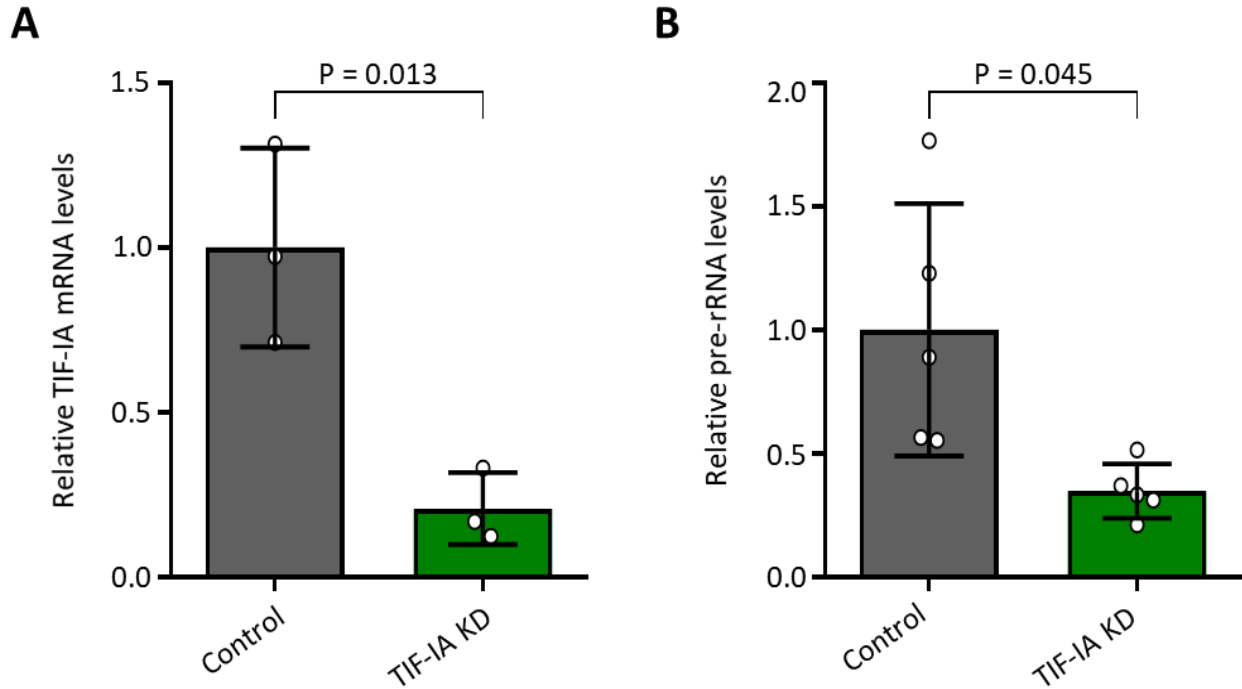


**Figure 5: TIF-IA knockdown decreases rRNA gene activity.** RT-qPCR analysis of **(A)** TIF-IA mRNA and **(B)** pre-rRNA levels comparing worms upon TIF-IA KD to control RNAi at 15 °C. Shown are the relative expression levels  $\pm$ SD normalized to tubulin mRNA levels, and each data point indicates an independent experiment. Three **(A)** and five **(B)** independent experiments were performed with sixty worms per condition in each experiment. Statistical significance was calculated using the unpaired Student's *t*-test in A, and the Welch's *t*-test in B (due to unequal variance).

### 5.1.3 rRNA gene activity is inversely correlated to healthspan

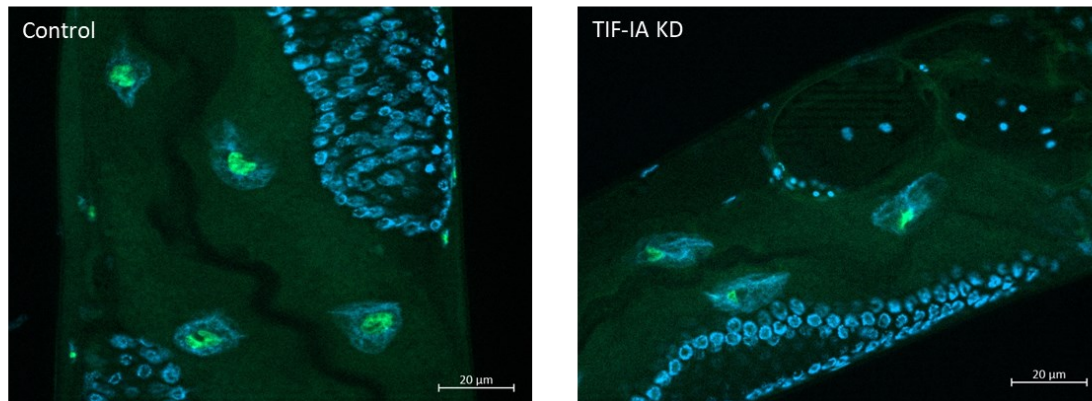
Loss-of-function mutations in the gene encoding TIF-IA lead to arrest in early development and lethality in mice and flies [131, 135]. Thus, the observation that a potent knockdown of TIF-IA over two generations extends lifespan raises the question of how manipulation of pre-rRNA synthesis affects the health of worms. As a first health indicator, body size was analyzed, which is regulated by developmental and environmental factors and has been shown to depend on food intake and cellular protein synthesis capacity in *C. elegans* [136, 137]. Measuring the surface area of worms as a proxy for body size, opposing effects of TIF-IA and NCL-1 knockdowns were observed. Relative to worms treated with control RNAi, TIF-IA RNAi treatment significantly reduced body size, while NCL-1 RNAi increased it (**Figure 7**). These differences occurred already early in life (AD2) and were maintained at old age (AD12),



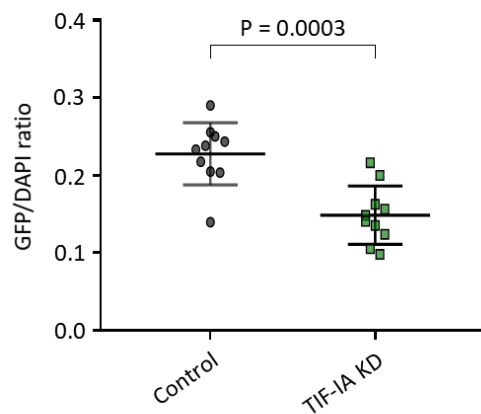
albeit worms overall grew bigger under all three conditions. These findings are in line with the observation that, within a species, there is generally a negative correlation between adult body size and longevity [138]. However, the bulkier NCL-1 KD worms might have a fitness advantage at a young age.

**A**

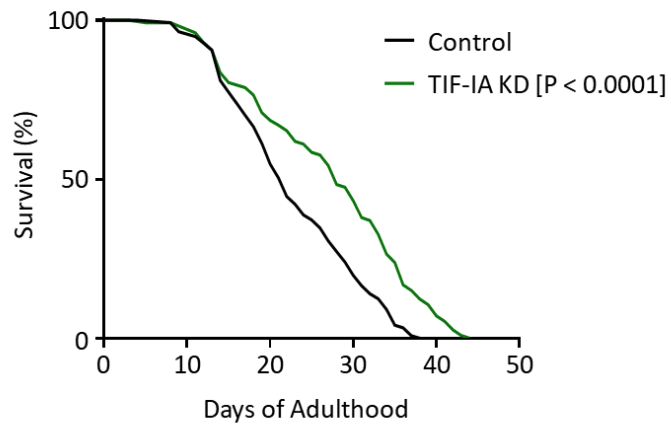
FIBRILLARIN/DAPI



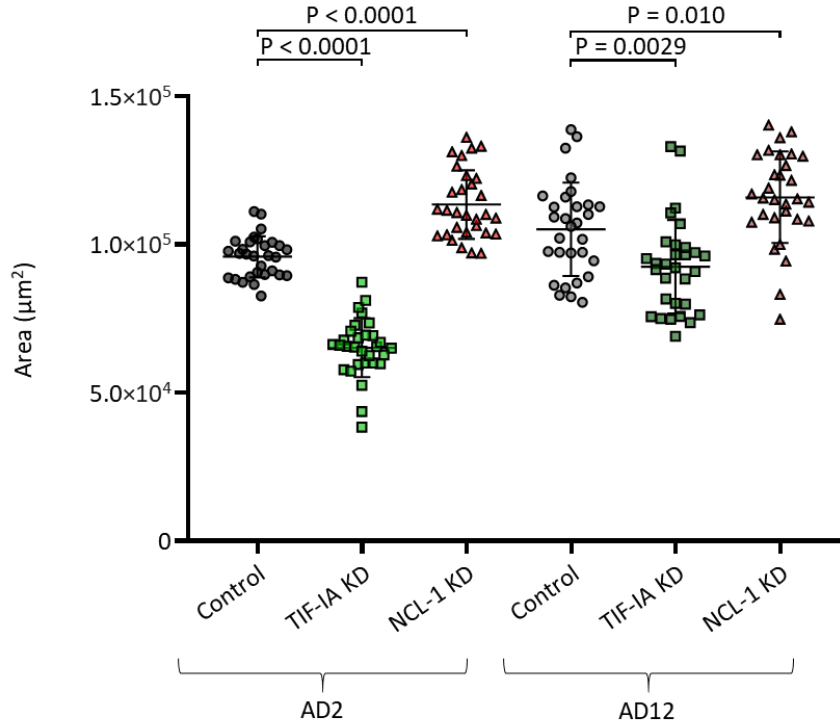
**B**



**C**

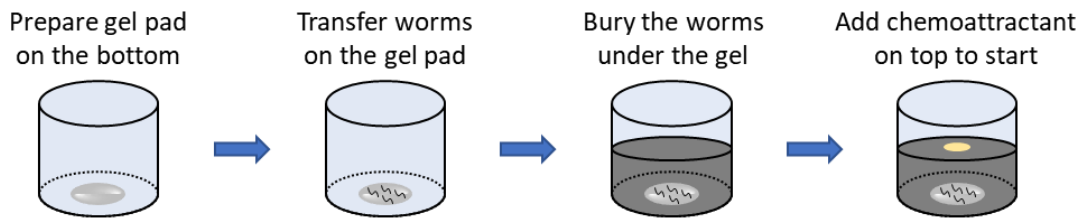
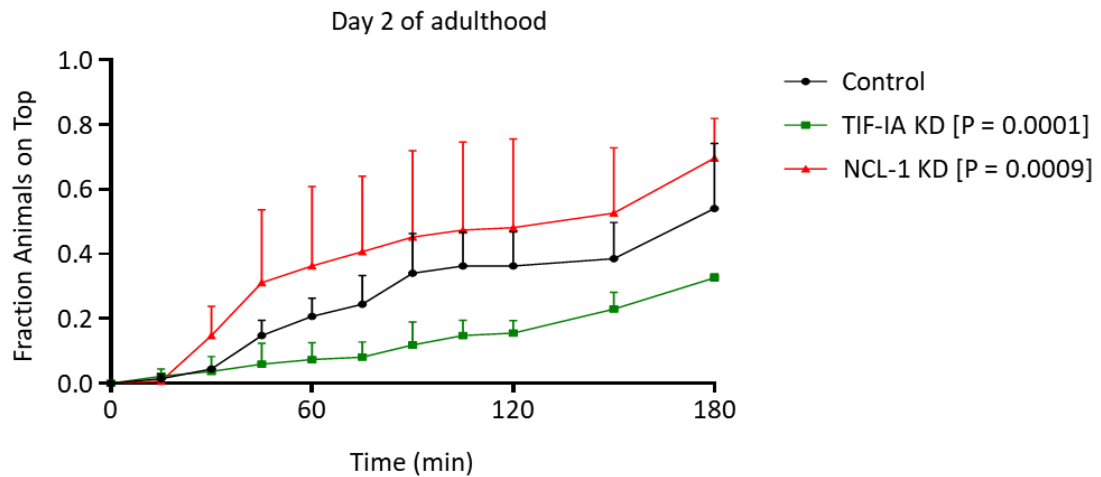
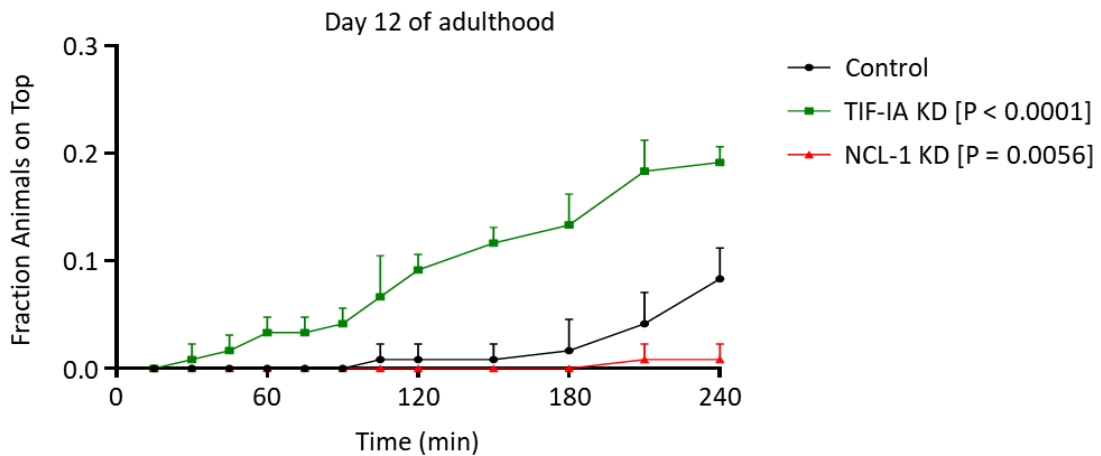


**Figure 6: TIF-IA knockdown decreases nucleolar size and extends lifespan. A & B)** FIB-1::GFP worms treated with control RNAi and TIF-IA RNAi. On day 2 of adulthood, the worms were permeabilized, stained with DAPI, and imaged using fluorescence microscopy. **A)** Representative images of the nuclei (blue) and nucleoli (green) **B)** Quantification of nucleolar size. Plotted is the mean nucleolar area  $\pm$ SD. Each data point represents a single worm. Two independent experiments were performed at 15 °C, with five worms per condition in each experiment. Nuclear area (DAPI) was used as normalization. Significance was calculated using the Student's *t*-test. **C)** Plotted is a representative lifespan analysis of worms treated with TIF-IA RNAi and control RNAi at 15 °C. Three independent experiments were performed. In each experiment, 140 worms were used per condition. Statistical significance was determined using the Mantel-Cox test.



**Figure 7: Knockdown of TIF-1A and NCL-1 affect body size in opposite directions.** Worm area was measured in TIF-1A KD and NCL-1 KD worms at young (AD2) or old (AD12) age. The mean worm area  $\pm$ SD was plotted, and each data point represents one worm. Ten worms per condition in each independent experiment were used, three independent experiments were performed. Statistical significance was calculated with the unpaired Student's *t*-test. Welch's correction was used for the comparison of control AD2 versus NCL-1 KD AD2 due to a significant difference in variance. [AD = adulthood day]

To further evaluate this hypothesis, the neuromuscular performance of worms was tested in burrowing assays [127, 128]. This assay makes use of a pluronic gel, which can be layered on top of worms and solidifies at room temperature. The buried animals crawl to a chemoattractant placed on top of the gel, depending on their locomotive capacity (**Figure 8A**). In keeping with being taller and fitter, NCL-1 KD worms clearly outperformed control and TIF-1A KD animals at young age (AD2) (**Figure 8B**). However, at AD12, TIF-1A-depleted worms exhibited the highest fraction of top crawlers, whereas NCL-1 KD animals performed the worst (**Figure 8C**). These findings indicate that elevated pre-rRNA synthesis provides an advantage in body movement and three-dimensional locomotion early in life but leads to a rapid decline with age. In contrast, moderation of pre-rRNA synthesis facilitates maintenance of neuromuscular performance throughout life, albeit at an initially lower level.

**A****B****C**

**Figure 8: Aging-associated loss of neuromuscular health is worsened by knocking down NCL-1 but improved upon TIF-IA knockdown. A)** Schematic overview of the burrowing assay setup. **B & C)** Shown is a representative plot of the burrowing assay at **(B)** young (AD2) or **(C)** old age (AD12) displaying the animals on top +SD over time in minutes (min), comparing TIF-IA KD, NCL-1 KD and control worms. Three independent experiments were performed; at least 120 worms per condition in each experiment were used. Statistical significance was calculated using paired Student's *t*-test. [AD = adulthood day]

In *C. elegans* and *D. melanogaster*, aging-dependent deterioration of health is tightly linked to functional and structural disintegration of the intestine [139]. To investigate why the performance of NCL-1 KD worms dissipates so dramatically with age, the so-called “Smurf assay”, which assesses intestinal barrier function, was employed [128]. Nematodes were fed with a blue dye (Brilliant Blue FCF), which did not cross the intact intestine. However, if gut integrity was compromised, the dye leaked into the body cavities, causing overall blue staining (Smurf). When young (AD2) control, TIF-IA KD, and NCL-1 KD worms were assayed, less than 10% showed a Smurf phenotype, with no significant difference between the three conditions (**Figure 9A,B**). In line with previous observations, leakiness of the intestine increased with age, and Smurf formation was prevalent at AD12 [128]. However, depending on the RNAi treatment, the frequency of Smurfs differed. Whereas in control and TIF-IA KD worms about 40-50% became Smurfs, NCL-1 KD led to a significantly higher portion of about 80% Smurfs at AD12 (**Figure 9A,C**). Thus, elevated pre-rRNA synthesis is linked to accelerated deterioration of intestinal integrity and, consequently, a reduced healthspan. Together, the results show that high pre-rRNA synthesis renders *C. elegans* fitter at a young age, but this advantage comes at the cost of an accelerated health decline (NCL-1 KD). In contrast, depletion of TIF-IA and concomitantly pre-rRNA throttles fitness early in life but extends health maintenance in aged animals.

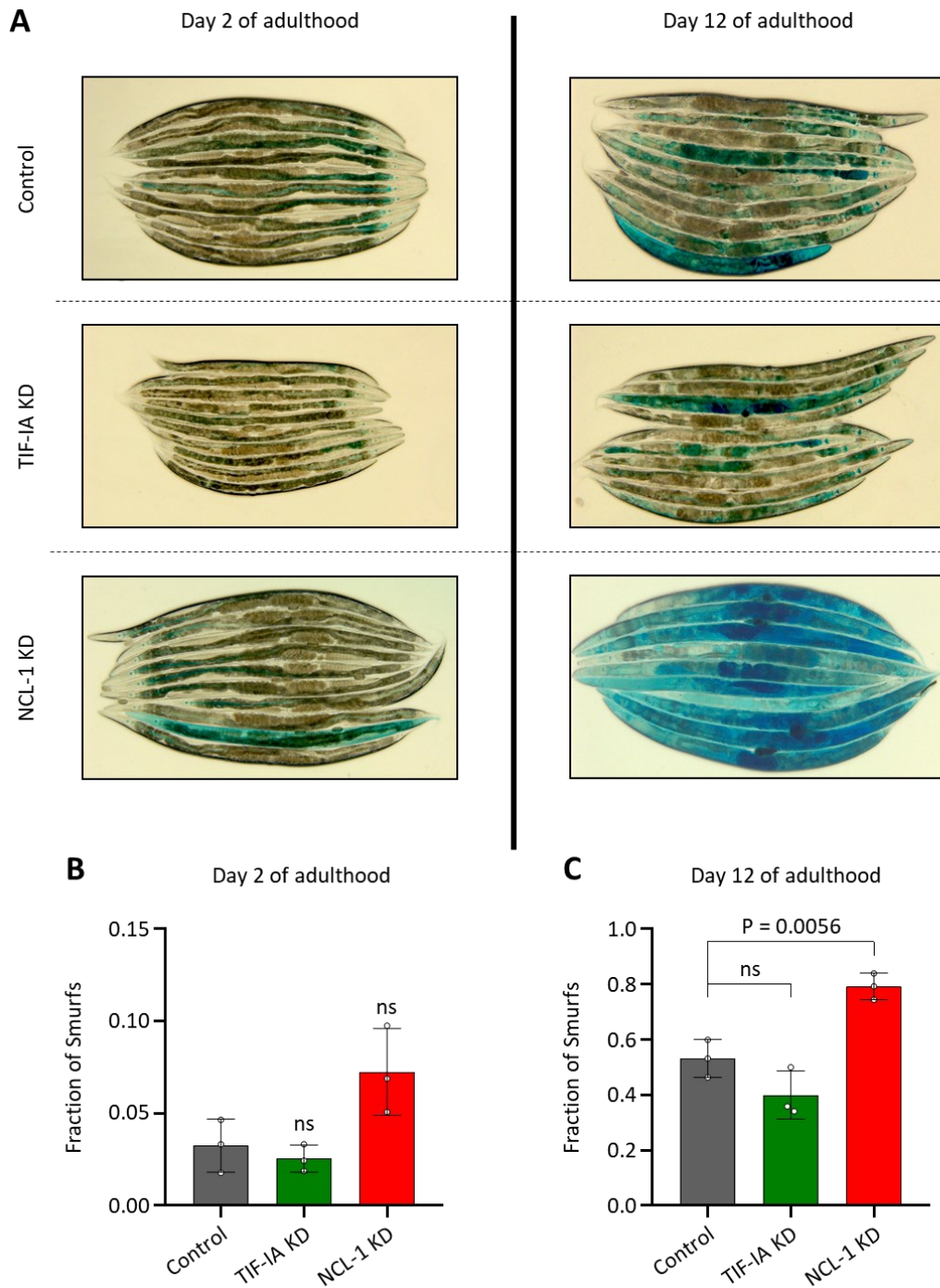


**Figure 9: Loss of intestinal integrity at old age due to knockdown of NCL-1.** Control, TIF-1A KD, or NCL-1 KD worms were treated with 5% Brilliant Blue FCF at young (AD2) and old age (AD12) (Smurf assay). Three independent experiments were performed at 15 °C, with 40-60 worms per condition in each experiment. **A)** Representative images are shown. **B & C)** Quantification of body-cavity leakage (Smurfs). Displayed is the fraction of Smurfs  $\pm$ SD from the total number of worms at **(B)** AD2 or **(C)** AD12. Each data point indicates an independent experiment. Statistical significance was determined using the unpaired Student's *t*-test. [AD = adulthood day, ns = not significant]

## 5.2 Proteomic adaptations to curbed rDNA activity

### 5.2.1 Moderation of rRNA gene activity adjusts metabolism at old age

To unravel how moderation of rRNA gene activity extends both lifespan and healthspan, molecular changes mediated by knockdown of TIF-IA were further assessed. Recent studies have shown that aging of *C. elegans* is tightly linked to perturbation of proteome homeostasis (proteostasis) [46, 140]. Therefore, the proteomes of control and TIF-IA-depleted worms were analyzed at days 2, 6, and 12 of adulthood by mass spectrometry (in collaboration with the FLI proteomics core facility). Thereby, over 5,000 different proteins were identified, and principal component analysis (PCA) demonstrated high reproducibility between biological replicates as well as treatment- and age-dependent proteome remodeling (**Figure 10A**).

The acquired proteome data were further analyzed by pairwise relative quantification of proteins. The age trajectory was monitored by comparing the protein abundance between old (AD12) and young (AD2) control worms. For testing the impact of TIF-IA depletion, control and knockdown animals at AD12 were compared. From both comparisons, proteins that were differentially regulated by at least 1.5-fold were extracted. Next, the overlap between proteins upregulated with age (1<sup>st</sup> comparison) and down-regulated by TIF-IA knockdown (2<sup>nd</sup> comparison) was assessed, yielding 298 proteins (**Figure 10B**). A similar number of proteins (309) was retrieved from the complementary approach, i.e., proteins decreased with age versus proteins increased by TIF-IA KD at AD12 (**Figure 10C**). Thus, the two protein lists contained the candidates whose age-dependent remodeling is counteracted by reduced TIF-IA and pre-rRNA levels.

Further segmentation analyses using WormCat, a web-based tool for genome-scale data from *C. elegans* [141], revealed that a large fraction of these candidates is involved in metabolism, especially lipid metabolism (**Figure 10D,E**). Interestingly, the loss of mitochondrial proteins in aged worms was ameliorated by treatment with TIF-IA RNAi, indicating that knockdown of TIF-IA could counteract the functional decline of mitochondria upon aging (**Figure 10E**) [142].

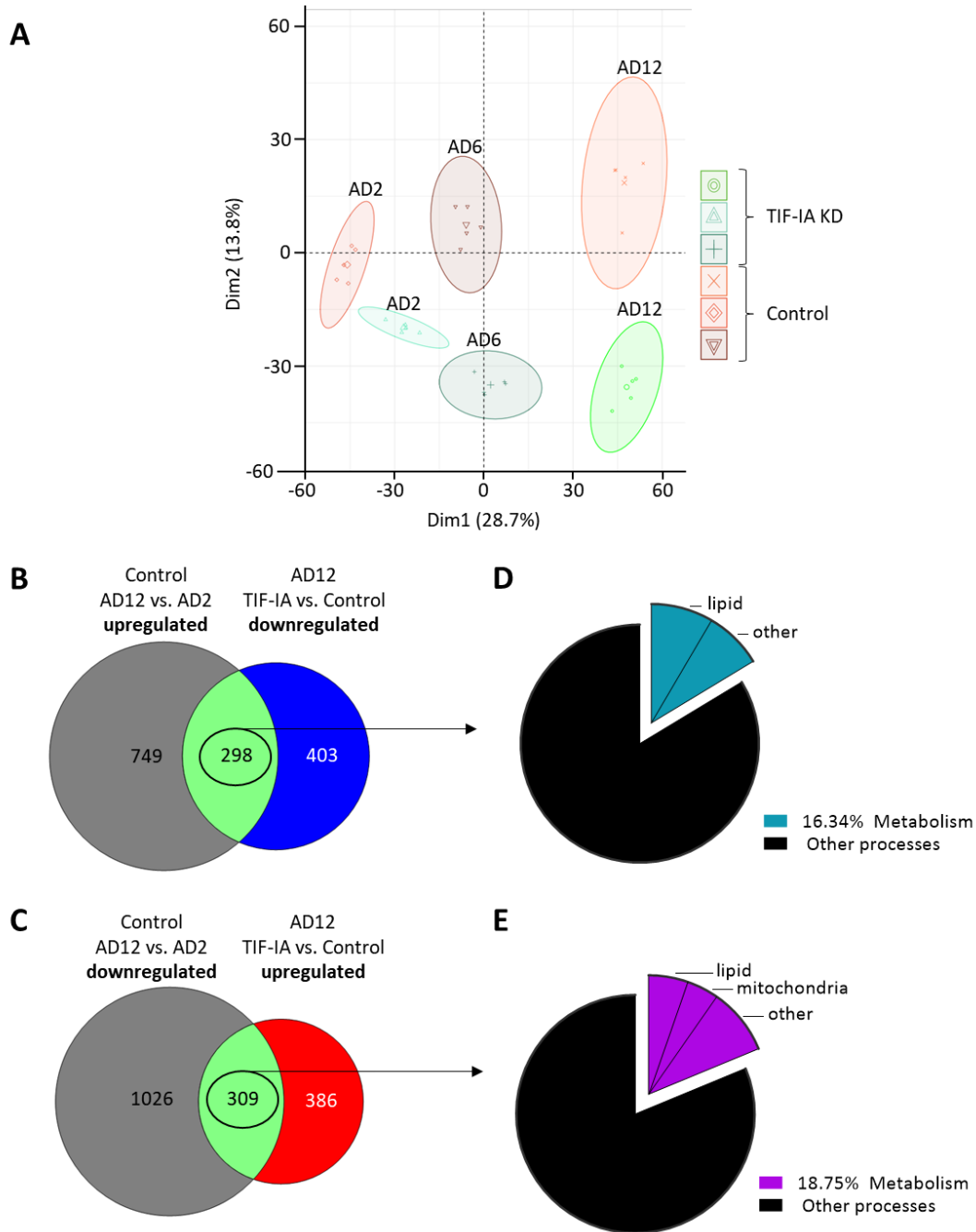


**Figure 10: TIF-IA knockdown rescues proteins involved in aging-related metabolic decline. A)** Principal component analysis of proteomic data of TIF-IA KD and control worms at young (AD2), middle (AD6), and old (AD12) age. Five independent experiments were performed, with 700 worms per experiment. **B & C)** Venn diagram comparing proteins that were at least 1.5 times **(B)** increased upon aging to decreased in old TIF-IA KD worms (Control – AD12 vs. AD2 to **AD12 – TIF-IA KD vs. Control**) or **(D)** decreased upon aging to increased in old TIF-IA KD worms (Control – AD12 vs. AD2 to **AD12 – TIF-IA KD vs. Control**). The overlap is encircled (**green**). **D & E)** WormCat segmentation analysis of overlapping proteins from the comparison in B and C, respectively (indicated with an arrow). Shown is the highest-ranked cellular process in terms of candidate numbers and its largest subgroups. [AD = adulthood day]

### 5.2.2 Abundance of vitellogenins is reduced in TIF-IA knockdown worms

In contrast to the preservation of mitochondrial proteins, TIF-IA knockdown led to a substantial reduction of vitellogenins that constitute a family of six yolk proteins (VIT-1 to VIT-6). Vitellogenins are highly expressed in the intestine of *C. elegans* and accumulate upon aging of post-reproductive animals [47, 60, 140]. Notably, upregulation of all six vitellogenins was strongly curbed by TIF-IA KD, starting early in life, but becoming even more pronounced in old age (**Figure 11**). This finding is reminiscent of the reduced expression of the genes encoding VIT-2 and VIT-5 in long-lived *daf-2* mutant nematodes [58]. Given that RNAi-mediated knockdown of VIT-2 and VIT-5 extends lifespan in the context of an intact DAF-2/DAF-16 pathway [58], the reduced levels of vitellogenins in TIF-IA KD worms are likely to contribute to their decelerated aging.

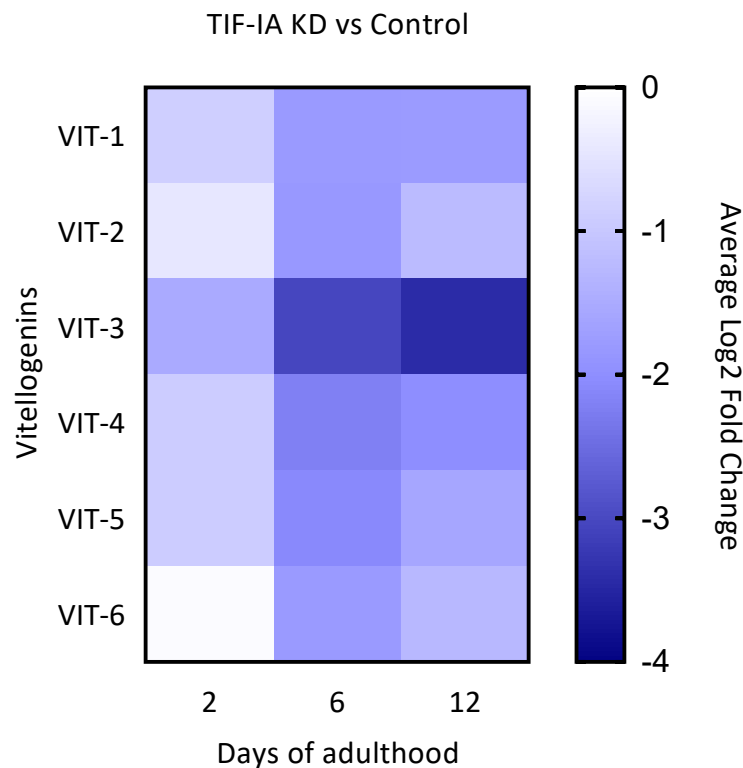


**Figure 11: Restriction of rRNA synthesis lowers the expression of vitellogenins.** Heatmap of changes in vitellogenin expression (VIT-1 to 6) upon TIF-IA knockdown at young (AD2), middle (AD6), and old age (AD12). Protein abundance was measured by mass spectrometry, and pairwise relative quantification for each age stage was carried out. [AD = adulthood day]



### 5.2.3 TIF-IA knockdown promotes longevity only partly via translation inhibition

The synthesis of pre-rRNA is a critical regulatory step in ribosome biogenesis [96]. Accordingly, reduced pre-rRNA synthesis in TIF-IA-depleted worms decreased the abundance of cytosolic but not mitochondrial ribosome subunits, the levels dropping on average by about 1.5-fold throughout adulthood (**Figure 12A**). Interestingly, the mitochondrial ribosomal proteins (RPs) at old age (AD12) were slightly upregulated, hinting again that TIF-IA knockdown might counteract aging-mediated mitochondrial functional decline. Given that ribosome abundance dictates protein synthesis capacity, total protein content in TIF-IA KD worms was moderately but significantly lower than in control animals (**Figure 12B**).

Previous studies have shown that throttling protein synthesis by depleting either RPs or translation factors can extend lifespan in *C. elegans* and other model organisms [121]. Hence, diminished protein production in the wake of perturbed rRNA gene activity was likely to contribute to the longevity of TIF-IA-depleted nematodes. To dissect this relation further, TIF-IA knockdown was compared with the genetic abrogation of IFE-2, an isoform of the eukaryotic translation initiation factor 4E (eIF-4E), which binds 7-methylguanosine caps of mRNAs. A *C. elegans* strain (KX15) with a partial deletion of the *ife-2* gene is a well-characterized translation inhibition mutant shown previously to have an extended lifespan [80, 143]. In accord with these data, the median lifespan of *ife-2* worms (AD23) was two days longer than that of control worms (AD21) (**Figure 13A**). Furthermore, TIF-IA KD animals lived four days longer (AD27); however, the knockdown of TIF-IA in *ife-2* mutants did not give further lifespan extension. Based on these findings, two conclusions can be drawn. Firstly, perturbation of pre-rRNA synthesis by TIF-IA KD throttles protein synthesis efficiently so that the concomitant impairment of IFE-2 does not affect lifespan. Secondly, interference with the protein synthesis machinery upstream of translation promotes longevity more potently than the *ife-2* mutation.

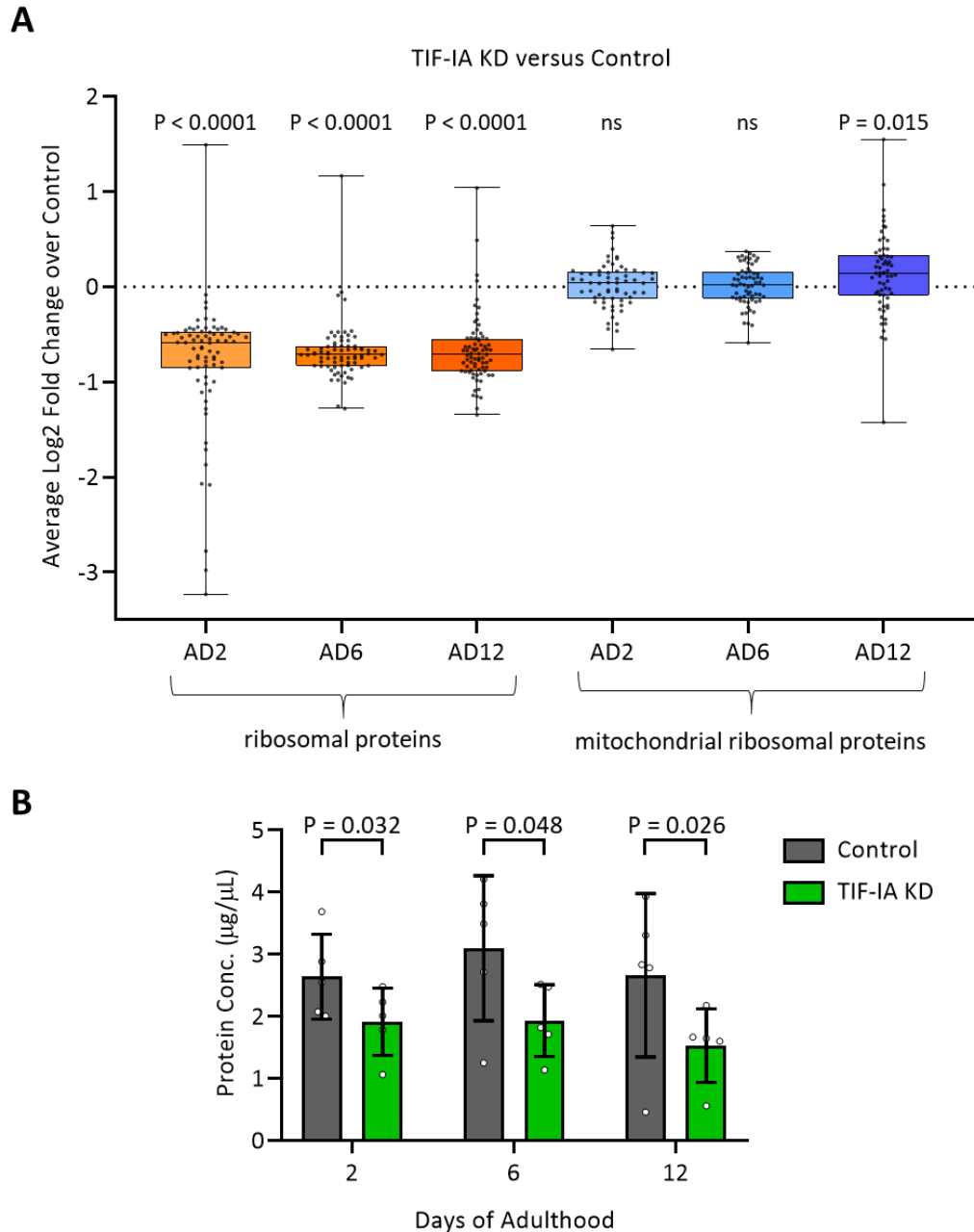


**Figure 12: Production of ribosomal proteins and total protein content is reduced upon TIF-IA knockdown. A)** Proteomic analysis of cytoplasmic and mitochondrial ribosomal proteins. Shown are boxplots of the average Log2 fold change of cytoplasmic (orange) and mitochondrial ribosomal (blue) proteins upon TIF-IA KD over control at young (AD2), middle (AD6), and old (AD12) age. Whiskers indicate the full range (min. to max.). Each data point indicates a protein. **B)** Total protein concentration of control and TIF-IA KD at AD2, AD6, and AD12. Displayed is the average total protein concentration  $\pm$ SD, and each data point indicates an independent experiment. **A & B)** Five independent experiments were performed. For each experiment, 700 worms per condition were cultivated. Statistical significance was determined in (A) with the one-sample *t*-test and in (B) with the paired Student's *t*-test. [AD = adulthood day, ns = not significant]

While *ife-2* worms are partially impaired in translation initiation, treatment of nematodes with cycloheximide (CHX) interferes with translation elongation and also prolongs lifespan [79]. Notably, when combining CHX treatment with TIF-IA knockdown, the results were akin to the previous experiments. Worms on control RNAi lived moderately longer in the presence of CHX. However, lifespan was even more extended when worms were cultivated on bacteria producing TIF- IA dsRNA, regardless of whether CHX was administered or not (**Figure 13B**). Together, these data support the view that downregulation of rRNA gene activity boosts longevity partly by inhibition of protein synthesis but, beyond that, induces additional anti-aging mechanisms.

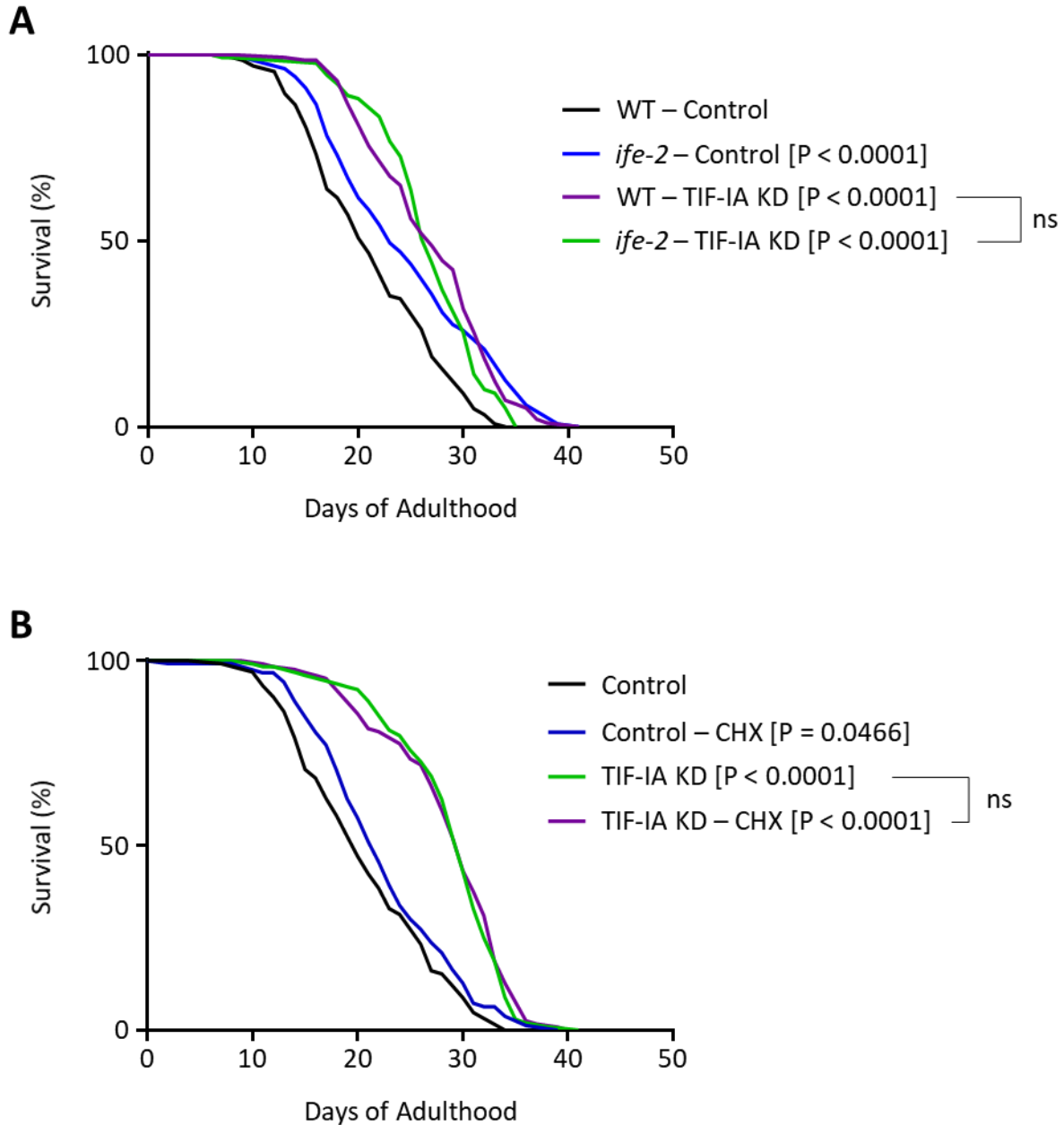


**Figure 13: Lifespan extension by TIF-IA knockdown is not improved by concomitant translation inhibition. A)** Lifespan analysis of wild-type (WT) and *ife-2* mutant worms, treated either with unspecific (control) or TIF-IA RNAi. **B)** Lifespan analysis of control and TIF-IA-depleted worms in the absence or presence of 1  $\mu$ M cycloheximide (CHX). **A & B)** Three independent experiments were performed at 15 °C, with 140 worms per condition in each experiment. A representative experiment is shown. Statistical significance was calculated using the Mantel-Cox test. [ns = not significant]

## 5.3 Reduction of rRNA gene activity remodels energy and lipid metabolism

### 5.3.1 Curtailment of rRNA gene activity increases cellular ATP levels

There is accumulating experimental evidence that sustainment of the cellular energy pool is vital for longevity [144]. Ribosome biogenesis is a highly energy-consuming process, requiring not only the extensive synthesis of the ribosome building blocks, i.e., rRNAs and ribosomal proteins, but also the activity of many ATPases, GTPases, and kinases for pre-rRNA processing and ribosome assembly [93, 95, 145]. Given that moderation of rRNA gene transcription curbs all these processes, it should lower energy expenditure profoundly. In accord with this notion, bioluminescent ATP measurements revealed about 1.5-fold higher ATP levels in TIF-IA KD worms relative to control worms at AD2 (**Figure 14A**). Moreover, ATP levels were similar between wild type and *ife-2* mutant animals, either in the absence or presence of TIF-IA RNAi. This observation suggests that inhibition of pre-rRNA synthesis, but not of translation, conserves cellular energy significantly. As ATP levels drop sharply with age in *C. elegans* [122], the energy-saving effect of TIF-IA depletion may contribute to the improvement of lifespan and healthspan. Further ATP measurements supported this notion by showing that despite a general age-dependent decline of the ATP pool, old (AD12) TIF-IA KD worms exhibited ATP levels comparable to young (AD2) control worms (**Figure 14B**).

The drug metformin is widely used to treat type II diabetes in humans and acts at the molecular level by inhibiting mitochondrial respiration [146]. A recent study has shown that metformin promotes longevity when given to young nematodes but causes ATP exhaustion and toxicity in aged *C. elegans* [147]. To test whether higher ATP availability owing to reduced pre-rRNA synthesis renders old worms more resilient to mitochondrial impairment, metformin was given to control and TIF-IA KD animals at AD12, and survival was monitored. This analysis showed that most control worms died within 72 hours after metformin treatment, reducing the median lifespan drastically from AD22 to AD15 compared to the untreated group. In contrast, immediate survival after metformin administration was better preserved in TIF-IA KD worms, causing a median lifespan similar to untreated control worms (**Figure 15**). However, also in this case, long-term survival was reduced in comparison to the untreated group.

These results suggest that TIF-IA depletion delays rather than prevents aging-associated changes in energy metabolism that confer metformin sensitivity at old age.

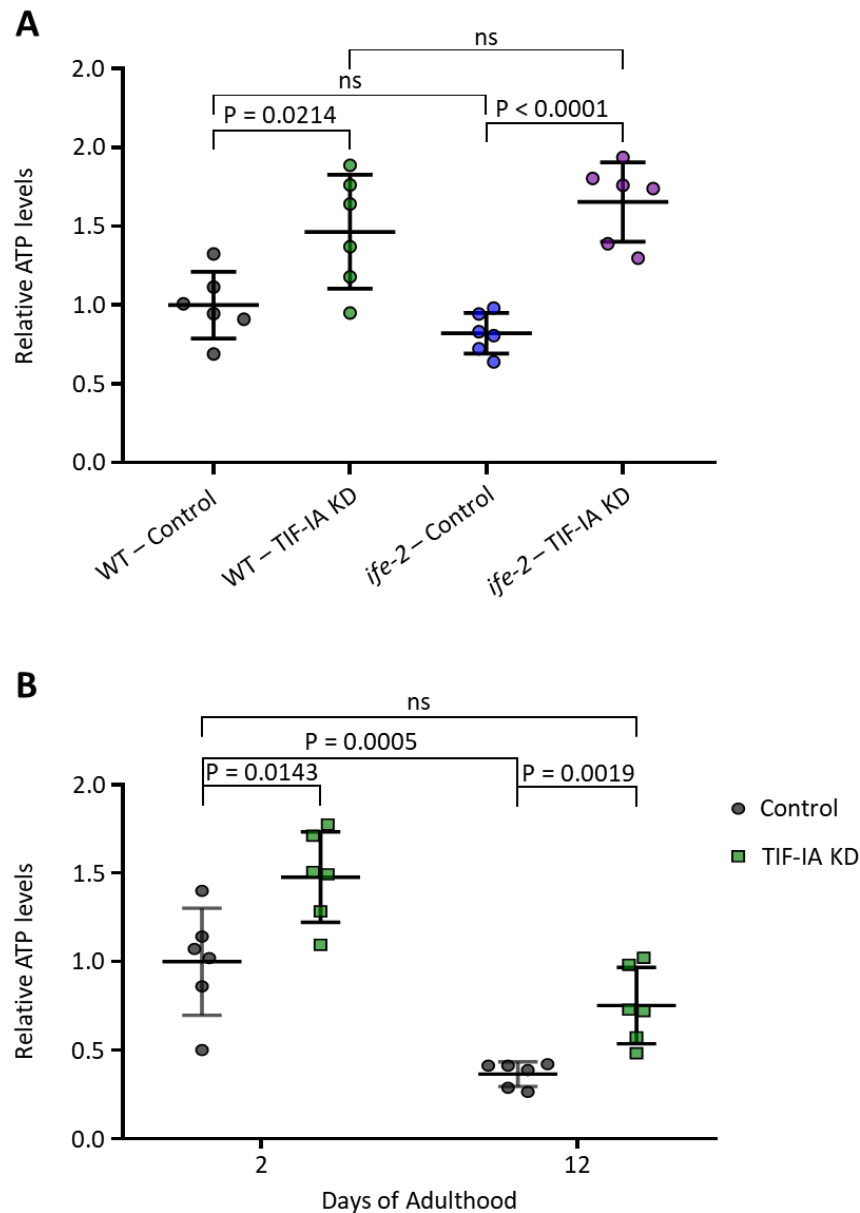


**Figure 14: Reduction of rRNA gene activity increases ATP levels and counteracts the loss of cellular energy upon aging. A)** Total cellular ATP of wild type and *ife-2* mutant treated with control RNAi or TIF-IA RNAi at AD2 was measured using an ATP bioluminescence assay. **B)** ATP levels of young (AD2) and old (AD12) worms upon TIF-IA KD relative to control were monitored. **A & B)** Shown are the relative ATP levels  $\pm$ SD; single data points indicate an independent experiment. Six independent experiments were performed at 15 °C, and fifty worms per condition were used in each experiment. Data was normalized against total protein content. Statistical significance was determined using the unpaired Student's *t*-test. [AD = adulthood day]

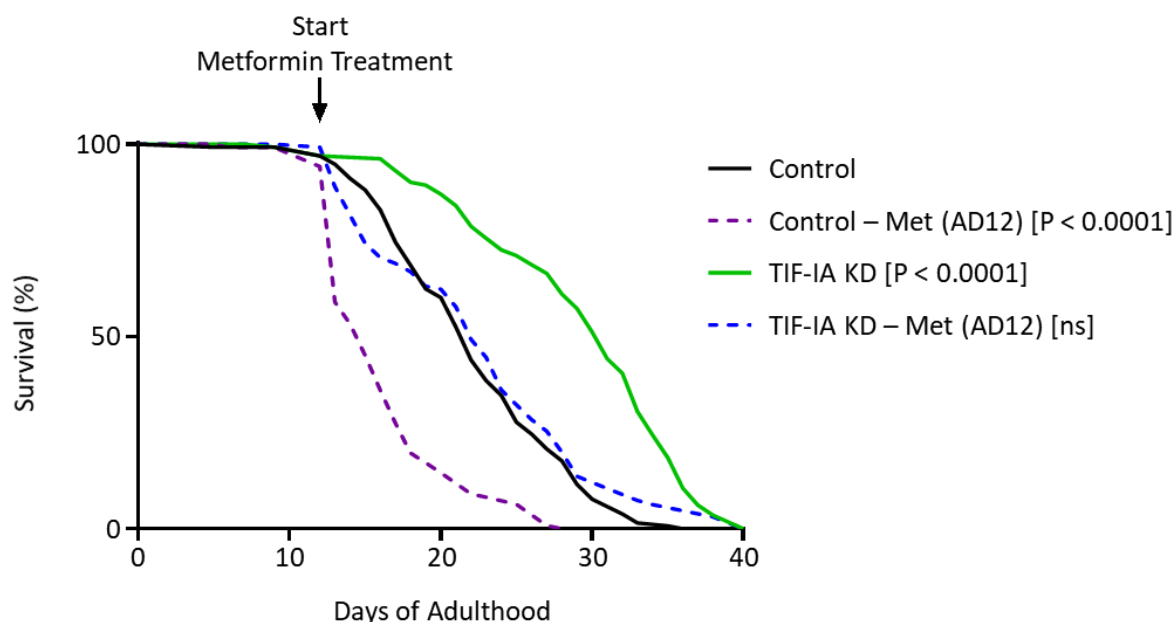


**Figure 15: Moderation of pre-rRNA synthesis partially rescues worms from age-related metformin toxicity.** Survival was monitored of worms fed on bacteria producing either control or TIF-IA dsRNA. From AD12 on, cultures were left untreated or 50 mM metformin (Met) was added. Three independent experiments were performed with 140 worms per condition. Representative data is shown. Statistical significance was calculated using the Mantel-Cox test. [AD = adulthood days, ns = not significant]

### 5.3.2 Moderation of rRNA gene activity alters lipid metabolism

Energy balance in *C. elegans* is tightly linked to metabolism, and the profile of membrane and storage lipids has been shown to have a substantial impact on longevity [148]. Based on the observations that knockdown of TIF-IA has a profound effect on proteins involved in lipid metabolism and ameliorates energy availability, the abundance and composition of fat in control and TIF-IA KD worms were analyzed at days 2, 6, and 12 of adulthood. To this end, lipidomics analysis by ultra-performance liquid chromatography-tandem mass spectrometry (UPLC-MS/MS) was used (in collaboration with Prof. Dr. Oliver Werz and PD Dr. Andreas Koeberle, FSU). Consistent with lower metabolic activity and smaller size of TIF-IA KD animals, the abundance of all membrane phospholipids was reduced compared to control worms at all age stages (**Figure 16A**).

Detailed analysis of the fatty acid (FA) composition of phosphatidylcholines (PCs) and phosphatidylethanolamines (PEs) revealed that the ratio between monounsaturated FAs (MUFAs) and polyunsaturated FAs (PUFAs) was increased throughout adulthood upon TIF-IA RNAi treatment (**Figure 16B,C**). Notably, higher MUFA levels in PCs and PEs have been reported for several life-extending interventions in *C. elegans* [62, 65, 69, 149, 150]. Regarding the storage lipids, the abundance of triacylglycerols (TAGs) was measured, and in contrast to the membrane lipids, TIF-IA KD worms exhibited a slight increase relative to control worms at AD6 and AD12 (**Figure 16A**). Given that TAGs serve as the primary energy reserve, this observation is consistent with the energy surplus of TIF-IA KD worms and has also been associated with prolonged lifespan [150-152]. Likewise, the level of TAG species containing medium-chain FAs (MCFAs) is positively correlated with longevity in nematodes [62, 150]. Although the ratio between MCFAs and long-chain FAs (LCFAs) in TAGs decreased with age in the absence and presence of TIF-IA RNAi, TIF-IA KD worms retained higher MCFA/LCFA ratios at AD12 (**Figure 16D**). Together, these findings indicate that downregulation of pre-rRNA synthesis owing to TIF-IA depletion remodels the lipid metabolism, thereby causing pro-longevity changes in the composition of membrane and storage lipids.



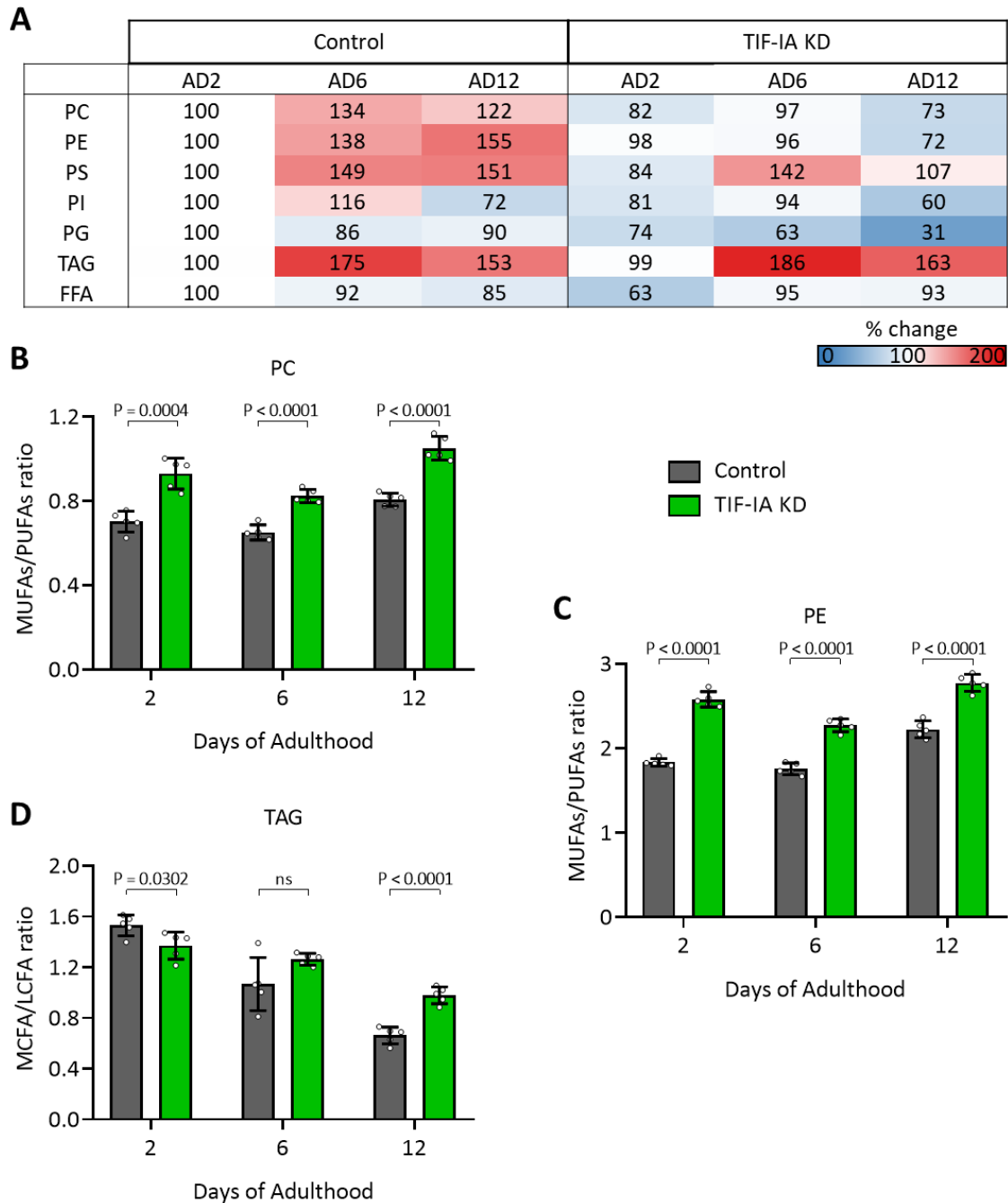
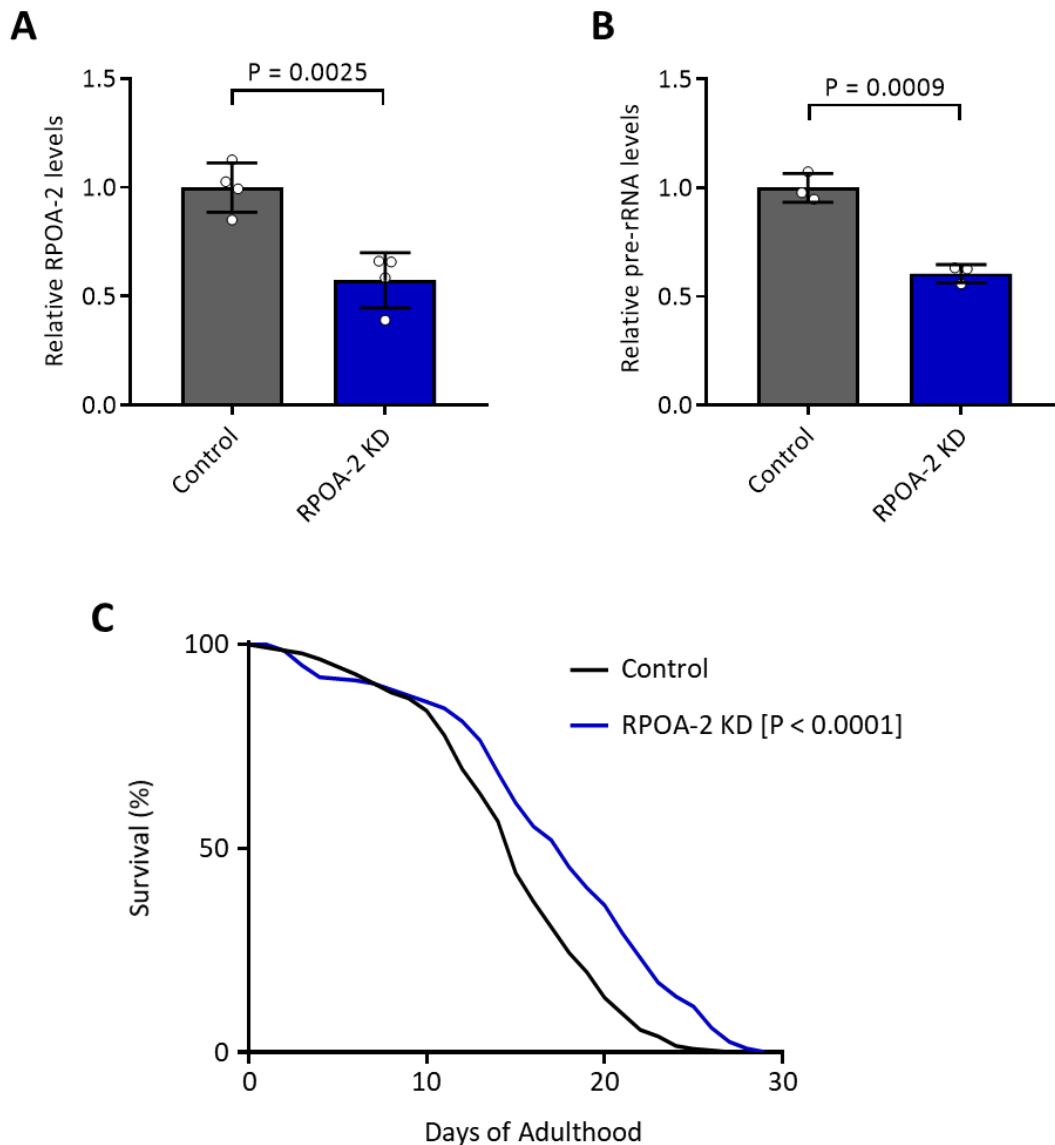


**Figure 16: Knockdown of TIF-IA changes the composition of membrane and storage lipids.** Lipid analysis of TIF-IA KD worms at young (AD2), middle (AD6), and old (AD12) age by UPLC-MS/MS **A)** Displayed are the relative intensities of different lipids. **B-D)** Plotted are the monounsaturated fatty acids : polyunsaturated fatty acids (MUFAs/PUFAs) ratios of **(B)** phosphatidylethanolamine (PE) and **(C)** phosphatidylcholine (PC), and **(D)** the medium-chain fatty acid : long-chain fatty acid (MCFA/LCFA) ratio of triglycerides (TAG). Data are from five independent experiments. In each experiment, 700 animals per condition were used. Data were normalized to total protein levels. Statistical significance was determined using unpaired Students *t*-test. [AD = adulthood day, FFA = free fatty acid, ns = not significant, PG = phosphatidylglycerol, PI = phosphatidylinositol, PS = phosphatidylserine]

## 5.4 Inhibition of rDNA activity late in life promotes healthy longevity

### 5.4.1 Knockdown of RNA polymerase I subunit RPOA-2 extends lifespan

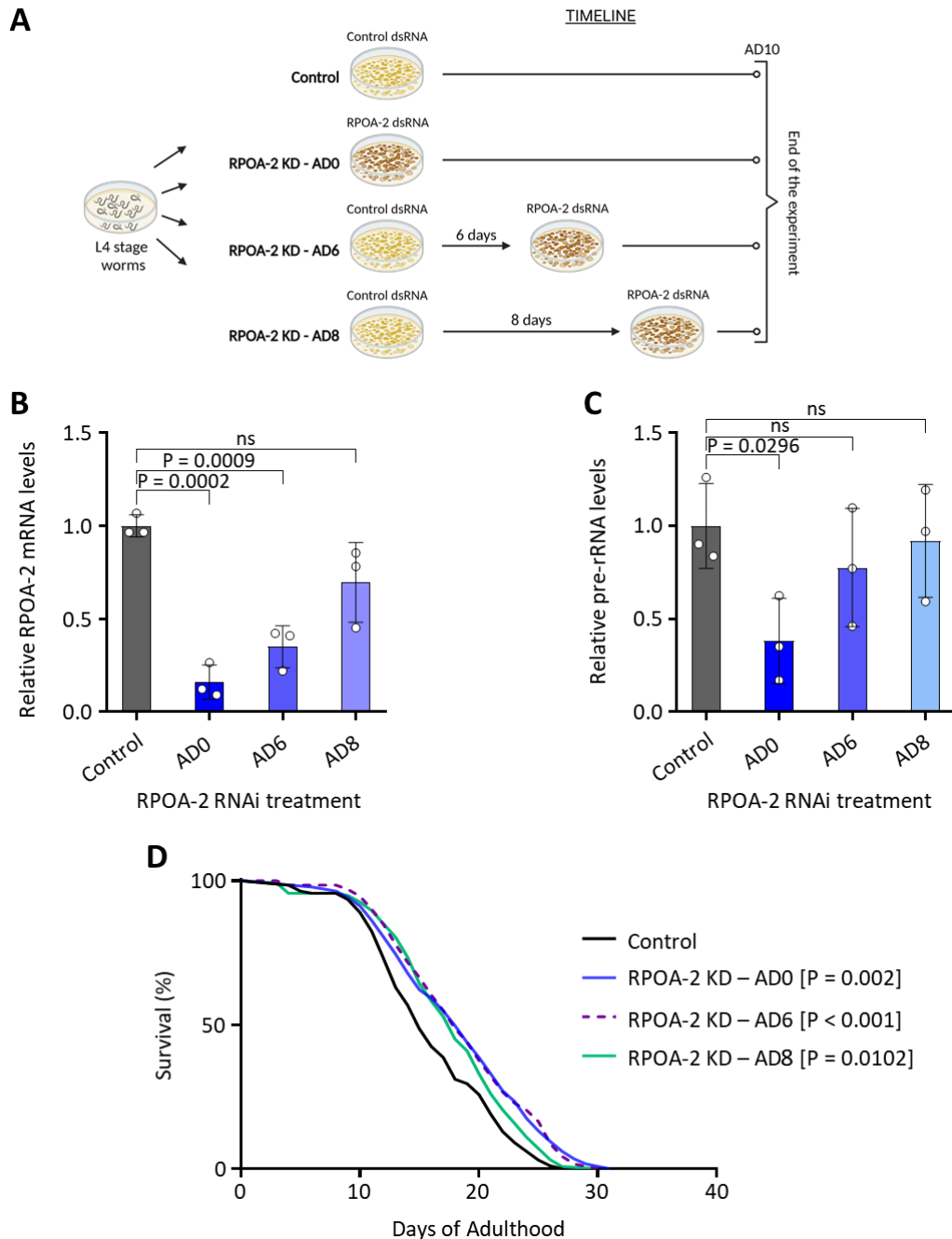
In all experiments so far, rRNA gene activity was downregulated through the knockdown of TIF-IA. To test if the observed lifespan extension was indeed caused by reduced pre-rRNA synthesis and did not involve another, so far unknown, functions of TIF-IA, an alternative perturbation of the Pol I machinery was carried out. Worms were fed with dsRNA against RPOA-2, the *C. elegans* homolog of the second-largest Pol I subunit in mammals (POLR1B) [153]. In contrast to the TIF-IA knockdown, which required RNAi treatment for two generations and the cultivation of worms at 15 °C, RPOA-2 RNAi was more effective. When treated from the L4 stage onwards, worms grown at 20 °C to AD2 exhibited a reduction in RPOA-2 mRNA and pre-rRNA levels to about 60% (**Figure 17A,B**). Importantly, lifespan analysis under these RNAi conditions revealed that depletion of RPOA-2 resulted in a significant prolongation of survival (**Figure 17C**). Thus, the similar effects of RPOA-2 and TIF-IA RNAi support the notion that curbing rRNA gene transcription promotes longevity.



**Figure 17: Knockdown of the RNA polymerase I subunit RPOA-2 extends lifespan.** Gene expression analysis of **(A)** RPOA-2 mRNA and **(B)** pre-rRNA levels, comparing worms upon RPOA-2 KD to control RNAi treatment at AD2. Shown are the relative expression levels  $\pm$ SD normalized to tubulin mRNA levels. Data points indicate independent experiments. Four (A) and three (B) independent experiments were performed with sixty worms per condition in each experiment. **C)** Shown is a representative lifespan analysis of worms treated with RPOA-2 RNAi and control RNAi at 20 °C. Three independent experiments were performed. In each experiment, 140 worms were used per condition. Statistical significance was determined using the Mantel-Cox test.

#### 5.4.2 RPOA-2 knockdown late in life extends lifespan

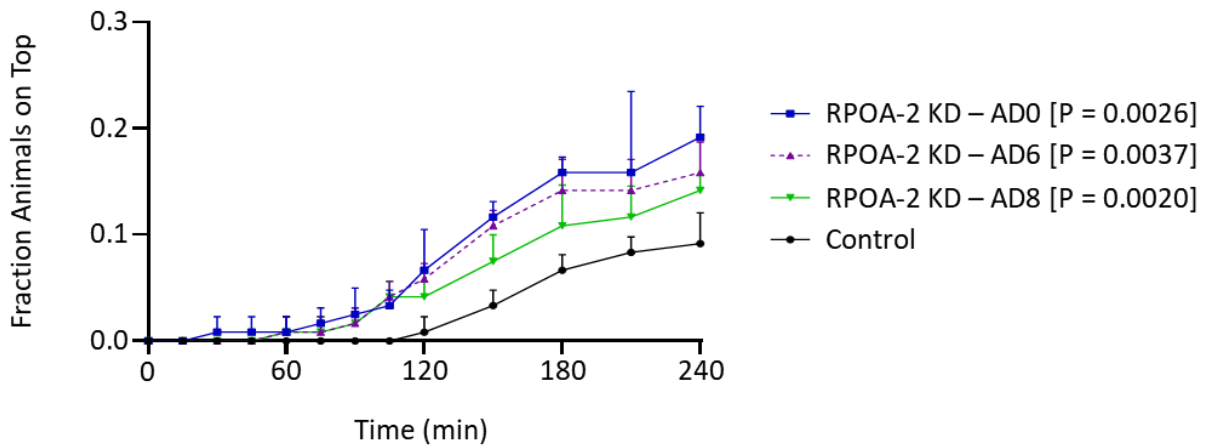
The fact that worms fed from the L4 stage onwards with RPOA-2 dsRNA lived longer than control worms ruled out the involvement of transgenerational or developmental effects. Moreover, the RPOA-2 RNAi efficacy provided the opportunity to initiate the knockdown at even later time points in adulthood. Therefore, feeding of worms with RPOA-2 dsRNA was initiated at L4 (AD0), AD6, or AD8, and the impact on RPOA-2 mRNA and pre-rRNA levels were assessed at AD10 (**Figure 18A**). Given that pharyngeal pumping and concomitant food ingestion declines with age [154], and later time points have less total exposure to RNAi, the reduction of both RPOA-2 mRNA and pre-rRNA was less efficient when RNAi was administered to AD6 and AD8 worms in comparison to administration to the AD0 worms (**Figure 18B,C**). Surprisingly, despite the alleviated RNAi potency when given later in life, the prolongation of the median lifespan was the same for all three time points (**Figure 18D**). However, maximum lifespan extension was less in worms only treated at AD6 and AD8, especially for the latest time point (AD8). Thus, throttling rRNA gene activity relatively late in life is sufficient to improve longevity. Still, the RNAi treatment has to start at the beginning of adulthood for the full extent of life prolongation.



**Figure 18: Knockdown of RPOA-2 late in life extends lifespan.** **A)** Schematic overview of the RPOA-2 RNAi late in life treatment. **B & C)** Gene expression analysis of **(B)** RPOA-2 mRNA and **(C)** pre-rRNA levels comparing RPOA-2 KD started at indicated time points. Shown are the relative expression levels  $\pm$ SD and data points from independent experiments. Tubulin mRNA levels were used for normalization. Three independent experiments were performed with sixty worms per condition in each experiment. **D)** Representative graph of the lifespan analysis from worms with knockdown of RPOA-2 started at AD0, AD6, AD8, or without knockdown (control). Three independent experiments were performed at 20 °C. In each experiment, 140 worms were used per condition. Statistical significance was determined using the Mantel-Cox test. [AD = adulthood day, ns = not significant]

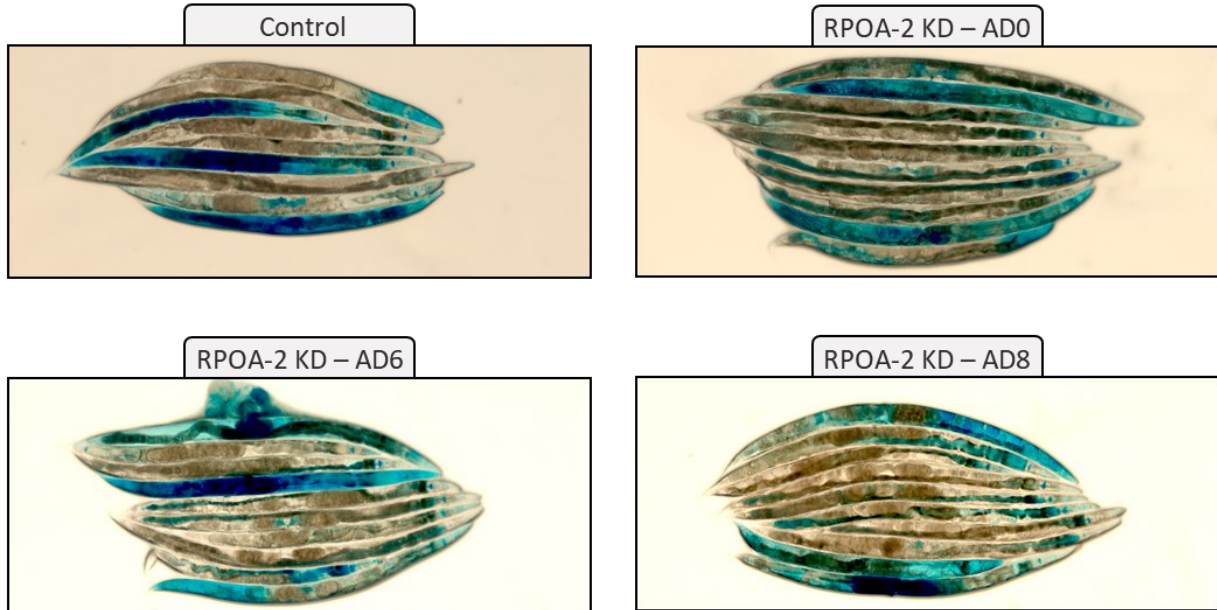
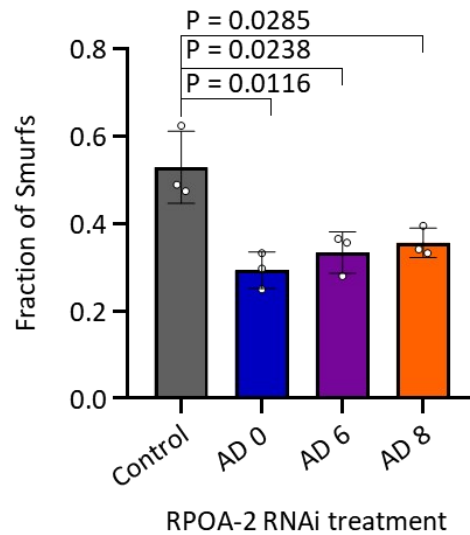
### 5.4.3 RPOA-2 knockdown late in life improves healthspan

Aging-associated tissue deterioration in nematodes has been shown to set in shortly after the reproductive phase, i.e., about AD6, with muscle and intestine being majorly affected [155, 156]. While inhibiting rRNA gene transcription early in life might extend lifespan by delaying the onset of the deterioration process, interventions starting during late adulthood would have to decelerate or even revert it. To determine whether knockdown of RPOA-2 starting at different adulthood stages improves neuromuscular performance at old age, treatment with RPOA-2 RNAi at L4 (AD0), AD6, or AD8 was followed by conducting burrowing assays at AD10 (**Figure 19**). Notably, control worms were clearly outperformed by all three treatment groups, the AD0 group having the highest fraction of top crawlers followed by AD6 and AD8 groups, respectively. This behavior reflected the strength of the pre-rRNA reduction (**Figure 18C**), suggesting that curbing rRNA gene activity improves neuromuscular health throughout life and does not only protract its decline.



**Figure 19: Moderation of rRNA gene activity late in life improves neuromuscular health.** Burrowing assay of old worms (AD10) where RPOA-2 was knocked down at different ages (AD0, AD6, AD8, or control). Shown is a representative experiment with the fraction of animals on top +SD over time. Three independent experiments were performed at 20 °C, with 120 worms per condition in each experiment. Statistical significance was determined using paired Student's *t*-test. [AD = adulthood day]

To test how the RPOA-2 KD late in life affects the intestinal barrier function, the AD0, AD6, and AD8 RNAi regimens were combined with the Smurf assay (**Figure 20A,B**). Relative to control worms, a moderate but significant decrease in the Smurf phenotype was again observed for all three knockdown groups, demonstrating that RPOA-2 depletion starting either early or late in life preserves the integrity of the intestine. Together, the data show that moderation of pre-rRNA synthesis is an effective intervention to extend both lifespan and healthspan and has a wide application window, covering virtually the whole *C. elegans* life cycle.

**A****B**

**Figure 20: Knockdown of RPOA-2 late in life improves intestinal integrity in old worms.** Smurf assay was performed on worms with different RPOA-2 knockdown initiation times using 5% Brilliant Blue FCF. Three independent experiments were performed at 20 °C, with 40-60 worms per condition in each experiment. **A)** Representative images are shown. **B)** Smurfs from the three independent experiments were quantified. Displayed is the fraction of Smurfs  $\pm$ SD. Statistical significance was determined using the unpaired Student's *t*-test. [AD = adulthood days]



## 6 DISCUSSION

Synthesis of pre-rRNA is the limiting step of ribosome biogenesis [157], thus dictating the number of ribosomes in cells and, consequently, the capacity for mRNA translation. rRNA gene transcription is regulated by central nutrient-sensing pathways, i.e., mTOR, IIS, AMPK, and SIRT1, which also affect longevity [96, 158-160]. Additionally, pre-rRNA is produced at a high rate, requiring a substantial energy investment from the cell [145]. Cellular energy levels become scarce during aging, thus compromising the maintenance of cellular homeostasis, including proteostasis [144, 161]. Curbing a highly energy-consuming process, such as rRNA gene transcription, could preserve cellular energy levels and thereby improve cellular homeostasis during aging. Therefore, it was hypothesized that Pol I transcription itself is a determinant of longevity.

### 6.1 RNA polymerase I transcriptional activity is a modulator of longevity

This work showed that NCL-1, a master regulator of ribosome biogenesis, also directly regulates Pol I transcription. Knockdown of NCL-1 overlocks the rRNA gene activity resulting in a decrease of both lifespan and healthspan in *C. elegans* (**Figures 3, 8**). Furthermore, TIF-IA was overexpressed in *C. elegans*, causing increased rRNA gene activity akin to fruit flies and mice [130, 131]. Overexpression of TIF-IA had a similar life-shortening effect as the NCL-1 knockdown (**Figure 4**), demonstrating the causative role of pre-rRNA synthesis in modulating longevity. Accordingly, decreasing Pol I transcriptional activity by knockdown of TIF-IA improved healthspan and extended lifespan (**Figures 6, 8**). In conclusion, curbing Pol I transcription improves both lifespan and healthspan in *C. elegans*. Therefore, rRNA gene transcription is a potential novel target to intervene with aging.

However, decreasing rDNA activity has a drawback because rRNA gene activity is positively correlated with body size and neuromuscular capacity at a young age in *C. elegans* (**Figures 7, 8**). These findings fit the antagonistic pleiotropy theory [2]. Elevated pre-rRNA synthesis enables worms to become bulkier and have a better locomotive performance early in adulthood. Therefore, they are likely to reach food faster and have better chances to escape

from predators. However, the higher metabolic activity accelerates aging, leading to a fitness disadvantage late in life. Hence, rRNA gene activity presents a trade-off between early life advantage caused by high activity and improved longevity owing to low activity. Since increased Pol I transcriptional activity gives worms an advantage in their reproductive phase, which is around 3 to 6 days, why is the pre-rRNA synthesis in wild-type worms not higher? A possible explanation would be that the energy expenditure that comes with increased rRNA gene activity must be sustained by food intake. In the natural habitat of *C. elegans*, food is likely to become scarce and thus will not meet the high energy demand induced by elevated Pol I transcription. This notion is supported by genetic abrogation of NCL-1 in *eat-2* mutant worms, which are long-lived due to reduced food uptake. The survival of animals carrying both mutations is severely diminished, their lifespan falling below wild-type and *ncl-1* single mutant worms [81].

## 6.2 Lowering rRNA gene activity is a promising late-life intervention

To achieve a sufficient knockdown of NCL-1 and TIF-IA, worms were treated for two generations with the corresponding RNAi. Hence, the pro-longevity effect could be either due to transgenerational or development effects; for example, a general slowdown in development could prolong lifespan. However, the lifespan extension caused by RPOA-2 RNAi treatment initiated at the L4 stage for one generation argues against this possibility. Nevertheless, knockdown of RPOA-2 initiated at L4 stage reduced rDNA activity during the reproductive phase and thus could have impacted the production of oocytes (**Figure 17**). In fact, the germline stem cells (GSCs) influence the aging of both *C. elegans* and *D. melanogaster*, and the ablation of GSCs extends their lifespan by about 60% and 40%, respectively [162, 163]. Given that the ribosome biogenesis facilitates stem cell differentiation and maintenance [164], curtailment of rRNA synthesis could delay aging through the restriction of GSCs. However, post-reproductive knockdown of RPOA-2 (AD6) illustrated that the pro-longevity mechanism is not dependent on the GSCs (**Figure 18**).

Initiating RPOA-2 knockdown even later, at AD8, still promoted longevity, despite the lower knockdown efficiency. Even though the median lifespan extension upon RPOA-2

knockdown was similar among the different treatment times, improvement in healthspan and maximum lifespan negatively correlated with the onset of the knockdown (**Figures 18, 19, 20**). However, it is difficult to determine whether RPOA-2 knockdown is less beneficial in old worms, because initiation of the treatment at later time points comes with the disadvantage of less exposure time to the RNAi. Besides, the pharyngeal pumping rate declines with age [154], meaning that the ingestion of bacteria becomes compromised. Consequently, the later the worms are transferred onto dsRNA-producing bacteria, the more the knockdown is delayed. Given this technical hurdle, other means of RNAi delivery, e.g., "RNAi by soaking" [165], may be employed in the future to reveal the full pro-longevity potential of RPOA-2 knockdown late in life. Nevertheless, the data presented in this thesis already suggest a wide application window for curbing rRNA gene activity to promote healthy aging.

### 6.3 Moderate rDNA activity provides geroprotection through preserving energy levels

The mitochondrial function has been long known to decline with age [166]. Aside from their activity, the number of mitochondria also reduces with age, and there is a decrease in ATP levels observed in old worms and flies [122, 167]. A lower ATP supply will consequently hold up the activity of ATP-demanding processes, including processes involved in cellular homeostasis. A drop in ATP levels can cause a homeostatic imbalance, contributing to aging [144]. Ribosome biogenesis is a major energetic burden for the cell [168]. By downregulating rRNA gene activity, which dictates ribosome biogenesis, the protein synthesis capacity will eventually be affected. Aside from pre-rRNA synthesis, its processing and folding, as well as ribosome assembly, translation, and degradation of ribosomal proteins (RPs), demand energy in order to synthesize ribosomes [93, 95, 169]. As TIF-1A KD worms exhibit decreased pre-rRNA synthesis, lower expression of RPs, and a decreased total protein content, knockdown of TIF-1A saves energy at all three levels, which is probably the reason for the gain in ATP levels. However, in contrast to previous findings showing that inhibition of protein synthesis in human neuronal cells increases ATP levels *in vitro* [170], perturbation of translation alone seems to be insufficient to significantly preserve energy in *C. elegans* (**Figure 14A**).

Importantly, the energy preservation in old TIF-IA KD worms raised the ATP level to a similar level as observed in young control worms (**Figure 14B**). Besides, TIF-IA KD protracted metformin-induced death at old age (**Figure 15**), suggesting that moderation of pre-rRNA synthesis counters age-dependent loss of metabolic plasticity, with which young worms adapt to metformin toxicity [147]. On the whole, reducing Pol I transcriptional activity relieves the cell from the metabolic burden owing to ribosome biogenesis and increases its survival chances when faced with an energy-requiring challenge.

Interestingly, ATP has hydrotropic properties, meaning that it solubilizes hydrophobic molecules in an aqueous solution. Therefore, other than serving as the cell's energy currency, ATP keeps proteins in solution by preventing and resolving the formation of aggregates [171]. Thus, the age-related drop in ATP levels might contribute to the age-related protein aggregation (see section 6.5), which would be alleviated by sustaining ATP levels upon moderation of rRNA gene activity.

In addition, the proteomic analysis showed that at old age, mitochondrial ribosomal protein content is maintained upon TIF-IA KD (**Figure 12A**). Furthermore, TIF-IA KD rescued a significant number of mitochondrial proteins from an age-related decline (**Figure 10D,E**). These data imply that moderation of rRNA gene activity does not only reduce ATP consumption but also protects mitochondria from age-associated dysfunction. Mitochondrial preservation maintains their bioenergetic competence, and this effect likely contributes to the increased ATP levels [172]. The degree of mitochondrial preservation upon curbed rRNA gene activity is still to be resolved. Therefore, investigating mitochondrial functional status in young and old TIF-IA KD or RPOA-2 KD worms, for example, by measuring mitochondrial respiration and glycolysis parameters, would elucidate how perturbation of rRNA gene activity affects age-related mitochondrial functional decline.

## 6.4 Curbed pre-rRNA synthesis modulates lipid metabolism and reduces lipotoxicity

Translation inhibition has been long known to extend lifespan and has been extensively studied in *C. elegans*, e.g., by deletion and mutation of RPs [41, 80, 173]. Proteomic analysis of TIF-IA KD worms showed lower ribosomal and total protein content (**Figure 12**). However, moderation of rRNA gene activity was only partly dependent on translational inhibition (**Figure 13**), suggesting that other mechanisms also come into play.

Further analysis of the proteome revealed that the largest fraction of proteins rescued by TIF-IA KD from age-related change were involved in metabolism, the largest category comprising proteins related to lipid metabolism (**Figure 10**). In this group, the vitellogenins stood out because all six VITs were downregulated upon TIF-IA KD (**Figure 11**). Vitellogenins are highly expressed yolk proteins in *C. elegans* that transport various nutrients and lipids from the intestine to the germline [60]. There is an increase of vitellogenins after the reproductive phase, mainly due to the accumulation of yolk. The massive yolk synthesis during the reproductive period seems not to be tightly shut down in the post-reproductive phase, resulting in vitellogenin accumulation and, importantly, their aggregation [47, 59, 60]. Knockdown of *vit-2* and *vit-5* extend lifespan, and it is proposed that age-related yolk accumulation leads to lipotoxicity [58, 174, 175]. Thus, the lower levels of vitellogenins could be due to less yolk production, thereby assisting the longevity of curbed rRNA gene activity.

Besides, TIF-IA KD worms had a lower membrane lipid content at any given age (**Figure 16A**). Importantly, TIF-IA KD provided a higher MUFA/PUFA ratio in membrane lipids (PCs and PEs) and a higher MCFA/LCFA ratio in storage lipids (TAGs) (**Figure 16**); both changes are positively correlated with longevity [62, 65, 69, 149, 150]. PUFAs have a higher peroxidation index than MUFAs, meaning that MUFAs are less prone to be damaged by reactive oxygen species, resulting in less lipoxidative stress [62]. However, increasing MUFAs lowers the membrane fluidity, but this can be compensated by shortening the chain length, which raises the question of whether this also holds true in TIF-IA KD worms. In sum, attenuation of pre-rRNA synthesis through TIF-IA depletion results in a longevity signature of the lipidome that likely acts as an additional geroprotection mechanism.

## 6.5 Decreased rRNA gene activity alleviates proteostatic stress

Key players in the maintenance of the proteostasis are the proteasome, the lysosome, and heat-shock proteins (HSPs). Whereas the HSPs rescue unfolded and misfolded proteins, the lysosome and proteasome degrade them [176, 177]. Loss of protein homeostasis has been characterized as one of the hallmarks of aging and is termed proteostasis collapse [1, 178]. TIF-IA knockdown worms have lower protein content, and part of their lifespan extension is due to translation inhibition (**Figure 12, 13**). Lower protein synthesis will decrease the load of nascent polypeptides processed by the proteostasis machinery, improving the efficiency of protein homeostasis.

In addition, the turnover of RPs decreases with age. More importantly, most of these proteins tend to aggregate in aged worms (63%) [47]. The age-related aggregation of RPs has also been observed in the brain of the killifish *Nothobranchius furzeri* due to proteostatic functional decline [179]. This suggests that RPs tend to be a burden for the aged proteostasis. Therefore, a lower abundance of RPs on account of TIF-IA knockdown could relieve the pressure on the proteostasis, reducing proteolytic stress during aging. Besides, RPs are produced in excess and, if not incorporated into the ribosomes, quickly degraded by the proteasome. Accordingly, inhibition of the proteasome leads to the accumulation of RPs [169], implying that the proteasome is continuously engaged in ribosomal protein degradation. TIF-IA KD worms have from a young age lower expression of RPs (**Figure 12A**); hence fewer ribosomal proteins have to be degraded, allowing the proteostasis to focus on other homeostatic duties.

Aside from RPs, the increased levels of vitellogenins are also partly due to aggregation with age [47]. Hence, post-reproductive yolk accumulation would not only lead to lipotoxicity but also turn into a proteotoxic insult. Also here does perturbation of rRNA gene activity by TIF-IA KD lightens the pressure on the proteolytic system. Moreover, the levels of vitellogenins are lower from a young age, and thus, it is more likely that vitellogenins are less expressed rather than better degraded. Decreased vitellogenin expression would preserve energy by reducing the synthesis and degradation of the vitellogenins.

Aside from decreasing proteotoxic insults, knockdown of TIF-IA counteracts against aging-associated cellular energy decline (section 5.3). Folding and, especially, degradation of

proteins are energy-intensive [161, 180]. Therefore, curbing rRNA gene activity could indirectly provide a more functional proteostasis during aging by preserving energy.

The evidence in this study and the literature indirectly imply that low rRNA gene activity prevents age-related proteostasis collapse [144, 181]. However, this thesis did not cover how and to what degree perturbation of rDNA affects proteostasis. Hence, quantifying aggregates in old worms upon perturbed rDNA activity would elucidate whether rRNA gene activity affects aggregate formation. In addition, interfering with the proteostasis in TIF-1A or RPOA-2 knockdown worms, for example, by RNAi treatment against proteasome subunits, would provide insight into whether and to what degree the proteostasis contributes to the pro-longevity effect upon curbing rRNA gene activity.

## 6.6 Perturbation of pre-rRNA synthesis as an anti-aging strategy

This work investigated a novel strategy to promote longevity by targeting rRNA gene transcription. Additionally, this study uncovered that reducing RNA activity has five molecular consequences, thereby promoting longevity: i) reduced ribosome biogenesis, ii) translation inhibition, iii) low yolk protein accumulation, iv) preservation of cellular energy, and v) altered lipid profile. Each of these five processes has been associated with longevity [58, 65, 69, 94, 144, 150, 175]. Therefore, I propose that curbing rRNA gene activity provides geroprotection through these means (**Figure 21**).

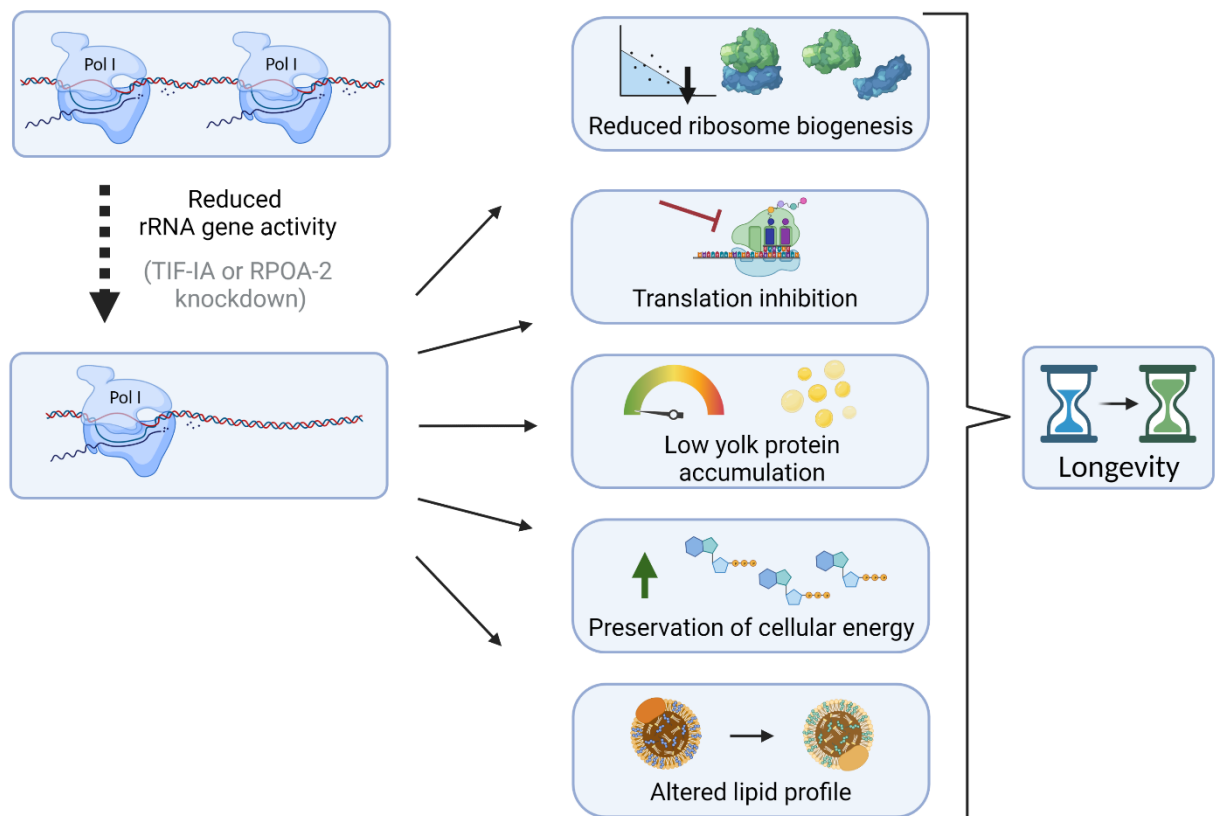


**Figure 21: Model depicting the geroprotective changes induced by moderation of rDNA activity.**

Upon TIF-1A or RPOA-2 knockdown, the rRNA gene activity is curbed. Downstream processes, i.e., ribosome biogenesis and translation, are reduced. Yolk proteins (VIT-1 to VIT-6) are decreased in the cell, and cellular ATP levels are increased. The lipid profile is remodeled towards longevity promotion. Together these changes mediate an increased healthspan and lifespan.



Reduced rRNA gene activity promotes longevity in *C. elegans*, but how does this translate to humans? The molecular mechanisms causing aging are conserved, i.e., mitochondrial functional decline and collapse of proteostasis. The ATP levels in human calf muscle have been shown to drop 8% per decade, mitochondrial proteins were reduced, and mitochondrial DNA was more damaged in aged muscles [182]. These findings show that in humans, a similar aging-related mitochondrial dysfunction can be observed. Additionally, senescent cells have been shown to have a decline in proteostasis function [183]. Moreover, proteostasis collapse has been associated with age-related neurodegenerative diseases, such as Alzheimer's, Parkinson's, and Huntington's disease, where the accumulation of protein aggregates is a major part of the etiology [184-186]. These observations reinforce that protein homeostasis also plays a role in human aging. Therefore, an approach to improve both cellular energy and protein homeostasis has potential as an anti-aging intervention in humans.

Considering the high conservation of ribosome biogenesis and translation in eukaryotes, the effects of Pol I perturbation on ribosome biogenesis, translation, and cellular energy levels would probably be similar. Moreover, the proposed intervention delayed aging in worms even when initiated later in life, making it a more practical intervention than whole life treatment. Thus, moderation of rDNA activity could be a promising anti-aging intervention in humans. However, the somatic cells of *C. elegans* are post-mitotic, and thus, how the inhibition of Pol I affects proliferative tissues is still unknown. Impairment of any step of the ribosome biogenesis, including rRNA synthesis, can lead to cell cycle arrest [187]. Thus, curbing pre-rRNA synthesis could result in the improper functioning of proliferative organs and tissues, such as the immune system and stem cells. Therefore, this has to be first carefully studied in a mammalian model organism. Furthermore, the degree of Pol I inhibition has to be fine-tuned so that it does not interfere with the function of proliferative cells.

There are currently two compounds available to pharmacologically intervene with rRNA gene activity in mammals: BMH-21 and CX-5461. BMH-21 is a DNA intercalator preferentially binding to the GC-rich rDNA [188]. CX-5461 inhibits Pol I transcription via disrupting the recruitment of SL1 to the promoter [189]. However, CX-5461 has recently been found to poison topoisomerase II, thereby inducing DNA damage [190]. Given that both

compounds are endangering the integrity of rDNA, they are not well suited for aging interventions. Therefore, in addition to developing safer Pol I transcription inhibitors, it will also be necessary to fully understand how pre-rRNA synthesis can be modulated by nutrition and lifestyle to promote healthy longevity in humans.

## 7 REFERENCES

1. López-Otín, C., et al., *The hallmarks of aging*. Cell, 2013. **153**(6): p. 1194-217.
2. Williams, G.C., Pleiotropy, natural selection, and the evolution of senescence. evolution, 1957: p. 398-411.
3. Kapahi, P., Protein synthesis and the antagonistic pleiotropy hypothesis of aging. Adv Exp Med Biol, 2010. **694**: p. 30-7.
4. Larsson, L., G. Grimby, and J. Karlsson, *Muscle strength and speed of movement in relation to age and muscle morphology*. J Appl Physiol Respir Environ Exerc Physiol, 1979. **46**(3): p. 451-6.
5. Lexell, J., *Human aging, muscle mass, and fiber type composition*. J Gerontol A Biol Sci Med Sci, 1995. **50 Spec No**: p. 11-6.
6. Franceschi, C. and J. Campisi, Chronic inflammation (inflammaging) and its potential contribution to age-associated diseases. J Gerontol A Biol Sci Med Sci, 2014. **69 Suppl 1**: p. S4-9.
7. Ayyaz, A. and H. Jasper, Intestinal inflammation and stem cell homeostasis in aging *Drosophila melanogaster*. Front Cell Infect Microbiol, 2013. **3**: p. 98.
8. Jandhyala, S.M., et al., *Role of the normal gut microbiota*. World J Gastroenterol, 2015. **21**(29): p. 8787-803.
9. Rera, M., R.I. Clark, and D.W. Walker, Intestinal barrier dysfunction links metabolic and inflammatory markers of aging to death in *Drosophila*. Proc Natl Acad Sci U S A, 2012. **109**(52): p. 21528-33.
10. Bitner, K., et al., *Predicting death by the loss of intestinal function*. PLoS One, 2020. **15**(4): p. e0230970.
11. *The top 10 causes of death*. 2020; Available from: <https://www.who.int/news-room/fact-sheets/detail/the-top-10-causes-of-death>.
12. Lee, B.C., A. Kaya, and V.N. Gladyshev, *Methionine restriction and life-span control*. Ann N Y Acad Sci, 2016. **1363**: p. 116-24.
13. Tanaka, Y., et al., Metformin activates KDM2A to reduce rRNA transcription and cell proliferation by dual regulation of AMPK activity and intracellular succinate level. Sci Rep, 2019. **9**(1): p. 18694.
14. Arslan-Ergul, A., A.T. Ozdemir, and M.M. Adams, *Aging, neurogenesis, and caloric restriction in different model organisms*. Aging Dis, 2013. **4**(4): p. 221-32.
15. Kenyon, C., et al., *A C. elegans mutant that lives twice as long as wild type*. Nature, 1993. **366**(6454): p. 461-4.
16. Tatar, M., et al., A mutant *Drosophila* insulin receptor homolog that extends life-span and impairs neuroendocrine function. Science, 2001. **292**(5514): p. 107-110.
17. Kappeler, L., et al., Brain IGF-1 receptors control mammalian growth and lifespan through a neuroendocrine mechanism. PLoS Biol, 2008. **6**(10): p. e254.
18. Murphy, C.T. and P.J. Hu, *Insulin/insulin-like growth factor signaling in C. elegans*. WormBook: The Online Review of C. elegans Biology [Internet], 2018.
19. Hay, N. and N. Sonenberg, *Upstream and downstream of mTOR*. Genes Dev, 2004. **18**(16): p. 1926-45.
20. Bareja, A., D.E. Lee, and J.P. White, Maximizing Longevity and Healthspan: Multiple Approaches All Converging on Autophagy. Front Cell Dev Biol, 2019. **7**: p. 183.
21. Sukumaran, A., K. Choi, and B. Dasgupta, Insight on Transcriptional Regulation of the Energy Sensing AMPK and Biosynthetic mTOR Pathway Genes. Front Cell Dev Biol, 2020. **8**: p. 671.
22. Dossou, A.S. and A. Basu, *The Emerging Roles of mTORC1 in Macromanaging Autophagy*. Cancers (Basel), 2019. **11**(10).

23. Tokunaga, C., K. Yoshino, and K. Yonezawa, *mTOR integrates amino acid- and energy-sensing pathways*. Biochem Biophys Res Commun, 2004. **313**(2): p. 443-6.
24. Vellai, T., et al., Genetics: influence of TOR kinase on lifespan in *C. elegans*. Nature, 2003. **426**(6967): p. 620.
25. Johnson, S.C., P.S. Rabinovitch, and M. Kaeberlein, *mTOR is a key modulator of ageing and age-related disease*. Nature, 2013. **493**(7432): p. 338-45.
26. Xu, J., J. Ji, and X.H. Yan, *Cross-talk between AMPK and mTOR in regulating energy balance*. Crit Rev Food Sci Nutr, 2012. **52**(5): p. 373-81.
27. Jeon, S.M., Regulation and function of AMPK in physiology and diseases. Exp Mol Med, 2016. **48**(7): p. e245.
28. Stenlesen, D., et al., Adenosine nucleotide biosynthesis and AMPK regulate adult life span and mediate the longevity benefit of caloric restriction in flies. Cell Metab, 2013. **17**(1): p. 101-12.
29. Cantó, C., et al., AMPK regulates energy expenditure by modulating NAD<sup>+</sup> metabolism and SIRT1 activity. Nature, 2009. **458**(7241): p. 1056-60.
30. Oberdoerffer, P., et al., SIRT1 redistribution on chromatin promotes genomic stability but alters gene expression during aging. Cell, 2008. **135**(5): p. 907-18.
31. Kaeberlein, M., M. McVey, and L. Guarente, The SIR2/3/4 complex and SIR2 alone promote longevity in *Saccharomyces cerevisiae* by two different mechanisms. Genes Dev, 1999. **13**(19): p. 2570-80.
32. Gottlieb, S. and R.E. Esposito, A new role for a yeast transcriptional silencer gene, SIR2, in regulation of recombination in ribosomal DNA. Cell, 1989. **56**(5): p. 771-6.
33. Zhang, L., et al., *Signal transduction, ageing and disease*. Biochemistry and Cell Biology of Ageing: Part II Clinical Science, 2019: p. 227-247.
34. Kou, X., et al., Ampelopsin attenuates brain aging of D-gal-induced rats through miR-34a-mediated SIRT1/mTOR signal pathway. Oncotarget, 2016. **7**(46): p. 74484.
35. Ghosh, H.S., M. McBurney, and P.D. Robbins, *SIRT1 negatively regulates the mammalian target of rapamycin*. PLoS One, 2010. **5**(2): p. e9199.
36. Rera, M., et al., Modulation of longevity and tissue homeostasis by the *Drosophila* PGC-1 homolog. Cell Metab, 2011. **14**(5): p. 623-34.
37. Zhou, Y., et al., SIRT1/PGC-1 $\alpha$  Signaling Promotes Mitochondrial Functional Recovery and Reduces Apoptosis after Intracerebral Hemorrhage in Rats. Front Mol Neurosci, 2017. **10**: p. 443.
38. Tissenbaum, H.A. and L. Guarente, Increased dosage of a sir-2 gene extends lifespan in *Caenorhabditis elegans*. Nature, 2001. **410**(6825): p. 227-30.
39. Satoh, A., et al., Sirt1 extends life span and delays aging in mice through the regulation of Nk2 homeobox 1 in the DMH and LH. Cell Metab, 2013. **18**(3): p. 416-30.
40. Chen, C., et al., *SIRT1 and aging related signaling pathways*. Mech Ageing Dev, 2020. **187**: p. 111215.
41. Hansen, M., et al., Lifespan extension by conditions that inhibit translation in *Caenorhabditis elegans*. Aging Cell, 2007. **6**(1): p. 95-110.
42. Liu, B., Y. Han, and S.-B. Qian, Cotranslational response to proteotoxic stress by elongation pausing of ribosomes. Molecular cell, 2013. **49**(3): p. 453-463.
43. Shcherbakov, D., et al., Ribosomal mistranslation leads to silencing of the unfolded protein response and increased mitochondrial biogenesis. Communications biology, 2019. **2**(1): p. 1-16.
44. Kelmer Sacramento, E., et al., Reduced proteasome activity in the aging brain results in ribosome stoichiometry loss and aggregation. Molecular systems biology, 2020. **16**(6): p. e9596.

45. Venkatraman, P., et al., Eukaryotic proteasomes cannot digest polyglutamine sequences and release them during degradation of polyglutamine-containing proteins. *Mol Cell*, 2004. **14**(1): p. 95-104.
46. Hipp, M.S., P. Kasturi, and F.U. Hartl, *The proteostasis network and its decline in ageing*. *Nat Rev Mol Cell Biol*, 2019. **20**(7): p. 421-435.
47. Dhondt, I., et al., *Changes of Protein Turnover in Aging Caenorhabditis elegans*. *Mol Cell Proteomics*, 2017. **16**(9): p. 1621-1633.
48. Samuel, B.S., et al., *Caenorhabditis elegans responses to bacteria from its natural habitats*. *Proc Natl Acad Sci U S A*, 2016. **113**(27): p. E3941-9.
49. Anderson, J.L., L.T. Morran, and P.C. Phillips, *Outcrossing and the maintenance of males within C. elegans populations*. *J Hered*, 2010. **101 Suppl 1**(Suppl 1): p. S62-74.
50. Altun, Z. and D. Hall, *Introduction to C. elegans anatomy*. In *WormAtlas*, 2009.
51. Corsi, A.K., B. Wightman, and M. Chalfie, *Transparent window into biology: A primer on Caenorhabditis elegans*. *WormBook*, 2015.
52. Zhang, B., et al., Environmental Temperature Differentially Modulates C. elegans Longevity through a Thermosensitive TRP Channel. *Cell Rep*, 2015. **11**(9): p. 1414-24.
53. Schwarz, E.M., Evolution: a Parthenogenetic nematode shows how animals become sexless. *Current Biology*, 2017. **27**(19): p. R1064-R1066.
54. Lai, C.H., et al., Identification of novel human genes evolutionarily conserved in Caenorhabditis elegans by comparative proteomics. *Genome Res*, 2000. **10**(5): p. 703-13.
55. Friedman, D.B. and T.E. Johnson, A mutation in the age-1 gene in Caenorhabditis elegans lengthens life and reduces hermaphrodite fertility. *Genetics*, 1988. **118**(1): p. 75-86.
56. Morris, J.Z., H.A. Tissenbaum, and G. Ruvkun, A phosphatidylinositol-3-OH kinase family member regulating longevity and diapause in Caenorhabditis elegans. *Nature*, 1996. **382**(6591): p. 536-9.
57. Weinkove, D., et al., Long-term starvation and ageing induce AGE-1/PI 3-kinase-dependent translocation of DAF-16/FOXO to the cytoplasm. *BMC Biol*, 2006. **4**: p. 1.
58. Murphy, C.T., et al., Genes that act downstream of DAF-16 to influence the lifespan of Caenorhabditis elegans. *Nature*, 2003. **424**(6946): p. 277-83.
59. Ackerman, D. and D. Gems, The mystery of C. elegans aging: an emerging role for fat. Distant parallels between C. elegans aging and metabolic syndrome? *Bioessays*, 2012. **34**(6): p. 466-71.
60. Perez, M.F. and B. Lehner, Vitellogenins - Yolk Gene Function and Regulation in Caenorhabditis elegans. *Front Physiol*, 2019. **10**: p. 1067.
61. Mutlu, A.S., J. Duffy, and M.C. Wang, *Lipid metabolism and lipid signals in aging and longevity*. *Dev Cell*, 2021. **56**(10): p. 1394-1407.
62. Shmookler Reis, R.J., et al., Modulation of lipid biosynthesis contributes to stress resistance and longevity of C. elegans mutants. *Aging (Albany NY)*, 2011. **3**(2): p. 125-47.
63. Hulbert, A.J., et al., Life and death: metabolic rate, membrane composition, and life span of animals. *Physiol Rev*, 2007. **87**(4): p. 1175-213.
64. Brown, M.K., J.L. Evans, and Y. Luo, Beneficial effects of natural antioxidants EGCG and alpha-lipoic acid on life span and age-dependent behavioral declines in Caenorhabditis elegans. *Pharmacol Biochem Behav*, 2006. **85**(3): p. 620-8.
65. O'Rourke, E.J., et al.,  $\omega$ -6 Polyunsaturated fatty acids extend life span through the activation of autophagy. *Genes Dev*, 2013. **27**(4): p. 429-40.
66. Benedetti, M.G., et al., Compounds that confer thermal stress resistance and extended lifespan. *Exp Gerontol*, 2008. **43**(10): p. 882-91.
67. Honda, Y., et al., Lifespan-extending effects of royal jelly and its related substances on the nematode Caenorhabditis elegans. *PLoS One*, 2011. **6**(8): p. e23527.

68. Sugawara, S., et al., Fish oil changes the lifespan of *Caenorhabditis elegans* via lipid peroxidation. *J Clin Biochem Nutr*, 2013. **52**(2): p. 139-45.
69. Han, S., et al., Mono-unsaturated fatty acids link H3K4me3 modifiers to *C. elegans* lifespan. *Nature*, 2017. **544**(7649): p. 185-190.
70. Qi, W., et al., The  $\omega$ -3 fatty acid  $\alpha$ -linolenic acid extends *Caenorhabditis elegans* lifespan via NHR-49/PPAR $\alpha$  and oxidation to oxylipins. *Aging Cell*, 2017. **16**(5): p. 1125-1135.
71. Nakatani, Y., et al., Sesamin extends lifespan through pathways related to dietary restriction in *Caenorhabditis elegans*. *Eur J Nutr*, 2018. **57**(3): p. 1137-1146.
72. Kim, S.H., et al., Phosphatidylcholine Extends Lifespan via DAF-16 and Reduces Amyloid-Beta-Induced Toxicity in *Caenorhabditis elegans*. *Oxid Med Cell Longev*, 2019. **2019**: p. 2860642.
73. Su, S. and M. Wink, Natural lignans from *Arctium lappa* as antiaging agents in *Caenorhabditis elegans*. *Phytochemistry*, 2015. **117**: p. 340-350.
74. Klass, M.R., Aging in the nematode *Caenorhabditis elegans*: major biological and environmental factors influencing life span. *Mechanisms of ageing and development*, 1977. **6**: p. 413-429.
75. Zhang, Y. and W.B. Mair, Dietary Restriction in *C. elegans*, in *Ageing: Lessons from C. elegans*. 2017, Springer. p. 355-391.
76. Avery, L., *The genetics of feeding in Caenorhabditis elegans*. *Genetics*, 1993. **133**(4): p. 897-917.
77. Lakowski, B. and S. Hekimi, *The genetics of caloric restriction in Caenorhabditis elegans*. *Proc Natl Acad Sci U S A*, 1998. **95**(22): p. 13091-6.
78. Lapierre, L.R., et al., Autophagy and lipid metabolism coordinately modulate life span in germline-less *C. elegans*. *Curr Biol*, 2011. **21**(18): p. 1507-14.
79. Takauji, Y., et al., Restriction of protein synthesis abolishes senescence features at cellular and organismal levels. *Sci Rep*, 2016. **6**: p. 18722.
80. Syntichaki, P., K. Troulinaki, and N. Tavernarakis, *eIF4E function in somatic cells modulates ageing in Caenorhabditis elegans*. *Nature*, 2007. **445**(7130): p. 922-6.
81. Tiku, V., et al., *Small nucleoli are a cellular hallmark of longevity*. *Nat Commun*, 2017. **8**: p. 16083.
82. Derenzini, M., et al., *Nucleolar function and size in cancer cells*. *Am J Pathol*, 1998. **152**(5): p. 1291-7.
83. McClintock, B., The relationship of a particular chromosomal element to the development of the nucleoli in *Zea mays*. *Zeit. Ze/lforsch. Mik. Anat*, 1934. **21**: p. 294-328.
84. Gonzalez, I.L. and J.E. Sylvester, Complete sequence of the 43-kb human ribosomal DNA repeat: analysis of the intergenic spacer. *Genomics*, 1995. **27**(2): p. 320-8.
85. Hempel, W.M., et al., The species-specific RNA polymerase I transcription factor SL-1 binds to upstream binding factor. *Mol Cell Biol*, 1996. **16**(2): p. 557-63.
86. Miller, G., et al., hRRN3 is essential in the SL1-mediated recruitment of RNA Polymerase I to rRNA gene promoters. *Embo j*, 2001. **20**(6): p. 1373-82.
87. Yuan, X., et al., Multiple interactions between RNA polymerase I, TIF-IA and TAF(I) subunits regulate preinitiation complex assembly at the ribosomal gene promoter. *EMBO Rep*, 2002. **3**(11): p. 1082-7.
88. Moorefield, B., E.A. Greene, and R.H. Reeder, *RNA polymerase I transcription factor Rrn3 is functionally conserved between yeast and human*. *Proc Natl Acad Sci U S A*, 2000. **97**(9): p. 4724-9.
89. Bodem, J., et al., TIF-IA, the factor mediating growth-dependent control of ribosomal RNA synthesis, is the mammalian homolog of yeast Rrn3p. *EMBO Rep*, 2000. **1**(2): p. 171-5.
90. Baßler, J. and E. Hurt, *Eukaryotic Ribosome Assembly*. *Annu Rev Biochem*, 2019. **88**: p. 281-306.
91. Peña, C., E. Hurt, and V.G. Panse, *Eukaryotic ribosome assembly, transport and quality control*. *Nat Struct Mol Biol*, 2017. **24**(9): p. 689-699.

92. Pelletier, J., G. Thomas, and S. Volarević, *Ribosome biogenesis in cancer: new players and therapeutic avenues*. Nat Rev Cancer, 2018. **18**(1): p. 51-63.
93. Strunk, B.S. and K. Karbstein, *Powering through ribosome assembly*. Rna, 2009. **15**(12): p. 2083-104.
94. MacInnes, A.W., The role of the ribosome in the regulation of longevity and lifespan extension. Wiley Interdiscip Rev RNA, 2016. **7**(2): p. 198-212.
95. Kressler, D., E. Hurt, and J. Bassler, *Driving ribosome assembly*. Biochim Biophys Acta, 2010. **1803**(6): p. 673-83.
96. Sharifi, S. and H. Bierhoff, Regulation of RNA Polymerase I Transcription in Development, Disease, and Aging. Annu Rev Biochem, 2018. **87**: p. 51-73.
97. Albertson, D.G., Localization of the ribosomal genes in *Caenorhabditis elegans* chromosomes by in situ hybridization using biotin-labeled probes. Embo j, 1984. **3**(6): p. 1227-34.
98. Ellis, R.E., J.E. Sulston, and A.R. Coulson, *The rDNA of C. elegans: sequence and structure*. Nucleic Acids Res, 1986. **14**(5): p. 2345-64.
99. Shaye, D.D. and I. Greenwald, *OrthoList: a compendium of C. elegans genes with human orthologs*. PLoS One, 2011. **6**(5): p. e20085.
100. Kaltenbach, L., et al., The TBP-like factor CeTLF is required to activate RNA polymerase II transcription during *C. elegans* embryogenesis. Mol Cell, 2000. **6**(3): p. 705-13.
101. Genome sequence of the nematode *C. elegans*: a platform for investigating biology. Science, 1998. **282**(5396): p. 2012-8.
102. Simonis, N., et al., Empirically controlled mapping of the *Caenorhabditis elegans* protein-protein interactome network. Nat Methods, 2009. **6**(1): p. 47-54.
103. Reboul, J., et al., *C. elegans* ORFeome version 1.1: experimental verification of the genome annotation and resource for proteome-scale protein expression. Nat Genet, 2003. **34**(1): p. 35-41.
104. Grob, A., C. Colleran, and B. McStay, UBF an essential player in maintenance of active NORs and nucleolar formation, in *The nucleolus*. 2011, Springer. p. 83-103.
105. Frank, D.J., B.A. Edgar, and M.B. Roth, The *Drosophila melanogaster* gene brain tumor negatively regulates cell growth and ribosomal RNA synthesis. Development, 2002. **129**(2): p. 399-407.
106. Connacher, R.P. and A.C. Goldstrohm, *Molecular and biological functions of TRIM-NHL RNA-binding proteins*. Wiley Interdiscip Rev RNA, 2021. **12**(2): p. e1620.
107. Frank, D.J. and M.B. Roth, ncl-1 is required for the regulation of cell size and ribosomal RNA synthesis in *Caenorhabditis elegans*. J Cell Biol, 1998. **140**(6): p. 1321-9.
108. Yi, Y.H., et al., A Genetic Cascade of let-7-ncl-1-fib-1 Modulates Nucleolar Size and rRNA Pool in *Caenorhabditis elegans*. PLoS Genet, 2015. **11**(10): p. e1005580.
109. Kobayashi, T., A new role of the rDNA and nucleolus in the nucleus--rDNA instability maintains genome integrity. Bioessays, 2008. **30**(3): p. 267-72.
110. Sinclair, D.A. and L. Guarente, *Extrachromosomal rDNA circles--a cause of aging in yeast*. Cell, 1997. **91**(7): p. 1033-42.
111. Ganley, A.R. and T. Kobayashi, Ribosomal DNA and cellular senescence: new evidence supporting the connection between rDNA and aging. FEMS Yeast Res, 2014. **14**(1): p. 49-59.
112. Ganley, A.R., et al., The effect of replication initiation on gene amplification in the rDNA and its relationship to aging. Mol Cell, 2009. **35**(5): p. 683-93.
113. Morlot, S., et al., Excessive rDNA Transcription Drives the Disruption in Nuclear Homeostasis during Entry into Senescence in Budding Yeast. Cell Rep, 2019. **28**(2): p. 408-422.e4.
114. Larson, K., et al., Heterochromatin formation promotes longevity and represses ribosomal RNA synthesis. PLoS Genet, 2012. **8**(1): p. e1002473.

115. Møller, H.D., et al., Circular DNA elements of chromosomal origin are common in healthy human somatic tissue. *Nature communications*, 2018. **9**(1): p. 1-12.
116. Shoura, M.J., et al., Intricate and Cell Type-Specific Populations of Endogenous Circular DNA (eccDNA) in *Caenorhabditis elegans* and *Homo sapiens*. *G3 (Bethesda)*, 2017. **7**(10): p. 3295-3303.
117. Filer, D., et al., *RNA polymerase III limits longevity downstream of TORC1*. *Nature*, 2017. **552**(7684): p. 263-267.
118. Martínez Corrales, G., et al., *Partial Inhibition of RNA Polymerase I Promotes Animal Health and Longevity*. *Cell Rep*, 2020. **30**(6): p. 1661-1669.e4.
119. Boulon, S., et al., *The nucleolus under stress*. *Mol Cell*, 2010. **40**(2): p. 216-27.
120. Le Bourg, E., *Hormesis, aging and longevity*. *Biochim Biophys Acta*, 2009. **1790**(10): p. 1030-9.
121. Steffen, K.K. and A. Dillin, *A Ribosomal Perspective on Proteostasis and Aging*. *Cell Metab*, 2016. **23**(6): p. 1004-1012.
122. Braeckman, B.P., et al., *Assaying metabolic activity in ageing *Caenorhabditis elegans**. *Mech Ageing Dev*, 2002. **123**(2-3): p. 105-19.
123. Brookman, J.L., et al., *An immunological analysis of Ty1 virus-like particle structure*. *Virology*, 1995. **207**(1): p. 59-67.
124. Frøkjær-Jensen, C., et al., *Single-copy insertion of transgenes in *Caenorhabditis elegans**. *Nat Genet*, 2008. **40**(11): p. 1375-83.
125. Stiernagle, T., *Maintenance of *C. elegans**. *WormBook*, 2006: p. 1-11.
126. Porta-de-la-Riva, M., et al., Basic *Caenorhabditis elegans* methods: synchronization and observation. *J Vis Exp*, 2012(64): p. e4019.
127. Lesanpezeshki, L., et al., Pluronic gel-based burrowing assay for rapid assessment of neuromuscular health in *C. elegans*. *Sci Rep*, 2019. **9**(1): p. 15246.
128. Gelino, S., et al., Intestinal Autophagy Improves Healthspan and Longevity in *C. elegans* during Dietary Restriction. *PLoS Genet*, 2016. **12**(7): p. e1006135.
129. Popov, A., et al., Duration of the first steps of the human rRNA processing. *Nucleus*, 2013. **4**(2): p. 134-41.
130. Zhao, J., et al., ERK-dependent phosphorylation of the transcription initiation factor TIF-IA is required for RNA polymerase I transcription and cell growth. *Mol Cell*, 2003. **11**(2): p. 405-13.
131. Grewal, S.S., J.R. Evans, and B.A. Edgar, *Drosophila TIF-IA is required for ribosome synthesis and cell growth and is regulated by the TOR pathway*. *J Cell Biol*, 2007. **179**(6): p. 1105-13.
132. Allen, A.K., J.E. Nesmith, and A. Golden, *An RNAi-based suppressor screen identifies interactors of the Myt1 ortholog of *Caenorhabditis elegans**. *G3 (Bethesda)*, 2014. **4**(12): p. 2329-43.
133. Lozano, E., et al., *Regulation of growth by ploidy in *Caenorhabditis elegans**. *Curr Biol*, 2006. **16**(5): p. 493-8.
134. Tikv, V. and A. Antebi, *Nucleolar Function in Lifespan Regulation*. *Trends Cell Biol*, 2018. **28**(8): p. 662-672.
135. Yuan, X., et al., Genetic inactivation of the transcription factor TIF-IA leads to nucleolar disruption, cell cycle arrest, and p53-mediated apoptosis. *Mol Cell*, 2005. **19**(1): p. 77-87.
136. Tuck, S., *The control of cell growth and body size in *Caenorhabditis elegans**. *Exp Cell Res*, 2014. **321**(1): p. 71-6.
137. So, S., K. Miyahara, and Y. Ohshima, *Control of body size in *C. elegans* dependent on food and insulin/IGF-1 signal*. *Genes Cells*, 2011. **16**(6): p. 639-51.
138. Bartke, A., *Somatic growth, aging, and longevity*. *NPJ Aging Mech Dis*, 2017. **3**: p. 14.
139. Rera, M., M.J. Azizi, and D.W. Walker, *Organ-specific mediation of lifespan extension: more than a gut feeling?* *Ageing Res Rev*, 2013. **12**(1): p. 436-44.



140. Walther, D.M., et al., Widespread Proteome Remodeling and Aggregation in Aging *C. elegans*. *Cell*, 2015. **161**(4): p. 919-32.
141. Holdorf, A.D., et al., WormCat: An Online Tool for Annotation and Visualization of *Caenorhabditis elegans* Genome-Scale Data. *Genetics*, 2020. **214**(2): p. 279-294.
142. Sun, N., R.J. Youle, and T. Finkel, *The Mitochondrial Basis of Aging*. *Mol Cell*, 2016. **61**(5): p. 654-666.
143. Keiper, B.D., et al., Functional characterization of five eIF4E isoforms in *Caenorhabditis elegans*. *J Biol Chem*, 2000. **275**(14): p. 10590-6.
144. Chaudhari, S.N. and E.T. Kipreos, The Energy Maintenance Theory of Aging: Maintaining Energy Metabolism to Allow Longevity. *Bioessays*, 2018. **40**(8): p. e1800005.
145. Warner, J.R., *The economics of ribosome biosynthesis in yeast*. *Trends Biochem Sci*, 1999. **24**(11): p. 437-40.
146. Fontaine, E., Metformin-Induced Mitochondrial Complex I Inhibition: Facts, Uncertainties, and Consequences. *Front Endocrinol (Lausanne)*, 2018. **9**: p. 753.
147. Espada, L., et al., Loss of metabolic plasticity underlies metformin toxicity in aged *Caenorhabditis elegans*. *Nat Metab*, 2020. **2**(11): p. 1316-1331.
148. Schroeder, E.A. and A. Brunet, *Lipid Profiles and Signals for Long Life*. *Trends Endocrinol Metab*, 2015. **26**(11): p. 589-592.
149. Hillyard, S.L. and J.B. German, Quantitative lipid analysis and life span of the fat-3 mutant of *Caenorhabditis elegans*. *J Agric Food Chem*, 2009. **57**(8): p. 3389-96.
150. Admasu, T.D., et al., Lipid profiling of *C. elegans* strains administered pro-longevity drugs and drug combinations. *Sci Data*, 2018. **5**: p. 180231.
151. Kimura, K.D., et al., daf-2, an insulin receptor-like gene that regulates longevity and diapause in *Caenorhabditis elegans*. *Science*, 1997. **277**(5328): p. 942-6.
152. Ashrafi, K., et al., Genome-wide RNAi analysis of *Caenorhabditis elegans* fat regulatory genes. *Nature*, 2003. **421**(6920): p. 268-72.
153. Seither, P. and I. Grummt, Molecular cloning of RPA2, the gene encoding the second largest subunit of mouse RNA polymerase I. *Genomics*, 1996. **37**(1): p. 135-9.
154. Huang, C., C. Xiong, and K. Kornfeld, Measurements of age-related changes of physiological processes that predict lifespan of *Caenorhabditis elegans*. *Proc Natl Acad Sci U S A*, 2004. **101**(21): p. 8084-9.
155. Herndon, L.A., et al., Stochastic and genetic factors influence tissue-specific decline in ageing *C. elegans*. *Nature*, 2002. **419**(6909): p. 808-14.
156. McGee, M.D., et al., Loss of intestinal nuclei and intestinal integrity in aging *C. elegans*. *Aging Cell*, 2011. **10**(4): p. 699-710.
157. Moss, T. and V.Y. Stefanovsky, *Promotion and regulation of ribosomal transcription in eukaryotes by RNA polymerase I*. *Prog Nucleic Acid Res Mol Biol*, 1995. **50**: p. 25-66.
158. Hoppe, S., et al., AMP-activated protein kinase adapts rRNA synthesis to cellular energy supply. *Proc Natl Acad Sci U S A*, 2009. **106**(42): p. 17781-6.
159. Grummt, I. and A.G. Ladurner, *A metabolic throttle regulates the epigenetic state of rDNA*. *Cell*, 2008. **133**(4): p. 577-80.
160. James, M.J. and J.C. Zomerdijs, Phosphatidylinositol 3-kinase and mTOR signaling pathways regulate RNA polymerase I transcription in response to IGF-1 and nutrients. *J Biol Chem*, 2004. **279**(10): p. 8911-8.
161. Peth, A., J.A. Nathan, and A.L. Goldberg, The ATP costs and time required to degrade ubiquitinated proteins by the 26 S proteasome. *J Biol Chem*, 2013. **288**(40): p. 29215-22.
162. Flatt, T., et al., *Drosophila germ-line modulation of insulin signaling and lifespan*. *Proceedings of the National Academy of Sciences*, 2008. **105**(17): p. 6368-6373.

163. Hsin, H. and C. Kenyon, Signals from the reproductive system regulate the lifespan of *C. elegans*. *Nature*, 1999. **399**(6734): p. 362-6.
164. Sharifi, S., H.F.R. da Costa, and H. Bierhoff, *The circuitry between ribosome biogenesis and translation in stem cell function and ageing*. *Mech Ageing Dev*, 2020. **189**: p. 111282.
165. Maeda, I., et al., Large-scale analysis of gene function in *Caenorhabditis elegans* by high-throughput RNAi. *Curr Biol*, 2001. **11**(3): p. 171-6.
166. Shigenaga, M.K., T.M. Hagen, and B.N. Ames, *Oxidative damage and mitochondrial decay in aging*. *Proc Natl Acad Sci U S A*, 1994. **91**(23): p. 10771-8.
167. Vernace, V.A., et al., Aging perturbs 26S proteasome assembly in *Drosophila melanogaster*. *Faseb j*, 2007. **21**(11): p. 2672-82.
168. Granneman, S. and D. Tollervey, *Building ribosomes: even more expensive than expected?* *Curr Biol*, 2007. **17**(11): p. R415-7.
169. Sung, M.K., et al., Ribosomal proteins produced in excess are degraded by the ubiquitin-proteasome system. *Mol Biol Cell*, 2016. **27**(17): p. 2642-52.
170. Zheng, X., et al., Alleviation of neuronal energy deficiency by mTOR inhibition as a treatment for mitochondria-related neurodegeneration. *Elife*, 2016. **5**.
171. Patel, A., et al., *ATP as a biological hydrotrope*. *Science*, 2017. **356**(6339): p. 753-756.
172. Brys, K., et al., Disruption of insulin signalling preserves bioenergetic competence of mitochondria in ageing *Caenorhabditis elegans*. *BMC Biol*, 2010. **8**: p. 91.
173. Pan, K.Z., et al., Inhibition of mRNA translation extends lifespan in *Caenorhabditis elegans*. *Aging cell*, 2007. **6**(1): p. 111-119.
174. Seah, N.E., et al., Autophagy-mediated longevity is modulated by lipoprotein biogenesis. *Autophagy*, 2016. **12**(2): p. 261-272.
175. Gems, D. and Y. de la Guardia, Alternative perspectives on aging in *Caenorhabditis elegans*: reactive oxygen species or hyperfunction? *Antioxidants & redox signaling*, 2013. **19**(3): p. 321-329.
176. Hartl, F.U., A. Bracher, and M. Hayer-Hartl, *Molecular chaperones in protein folding and proteostasis*. *Nature*, 2011. **475**(7356): p. 324-32.
177. Mizushima, N., et al., *Autophagy fights disease through cellular self-digestion*. *Nature*, 2008. **451**(7182): p. 1069-75.
178. Ben-Zvi, A., E.A. Miller, and R.I. Morimoto, *Collapse of proteostasis represents an early molecular event in Caenorhabditis elegans aging*. *Proceedings of the National Academy of Sciences*, 2009. **106**(35): p. 14914-14919.
179. Kelmer Sacramento, E., et al., Reduced proteasome activity in the aging brain results in ribosome stoichiometry loss and aggregation. *Mol Syst Biol*, 2020. **16**(6): p. e9596.
180. Calderwood, S.K., A. Murshid, and T. Prince, The shock of aging: molecular chaperones and the heat shock response in longevity and aging--a mini-review. *Gerontology*, 2009. **55**(5): p. 550-8.
181. Santra, M., K.A. Dill, and A.M.R. de Graff, *Proteostasis collapse is a driver of cell aging and death*. *Proc Natl Acad Sci U S A*, 2019. **116**(44): p. 22173-22178.
182. Short, K.R., et al., *Decline in skeletal muscle mitochondrial function with aging in humans*. *Proc Natl Acad Sci U S A*, 2005. **102**(15): p. 5618-23.
183. Klaips, C.L., G.G. Jayaraj, and F.U. Hartl, *Pathways of cellular proteostasis in aging and disease*. *J Cell Biol*, 2018. **217**(1): p. 51-63.
184. Brehme, M., et al., A chaperome subnetwork safeguards proteostasis in aging and neurodegenerative disease. *Cell Rep*, 2014. **9**(3): p. 1135-50.
185. Yerbury, J.J., et al., *Walking the tightrope: proteostasis and neurodegenerative disease*. *J Neurochem*, 2016. **137**(4): p. 489-505.

186. Soares, T.R., et al., *Targeting the proteostasis network in Huntington's disease*. Ageing Res Rev, 2019. **49**: p. 92-103.
187. Turi, Z., et al., Impaired ribosome biogenesis: mechanisms and relevance to cancer and aging. Aging (Albany NY), 2019. **11**(8): p. 2512-2540.
188. Colis, L., et al., DNA intercalator BMH-21 inhibits RNA polymerase I independent of DNA damage response. Oncotarget, 2014. **5**(12): p. 4361-9.
189. Drygin, D., et al., Targeting RNA polymerase I with an oral small molecule CX-5461 inhibits ribosomal RNA synthesis and solid tumor growth. Cancer Res, 2011. **71**(4): p. 1418-30.
190. Bruno, P.M., et al., The primary mechanism of cytotoxicity of the chemotherapeutic agent CX-5461 is topoisomerase II poisoning. Proc Natl Acad Sci U S A, 2020. **117**(8): p. 4053-4060.

## ACKNOWLEDGMENTS

Throughout my work, I have received a great deal of support and guidance.

Special thanks to Dr. Holger Bierhoff for giving me the opportunity to work on this project. Moreover, he has been instrumental in defining the path of my research.

I would like to thank my thesis committee, Holger, Dr. Maria Ermolaeva, and PD Dr. Christian Kosan for their guidance throughout my Ph.D. research. I thank Holger for investing a substantial amount of time in his students, like a father in his teenage children, including in me. I thank Maria for taking me under her wing as one of her own.

I would like to thank Prof. Dr. Manja Marz, who was kind enough to fund me for the first few semesters. I would like to acknowledge Dr. Joanna Kirkpatrick and Norman Rahnis from the proteomics core facility at FLI Jena for their helpful and fruitful collaboration. I thank my collaborators Prof. Dr. Werz and PD Dr. Koeberle at the department of Pharmacy, FSU of Jena, for helping me getting other insights into my work.

I thank Yvonne for being the pillars of the lab. Her superpowers have been keeping the entropic force of the students in check, and she made our lives significantly more convenient. I would like to acknowledge Marina for constantly offering her help more than I can offer her work. I would also like to thank Lisa for supporting me in the CMB.

I would like to thank Tanya, Alex D., and Lilia for teaching me the way of the worm. I thank Prerna for always selflessly helping and supporting me. I thank Asya, Isabela, Melike, Pol, and Huahui for making my lab life much more entertaining.

I would like to thank Andy, Alex E., SoYoung, Hugo, Robert, and Lisa for always assisting me with a smile, even if they are busy. I thank all my colleagues at the department of biochemistry, who created a pleasant working atmosphere. I would like to thank Viola, who helped me out as my bachelor's student.

A special thanks to Ann-Sophie for always organizing everything for me, supporting, assisting, and pushing me. I would have probably been still writing my thesis if it was not for her. I would like to thank my mother for teaching me not to leave today's work for tomorrow. I would like to acknowledge my father for teaching me that everything should be done in moderation, this even holds true for rRNA synthesis, and for toughening me up, which helped me get through many challenges. Lastly, I would like to thank my daughter Ada, who can always melt the stress away with her warm smile.

## DECLARATION OF INDEPENDENT ASSIGNMENT

### EHRENWÖRTLICHE ERKLÄRUNG

Hiermit versichere ich, dass mir die geltende Promotionsordnung der Fakultät für Biowissenschaften der Friedrich-Schiller-Universität Jena bekannt ist. Ich habe die vorliegende Dissertation mit dem Titel **„Moderation of rRNA gene activity triggers metabolic adaptation promoting geroprotection in *Caenorhabditis elegans*“** selbst angefertigt und keine Textabschnitte eines Dritten oder eigener Prüfungsarbeiten ohne Kennzeichnung verwendet. Alle verwendeten Hilfsmittel, persönliche Mitteilungen und Quellen habe ich angegeben. Personen, welche mich bei der Auswahl und Auswertung des Materials sowie bei der Erstellung des Manuskriptes unterstützt haben, wurden in der vorliegenden Arbeit genannt. Es wurde keine Hilfe einer kommerziellen Promotionsvermittlung in Anspruch genommen und Dritte haben weder mittelbar noch unmittelbar geldwerte Leistungen von mir erhalten, welche im Zusammenhang mit dem Inhalt dieser Arbeit stehen. Die Promotionsarbeit wurde nie zuvor als Prüfungsarbeit für eine staatliche oder andere wissenschaftliche Prüfung eingereicht. Weiterhin wurde die vorliegende Arbeit sowie eine in wesentlichen Teilen ähnliche oder eine andere Abhandlung dieser Arbeit nie zuvor bei einer anderen Hochschule oder Fakultät als Dissertation eingereicht.

Jena, 29.06.2021

.....

Mohamed Samin Sharifi